Expanding the Development of Engineered Genetic Incompatibility in Three Plant Systems

A Dissertation
SUBMITTED TO THE FACULTY OF
THE UNIVERSITY OF MINNESOTA
BY

Jonathan Parker Cors

IN PARTIAL FULFILLMENT OF THE REQUIREMENTS
FOR THE DEGREE OF
DOCTOR OF PHILOSOPHY

Advisors: Dr. Eric Watkins, Dr. Michael Smanski

2026

Acknowledgements

Thank you to my fantastic mentors I've had since I first became a researcher, Dr. Dominic Petrella and Dr. Florence Sessoms. I owe so much of my career to both of you.

Thank you to my fantastic lab mates that trained me, helped me, and supported me: Dr. Matthew Zinselmier, Dr. Juan Armando Casas Mollano, and Dr. Savio Ferriera.

Thank you to members of the Voytas lab for your support and expertise: Dr. Colby Starker, Dr. Jon Cody, and Nick Klejeski.

Thank you to my advisors, Dr. Michael Smanski and Dr. Eric Watkins. This collaboration started seemingly out of nowhere, and looking back on everything I've achieved I can confidently say so much of it was thanks to both of you. Additionally, thank you to my committee members, Dr. Robert Stupar, Dr. Jacob Jungers, and Dr. Dominic Petrella. All of you joined and helped me during my time of need and have continued to offer me guidance and support since then.

Thank you to my friend and family for always supporting me.

Finally, thank you to my dog Ame. The joy of my life. Every bad day was instantly cured coming home to you wagging your tail.

Abstract

The rapid advancement of agricultural synthetic biology necessitates robust biocontainment strategies to prevent the ecological escape of transformative traits. Current methods, such as physical isolation and sterility-based systems, are insufficient due to environmental instability and biological leakage. This dissertation investigates Engineered Genetic Incompatibility (EGI) as a mechanism for synthetic speciation to enforce durable reproductive isolation in plants. EGI utilizes a programmable transcriptional activator to drive lethal overexpression of essential genes in hybrid offspring, while maintaining fertility within the engineered population through a refractory guide target site. This research addresses the biological hurdles of implementing EGI, across three plant systems of increasing complexity.

First, using the model organism *Arabidopsis thaliana*, this work optimizes EGI components to overcome incomplete lethality observed in previous prototypes. By shifting the lethal target from the developmental regulator *WUSCHEL* to the metabolic gene *ELO1*, and integrating intron-mediated enhancement with the *Rpl23* promoter, containment efficacy was improved to 93% lethality in hybrid lines. Second, these components were translated to the oilseed cover crop pennycress (*Thlaspi arvense*) to evaluate EGI in an agronomic context. This compared protoplast, viral, and stable transformation methodologies, revealing critical bottlenecks in guide RNA toxicity and the transferability of tools from model systems. Finally, this dissertation addresses transformation recalcitrance in perennial ryegrass (*Lolium perenne*), optimizing protocols to facilitate the future incorporation of EGI into the ecologically critical grass family.

Collectively, this work demonstrates that while barriers to absolute lethality remain, EGI represents a distinct maturation in biocontainment technology. By engineering bidirectional

incompatibility that mimics natural speciation, this strategy offers a pathway to secure the biosafety of next-generation crops while preserving germplasm integrity.

Table of Contents

Chapter 1 – Introduction: The Biocontainment Imperative and the Difficulties in Plants

Chapter Summary

The rapid advancement of agricultural synthetic biology necessitates robust biocontainment strategies to prevent the ecological escape of transformative traits. Current methods, such as physical isolation and sterility-based systems, are insufficient due to environmental instability and biological leakage. This dissertation investigates Engineered Genetic Incompatibility (EGI) as a mechanism for synthetic speciation to enforce durable reproductive isolation. EGI utilizes a programmable transcriptional activator to drive lethal overexpression of essential genes in hybrid offspring, while maintaining fertility within the engineered population through a refractory guide target site. However, translating EGI to plant systems faces significant barriers, including genomic complexity in polyploid crops, physiological resilience that buffers against lethality, and epigenetic silencing mechanisms. This work seeks to remove hurdles to EGIs success in multiple species, progressing from the model organism *Arabidopsis thaliana* to the oilseed cover crop pennycress *(Thlaspi arvense)* and the recalcitrant monocot perennial ryegrass (*Lolium perenne)*.

1.1 The Imperative of Biocontainment

The global agricultural landscape is currently undergoing a paradigm shift driven by the rapid maturation of synthetic biology. While the first generation of genetically modified (GM) crops focused primarily on single agronomic traits, herbicide tolerance, or insect resistance (Raman, 2017), the next generation of plant engineering aims to fundamentally alter plant metabolism and physiology. Efforts are now underway to engineer C_4 photosynthetic pathways into C_3 crops (Hibberd et al., 2008), introduce nitrogen-fixing capabilities into non-legumes (Santi et al., 2013), and utilize plants as bioreactors for high-value pharmaceuticals and industrial enzymes (Sharma and Sharma, 2009). As these engineered traits become more complex and potentially more ecologically transformative, the biosafety risks associated with their unauthorized spread increase commensurately. Consequently, the development of robust biocontainment strategies, defined as mechanisms that prevent the escape of transgenes into wild or non-target populations, has elevated from a regulatory precaution to an ecological and economic imperative.

The history of agricultural biotechnology is punctuated by costly failures of containment that illustrate the high stakes of transgene escape. For example, ‘StarLink’ maize (*Zea mays)*, which was engineered to produce the Cry9C protein to act as an insecticide against caterpillars, was approved only for animal feed, but in 2000, this GMO corn was detected in the human food supply (Bucchini and Goldman, 2002). The resulting recall and trade disruption depressed U.S. corn prices by an estimated 6.8% for a year and cost the developer, Aventis, and the U.S. agricultural sector nearly $1 billion in buybacks and lost revenue (Carter and Smith, 2006; Schmitz et al., 2005). Perhaps most concerning for future synthetic biology applications is the case of glyphosate-resistant creeping bentgrass (*Agrostis stolonifera*) in Oregon. Following a wind event at a 2003 field trial, the transgene escaped into the wild, establishing feral

populations that persisted more than a decade later despite extensive eradication efforts, threatening the state's grass seed export industry (Reichman et al., 2006; Zapiola et al., 2008). These examples demonstrate that zero-tolerance markets and ecological safety cannot be guaranteed by stewardship and physical isolation alone.

While these examples highlight different modes of transgene escape, the creeping bentgrass example escaped via vertical gene flow, specifically through pollen-mediated dispersal and introgressive hybridization with sexually compatible wild relatives. Introgression, the permanent incorporation of genes from one population into the gene pool of another, poses significant ecological risks. Transfer of fitness-enhancing traits (e.g., herbicide resistance, drought tolerance, or pest resistance) to weed species increases difficulty of removal and the erosion of genetic diversity in wild centers of origin (Ellstrand, 2003; Ellstrand et al., 2013; Lu and Snow, 2005). For synthetic biology applications involving the production of bioactive compounds or industrial precursors, the escape of such traits could have deleterious effects on non-target herbivores, pollinators, and soil microbiota, rendering zero-tolerance containment a prerequisite for field deployment.

1.2 A Critical Review of Existing Biocontainment Strategies

To address the risks of vertical gene flow, a diverse array of containment strategies has been developed, ranging from simple physical barriers to complex genetic circuits. However, each existing method is characterized by specific limitations that render them insufficient for the stringent requirements of next-generation synthetic biology. Several extensive reviews already exist describing biocontainment strategies (Clark and Maselko, 2020; Daniell, 2002; George et al., 2024; Lee et al., 2018), and as such this work only seeks to briefly highlight them.

1.2.1 Physical and Spatial Containment

Historically, the primary method for containment has been spatial isolation, which relies on the establishment of buffer zones between GM crops and sexually compatible relatives. While regulatory bodies like the Animal and Plant Health Inspection Service (APHIS) often mandate specific isolation distances, these are based on statistical probabilities of pollen travel rather than absolute containment. Meteorological events, such as high winds or convection currents, can carry pollen kilometers beyond established buffers , such as what happened with the previous example of creeping bentgrass (Ellstrand, 2003). Furthermore, physical containment relies heavily on human compliance and cannot mitigate the spread of propagules via anthropogenic transport or animal vectors.

1.2.2 Biological and Genetic Barriers

Many engineered biological strategies aim to disrupt the reproductive cycle to prevent gene flow. The most common approach, Cytoplasmic Male Sterility (CMS), prevents the formation of viable pollen through the expression of chimeric mitochondrial open reading frames (ORFs) that disrupt ATP synthesis or induce premature programmed cell death in the tapetum (Chen and Liu, 2014). This strategy has been widely deployed in hybrid breeding systems for crops such as maize (Bohra et al., 2016); however, the utility of CMS is constrained by its inherent instability. CMS is susceptible to breakdown via the spontaneous restoration of fertility through nuclear *Restorer-of-fertility (Rf)* genes. These nuclear-encoded proteins can post-transcriptionally silence the mitochondrial sterility-inducing ORFs, rendering the containment system ineffective if such genes are present in the wider population.

Transplastomics is the engineering of the chloroplast genome rather than the nuclear genome. The primary utility of transplastomics for biocontainment lies in the cytological mechanism of maternal inheritance observed in the majority of angiosperms, where plastids are excluded from the generative cell during pollen development or are actively degraded in the pollen tube (Bock, 2015; Hagemann, 2004). This ensures that the engineered trait is not transmitted via pollen dispersal, effectively neutralizing the primary vector for vertical gene flow to wild relatives. The efficacy of this strategy is challenged by documented paternal leakage, where plastids are transmitted via pollen at low but ecologically significant frequencies (Azhagiri and Maliga, 2007).

Apomixis, or asexual reproduction through seeds, allows for the fixation of hybrid vigor and clonal propagation. Apomixis is a complex trait maintained through several gene interactions, though recent efforts have successfully engineered it in rice *(Oryza sativa)* (Chen et al., 2025) and sorghum *(Sorghum bicolor)* (Simon et al., 2025). In a containment context, obligate apomixis prevents the reception of foreign pollen. However, unless coupled with complete male sterility, apomictic plants still produce viable pollen that can fertilize wild relatives. A significant risk involves the apomixis gene itself escaping: if introgressed into a weed population, it could fix heterosis in the weed, creating highly invasive weeds (Hojsgaard and Hörandl, 2019).

Cleistogamy, a reproductive strategy where pollination occurs within permanently closed flowers, offers a natural physical barrier to gene flow (Culley and Klooster, 2007). By preventing the release of pollen into the environment, cleistogamous crops significantly reduce the risk of outcrossing with wild relatives or neighboring non-GM fields. This trait is naturally present in crops like wheat (*Triticum aestivum*) and rice (*Oryza sativa*), contributing to their historically lower rates of pollen-mediated gene flow compared to open-pollinated species (Lu and Snow,

2005). However, the efficacy of cleistogamy as a containment strategy is often compromised by small yet ecologically significant ability for pollen to escape (Matus-Cádiz et al., 2004). Furthermore, engineering obligate cleistogamy into naturally open-pollinated crops presents significant morphological challenges as a result of inbreeding depression (Charlesworth and Charlesworth, 1987).

More advanced molecular methods attempt to restrict the use or transmission of the transgene itself through Genetic Use Restriction Technologies (GURTs). Broadly categorized into variety-specific (V-GURT) and trait-specific (T-GURT) systems, these technologies utilize complex multi-component genetic circuits to control gene expression via external chemical triggers (Lombardo, 2014). V-GURT, colloquially known as "Terminator" technology, aims to prevent unauthorized seed saving and transgene escape by rendering the second-generation (F2) seeds sterile. A classic V-GURT architecture involves a three-gene system: a recombinase (e.g., Cre) under the control of a chemically inducible promoter, a lethal effector gene (e.g., the ribosome-inactivating saporin or the barnase ribonuclease) under a late-embryogenesis-abundant (LEA) promoter, and a blocking sequence flanked by target sites (e.g., *loxP*) that separates the lethal gene from its promoter. Upon treatment with an inducer such as tetracycline, the recombinase is expressed, excising the spacer and allowing for the tissue-specific expression of the lethal gene during seed maturation. This ensures that while the first generation is agronomically viable, the resulting seeds fail to germinate (Lombardo, 2014). T-GURT systems, by contrast, regulate the expression of the transgene itself rather than the viability of the whole organism. In these systems, the added agronomic trait is only expressed following the application of a proprietary chemical activator, allowing for temporal control over the GM trait (Hills et al., 2007).

While GURTs offer a robust biological solution to seed-mediated escape and temporal gene flow, they have faced insurmountable socio-political opposition due to concerns regarding farmer seed sovereignty and the potential for monopolization of germplasm (Lombardo, 2014). Furthermore, from a biosafety perspective, these systems remain susceptible to transcriptional gene silencing or mutations within the lethal effector or the inducible promoter, which could lead to "leaky" phenotypes and a loss of containment over evolutionary time.

As summarized in Table 1, these limitations underscore the need for improved biocontainment designs that address the shortcomings of current strategies. Existing methods are often compromised by reliance on inducible triggers that may fail under environmental stress, incomplete efficiency due to biological leakage, or sterility mechanisms that impede breeding and seed saving. To ensure the biosafety of next-generation synthetic biology, containment strategies must be constitutive to prevent silencing, evolutionarily robust, and capable of enforcing reproductive isolation without sacrificing agronomic utility. This requires moving beyond sterility toward synthetic speciation. While this term has gained prominence with the rise of synthetic biology, it represents the engineering application of a century-old evolutionary theory: Bateson-Dobzhansky-Muller Incompatibilities (BDMI). First characterized in the 1930s and 40s (Dobzhansky, 1936; Orr and Turelli, 2001), BDMIs describe how incompatible gene combinations arise between diverging populations to enforce reproductive isolation. Synthetic speciation effectively fast-forwards this evolutionary process, using designed genetic systems to render a crop sexually incompatible with wild relatives while maintaining fertility within the crop population. Accordingly, this dissertation investigates Engineered Genetic Incompatibility (EGI) as a strategy to establish durable reproductive barriers and isolate engineered genomes from wild gene pools.

1.3 Engineered Genetic Incompatibility (EGI): A Mechanism for Synthetic Speciation

Engineered Genetic Incompatibility (EGI) represents a departure from traditional sterility-based containment. Instead of breaking the reproductive cycle, EGI establishes a species-like barrier based on extreme underdominance. The hybrid has lower fitness than either homozygote parent. In the case of EGI, the hybrid offspring between the engineered strain and the wild type are completely inviable, while matings within the engineered population remain fully fertile (Maselko et al., 2017).

1.3.1 Molecular Mechanism

The EGI system functions through a genetic circuit comprised of two essential components. The first is the lethal effector, which consists of a Programmable Transcriptional Activator (PTA), such as a CRISPR-dCas9 fused to one or multiple strong trans-activation domain (e.g., VPR, VP64, Dreb2). This PTA is programmed via a single guide RNA (sgRNA) to bind to the promoter of a tightly regulated, essential developmental gene, driving lethal overexpression or ectopic expression of the target gene. The second component is the resistance allele. To prevent self-destruction, the EGI strain carries a refractory version of the target promoter. This promoter contains precise mutations (indels or SNPs) at the sgRNA binding site that abolish PTA recognition while maintaining the promoter's native function and regulation by endogenous transcription factors.

1.3.2 Genetic Logic of the Incompatibility

The interaction between these components creates a conditional lethality that manifests only in hybrids. In the EGI parent, the organism is homozygous for both the PTA and the refractory promoter; although the lethal effector is present, it cannot bind to the mutated promoter, and the

target gene is expressed at normal, physiological levels. Similarly, the wild-type parent lacks the PTA and possesses the wild-type promoter, resulting in normal development. However, when an EGI parent mates with a wild-type plant, the resulting F1 hybrid inherits one copy of the PTA from the EGI parent and one copy of the wild-type promoter from the wild-type parent. The PTA recognizes and binds to the single wild-type promoter allele, driving lethal overexpression of the target gene.

This mechanism has been robustly demonstrated in model organisms. In *Saccharomyces cerevisiae*, EGI strains were created that were reproductively isolated from wild-type yeast but fully fertile with themselves (Maselko et al., 2017). Similarly, in *Drosophila melanogaster*, EGI was used to generate synthetic species barriers, proving that the system functions effectively in metazoans (Maselko et al., 2020). Recent work has also translated these components to *Arabidopsis thaliana*, demonstrating the feasibility of the transcriptional activation logic in plants, although complete lethality remains an optimization challenge (Zinselmeier et al., 2025).

Beyond basic isolation, the underlying mechanics of EGI have significant implications for pest control. In insects, EGI is being explored as a next-generation Sterile Insect Technique (SIT). Unlike traditional SIT, which relies on radiation that can damage insect fitness, EGI allows for the rearing of competitive, fertile males that produce non-viable offspring when mating with wild females. This offers a genetic approach to population suppression for agricultural pests and disease vectors without the regulatory complexity of gene drives (Maselko et al., 2020; Upadhyay et al., 2022).

In the context of plant biotechnology, the primary application of EGI is biocontainment. By enforcing a post-zygotic barrier, EGI prevents the introgression of engineered traits into wild

populations. This ensures that any gene flow event, whether pollen from the EGI crop fertilizing a wild relative or wild pollen fertilizing the EGI crop, results in seed abortion, thereby strictly enforcing genetic isolation and protecting natural ecosystems from potential transgene flow.

Finally, this bidirectional incompatibility has significant utility beyond biocontainment, particularly for maintaining cultivar purity in open-pollinated species (Yadav et al., 2022). Conventionally, maintaining the genetic identity of an open-pollinated variety requires substantial spatial isolation to prevent pollen contamination from neighboring fields. EGI internalizes this isolation; any foreign pollen that lands on the EGI crop fails to produce viable offspring, ensuring that harvested seed remains genetically pure without the need for buffer zones. Unlike sterility systems, EGI allows the engineered crop to be fertile and reproduce normally with itself, enabling seed saving and breeding programs, provided the genetic barrier is maintained.

1.3.3 Limitations and Potential Failure Modes

Despite its theoretical robustness, EGI is not immune to biological failure modes common to all transgenic systems. The primary vulnerability lies in the stability of the lethal effector. Since the incompatibility relies on the active expression of the PTA to kill hybrids, any mechanism that silences this transgene, such as RNA interference (RNAi) or promoter methylation, would render the lethal effector inert. In such a scenario, a hybrid offspring would survive, effectively breaking the containment barrier. This risk is particularly acute in plants, which possess robust gene silencing pathways designed to suppress foreign DNA (El-Sappah et al., 2021). Consequently, maintaining stable, high-level expression of the PTA over successive generations is a prerequisite for the long-term efficacy of the system.

A more subtle but equally critical failure mode involves the standing genetic variation within the wild population. The design of an EGI system assumes that the wild-type population possesses a consistent promoter sequence that the PTA can recognize and bind to. However, wild populations are genetically diverse (Salgotra and Chauhan, 2023). If a natural variant exists within the wild gene pool that contains a mutation or polymorphism at the sgRNA target site, this allele would effectively mimic the engineered refractory promoter. In this scenario, a hybrid formed between the EGI crop and a wild relative carrying this natural refractory allele would survive, as the PTA would fail to bind the target promoter. This would result in the immediate failure of the containment barrier. To mitigate this risk, the design of EGI systems requires extensive bioinformatic surveying of wild germplasm to ensure the selected target sequence is highly conserved and devoid of polymorphisms that could confer resistance. This approach was empirically demonstrated in *Drosophila suzukii* by Feltman et al., (2022), who developed the Haplotype-resolution analysis of Unique loci by bulk Genomic Extraction (HUGE) pipeline. By utilizing high-throughput amplicon sequencing on pooled genomic DNA from thousands of wild-caught individuals, they were able to quantify standing genetic variation at high resolution. This allowed for the identification of specific promoter regions that remained evolutionarily conserved across different geographic populations and growing seasons, thereby pinpointing safe targets for PTA binding that minimize the probability of pre-existing resistance alleles.

Finally, it is important to distinguish between introgression and persistence. EGI is specifically designed to prevent introgression, the flow of genes from the crop into the wild gene pool. It does not, however, prevent the persistence of the individual crop plant itself. Unlike Genetic Use Restriction Technologies (GURTs), which induce sterility, EGI plants are fully fertile with one another. Consequently, EGI does not prevent the establishment of volunteer populations, crop

plants that grow from spilled seed in subsequent seasons. While these volunteers would remain genetically isolated from wild relatives and would not pass their transgenes into the wild gene pool, they could still establish feral populations that pose agronomic challenges, acting as weeds that require chemical or mechanical control.

1.4 Challenges in Translating EGI to Crops

While EGI has been successfully demonstrated in model systems such as *Saccharomyces cerevisiae* and *Drosophila melanogaster*, its translation to the plant kingdom has been hindered by fundamental biological distinctions. The engineering of synthetic speciation requires precise manipulation of genomic architecture that is trivial in microbes but presents significant hurdles in higher species.

1.4.1 Genomic Complexity and the Challenge of Resistance Engineering

Translating EGI to major crops is immediately complicated by the synergistic challenges of polyploidy and DNA repair mechanisms. Unlike the diploid genomes of *Drosophila* and *S. cerevisiae* (in laboratory haploid/diploid cycling), many economically relevant crop species are polyploid. For example, wheat (*Triticum aestivum*) is hexaploid, possessing three sub-genomes (A, B, and D), while potato (*Solanum tuberosum*) is tetraploid (Heslop-Harrison et al., 2022). This genomic redundancy poses a mathematical challenge for EGI design: to create a viable EGI parent, every single allele of the target promoter, six in wheat, four in potato, must be precisely mutated to the refractory state. Failure to edit even one allele leaves a wild-type binding site available for the PTA, resulting in auto-lethality.

This mathematical challenge is compounded by the plant's inherent DNA repair preferences. To generate the resistance allele, the wild-type promoter sequence must be replaced with the

mutated, refractory sequence. In yeast, this is readily achieved via Homologous Recombination (HDR), which is the dominant DNA repair pathway. However, higher plants preferentially utilize Non-Homologous End Joining (NHEJ) to repair DNA double-strand breaks. NHEJ is an error-prone pathway that typically introduces random insertions or deletions rather than precise edits (Puchta, 2005). Consequently, the rate of precise promoter replacement via HDR in plants is historically low (often <1%) (Voytas, 2013). Thus, engineering EGI either relies upon random mutagenesis and several generations of selfing in higher ploidy plants to homologize a stable resistance allele or attempt a low efficient HDR reaction.

Furthermore, this genomic redundancy often manifests as functional buffering that directly opposes the lethality required for EGI. In *Drosophila*, developmental pathways are often highly canalized; for example, ectopic expression of the morphogen *Pyramus* typically triggers catastrophic embryonic failure (Maselko et al., 2020). In contrast, plants possess extraordinary plasticity, a trait likely evolved to ensure survival as sessile organisms in fluctuating environments (Sultan, 2000). This plasticity is genetically encoded through expansive gene families and negative feedback loops that buffer against transcriptional perturbations.

For instance, the *CLAVATA-WUSCHEL* (CLV-WUS) feedback loop, which maintains the shoot apical meristem, is remarkably robust. While *WUSCHEL* is a potent developmental regulator, its artificial overexpression often triggers compensatory downregulation of related pathways or activates parallel maintenance systems, resulting in somatic abnormalities, such as fasciated stems or ectopic shoots, rather than the binary "death" phenotype required for containment (Somssich et al., 2016; Zinselmeier et al., 2025). Similarly, the auxin signaling pathway is heavily buffered by redundancy in both biosynthesis (*YUCCA* family) and transport (*PIN* family) (Cheng et al., 2006). If an EGI system attempts to disrupt development by overexpressing a

specific auxin response factor, the plant can often re-establish homeostasis by altering auxin transport or sensitivity, converting a potentially lethal signal into a survivable, albeit distinct, morphological phenotype.

Another illustrative example of this resilience is the stress-induced transition to flowering. Plants possess a type of emergency response system where severe physiological stress, such as drought, pathogen attack, or transcriptional disruption, triggers the premature activation of floral integrator genes like *FLOWERING LOCUS T (FT)* and *SUPPRESSOR OF OVEREXPRESSION OF CONSTANS 1 (SOC1)* (Kazan and Lyons, 2016). This phenomenon allows the plant to escape lethal conditions by rapidly producing seeds before death. In the context of EGI, a PTA designed to cause vegetative lethality might inadvertently trigger this stress response. Instead of resulting in a sterile, necrotic seedling, the hybrid might exhibit a stress flowering phenotype, producing a miniature, fertile plant that successfully disperses transgenic seeds.

1.4.2 Physiological Autonomy and Structural Resilience

Beyond genomic buffering, the fundamental cellular physiology of plants presents a physical barrier to the efficacy of cytotoxic EGI effectors. In animal systems, cell death is often structurally catastrophic; the lysis of the plasma membrane leads to immediate tissue collapse, organ failure, or septic shock. Plants, however, are encased in a rigid cellulosic cell wall matrix. This allows plant tissues to maintain structural integrity and even mechanical function after the protoplast has died. This structural autonomy implies that cell death in plants is often a less binary event than in animals.

This is highlighted by the fact that plants have evolved to utilize targeted cell death as a developmental necessity rather than a pathology. The maturation of xylem vessels involves the

programmed autolysis of tracheary elements to create hollow, functional water-transport tubes (Bollhöner et al., 2012). Similarly, the hypersensitive response to pathogens relies on the rapid, localized necrosis of tissue to starve invaders. This strategy is made possible by the plant's unique ability to strictly compartmentalize damage. Through the rapid closure of plasmodesmata and the deposition of callose barriers, plants can physically isolate necrotic lesions from healthy tissue, effectively sacrificing a limb to save the body (Greenberg and Yao, 2004).

The inherent compartmentalization of plant tissues, paired with cellular totipotency, presents a significant challenge to the efficacy of EGI-mediated containment. Unlike animal systems where differentiation is typically terminal, somatic plant cells retain a high degree of developmental plasticity, allowing them to dedifferentiate and regenerate entire organs (Su et al., 2021; Sugimoto et al., 2011).

If an EGI effector induces widespread necrosis but fails to reach absolute cellular lethality, potentially due to mosaic expression or localized gene silencing, residual viable cells can utilize the existing tissue structure to initiate recovery. A single surviving meristematic niche, or even a small cluster of pluripotent parenchyma cells, is capable of re-initiating growth and restoring the organism from a severely damaged state. Consequently, for EGI to be successful in plants, it must overcome not only the plant’s immediate viability but also its robust capacity for regeneration.

1.4.3 Epigenetic Vigilance and Transgene Instability

A final, and often underestimated, barrier to EGI in plants is the genome's aggressive epigenetic immune system. While model eukaryotes like *S. cerevisiae* lack RNAi pathways (Drinnenberg et al., 2009), and *Drosophila* possesses manageable small-RNA regulatory networks (Ghildiyal and

Zamore, 2009), plants have evolved the RNA-directed DNA Methylation (RdDM) pathway as a potent defense against invasive genetic elements (Matzke and Mosher, 2014). This pathway specifically targets repetitive, highly expressed, or foreign DNA sequences, signatures that are inherent to synthetic biology constructs.

The EGI architecture necessitates the use of large, complex transgenes, including dCas9 fusions, viral trans-activation domains (e.g., VPR, VP64, Dreb2), and multiple repetitive sgRNA expression cassettes. These features can easily be recognized by the RdDM machinery. Once recognized, the transgene is targeted for de novo cytosine methylation, leading to transcriptional gene silencing that is both stable and heritable. This creates a scenario of trans-generational erosion, where an EGI line may demonstrate perfect lethality in the T1 generation, only to have the lethal effector silenced in the T2 or T3 generation without any changes to the underlying DNA sequence (Huang and Jin, 2022; Mathieu et al., 2007)

This vulnerability is exacerbated by the mechanism of plant transformation itself. The standard method for delivering these constructs is *Agrobacterium*-mediated transformation, which results in the semi-random integration of the T-DNA into the host genome. This introduces a position effect variable: if the EGI construct integrates into a region of highly condensed heterochromatin or a transcriptionally repressed locus, the lethal effector may be silenced immediately or fail to reach the expression threshold required for lethality (Gelvin, 2017). Unlike site-specific integration in yeast, where chromatin context is controlled, plant engineers must screen upwards of hundreds of independent events to find a locus that is both transcriptionally active and epigenetically stable.

1.4.4 The Design-Build-Test Cycle

The rate of iteration in plant synthetic biology is severely constrained by the extended timescales inherent to plant growth and the technical bottlenecks of transformation. A complete design-build-test cycle in yeast can be executed in less than a week (Botstein et al., 1997). In *Arabidopsis thaliana*, the fastest plant model, the cycle takes 2-3 months (Koornneef and Meinke, 2010). However, for major crop species, this timeline expands to years. This temporal constraint is exacerbated by the multi-component nature of EGI. Establishing a stable EGI line requires more than a simple transgenic insertion; it necessitates the homogenization of complex genotypes. An EGI parent must be homozygous for the lethal effector transgene and, crucially, homozygous for the refractory promoter mutations across all alleles. Achieving this state often requires multiple generations of selfing and segregation to fix the desired edits while removing any CRISPR machinery used to generate them.

Furthermore, the physical delivery of these genetic components remains a primary bottleneck. While *Arabidopsis* benefits from the robust floral dip method (Clough and Bent, 1998), the majority of crop species are recalcitrant to transformation and lack standardized, high-efficiency protocols (Anjanappa and Gruissem, 2021). Transformation pipelines for species like maize, wheat, or soybean typically rely on laborious tissue culture procedures to regenerate whole plants from single transformed cells. These protocols are often genotype-specific, meaning a method optimized for a laboratory cultivar like 'Nipponbare' rice may fail completely in a commercially relevant variety (Matsumoto et al., 2016). This biological friction converts the "Build" phase of the cycle into a multi-month or multi-year endeavor, severely limiting the researcher's ability to empirically optimize PTA expression levels or screen large libraries of promoter mutations in a relevant agronomic context.

1.5 Conclusion

It is crucial to recognize that the barriers described above, genomic complexity, physiological resilience, and epigenetic surveillance, are not specific defects of the EGI architecture, but rather fundamental properties of the plant kingdom that challenge all synthetic biology endeavors. Any sophisticated biocontainment strategy operating in the complex genomic environment of a crop species must contend with these same limitations. For instance, GURT and apomixis are equally susceptible to RdDM-mediated silencing and working in a polyploid crop like wheat would require the homogenization of six alleles across three genomes, facing a similar editing probability cliff as EGI.

Thus, while the hurdles to achieving EGI in plants are significant, they are not unique. The distinction, and the imperative for pursuing EGI, lies in the unique outcome it offers. Unlike containment strategies that rely on fragility (sterility) or physical isolation, EGI constructs a bidirectional containment that mimics natural speciation events, enforcing reproductive isolation through the active elimination of hybrid offspring rather than the passive failure of fertilization. This mechanism offers three benefits: it strictly prevents the escape of transgenes into wild populations (biocontainment), protects the crop from pollination by wild relatives (cultivar purity), and critically, maintains full fertility within the engineered population. This capacity to combine absolute genetic isolation with normal agronomic performance and seed viability represents the gold standard for next-generation biotechnology, transforming biocontainment from a regulatory burden into an intrinsic trait that secures both ecological safety and germplasm integrity.

1.6 Dissertation Overview

This dissertation seeks to address some of the biological hurdles described above by systematically developing and testing EGI components across a spectrum of plant complexity. The research presented herein moves from model systems to agronomic crops, investigating the feasibility of synthetic speciation in increasingly complex genomic and physiological contexts.

Chapter 2 focuses on the model organism *Arabidopsis thaliana* as a proving ground for EGI design. This chapter details the testing of unique genetic constructs and Programmable Transcriptional Activators (PTAs) to identify optimal lethal effectors that can overcome the robust buffering capacity of plant developmental networks.

Chapter 3 translates these findings to *Thlaspi arvense* (pennycress), an emerging oilseed crop. This chapter tests the validity of transferring EGI components from the *Arabidopsis* model to a closely related agronomic species, evaluating whether the genetic logic of incompatibility holds true in a crop environment and assessing the efficacy different ways to test the EGI components.

Chapter 4 tackles the challenge of transformation recalcitrance in *Lolium perenne* (perennial ryegrass), a monocot species with significant economic importance but limited genomic tools. This chapter focuses on expanding and optimizing transformation methods to facilitate the future incorporation of EGI, laying the groundwork for synthetic speciation in the ecologically critical grass family.

1.7 Tables

Strategy	Mechanism of Action	Primary Containment Failure Mode
Physical Isolation	Spatial separation (Buffer zones)	Extreme weather; Anthropogenic error; Pollen viability duration.
Cytoplasmic Male Sterility (CMS)	Mitochondrial dysfunction prevents pollen formation	Does not stop seed dispersal; Environmental restoration of fertility.
Transplastomics	Chloroplast engineering (Maternal inheritance)	Paternal leakage (low freq); Does not stop seed dispersal; Technical difficulty in monocots.
Cleistogamy	Pollination occurs within closed flowers	"Open flower" leakage under stress; Not applicable to all crop architectures.
Apomixis	Asexual seed production (Clonal)	Pollen flow to wild relatives (if not male sterile); Risk of "apomixis gene" escape.
GURTs (Terminator)	Embryonic lethality in F2 seeds	Gene silencing of the lethal construct; Social/Regulatory rejection.

Table 1. Summary of biocontainment strategies

Chapter 2 – Progress Towards EGI in Arabidopsis Thaliana

Chapter Summary

The containment of transgenes within genetically modified crops is a pivotal challenge in agricultural biotechnology. Engineered Genetic Incompatibility (EGI) offers a solution by establishing species-like reproductive barriers; however, the initial implementation in *Arabidopsis thaliana* targeting the *WUSCHEL* (*WUS*) promoter failed to guarantee complete lethality in hybrid progeny. This study focuses on optimizing the EGI system to eliminate survivors through four primary strategies: multiplexing sgRNAs to increase transcriptional output, introducing introns into dCas9 for enhanced expression, evaluating alternative promoters (*RPS5a*, *Rpl23*, and *GmGlycinin*), and shifting the lethal target from the developmental regulator *WUS* to the metabolic gene *ELO1*. Results demonstrate that targeting the metabolic pathway via *ELO1* yields superior lethality compared to *WUS* overexpression. While seed-specific activation proved insufficient, the integration of intron-mediated enhancement with the *Rpl23* promoter achieved the highest containment efficacy, resulting in 93% lethality in hybrid lines. Molecular analysis of surviving "escapers" revealed a lack of target overexpression correlated with the downregulation of the engineered activation machinery. These findings represent a significant refinement of the EGI mechanism, though further optimization is required to achieve the absolute lethality necessary for commercial biocontainment.

2.1 Introduction

The containment of transgenes within genetically modified crops remains a pivotal challenge in agricultural biotechnology. Potential for gene flow between genetically modified crops and their wild or weedy relatives poses significant regulatory and ecological hurdles (Clark and Maselko, 2020). Engineered Genetic Incompatibility (EGI) offers a synthetic biology solution to this problem by establishing species-like reproductive barriers that function independently of physical isolation (Maselko et al., 2020). By coupling a Programmable Transcriptional Activator (PTA) with a target gene essential for development, EGI ensures that any hybridization event between the engineered crop and a wild relative results in lethal overexpression of the target gene, effectively culling the hybrid progeny.

The preceding work described by Zinselmeier et al., (2025), established the first functional EGI system in a model plant species, *Arabidopsis thaliana*. That study utilized a CRISPR-based activation system known as MoonTag (Casas-Mollano et al., 2023) to target the endogenous *WUSCHEL* (*WUS*) promoter. The results demonstrated the molecular validity of the EGI mechanism where the engineered strains harboring promoter mutations were immune to the PTA, while hybrid offspring possessing a wild-type promoter from the non-engineered parent suffered from ectopic gene activation. However, while the initial prototype validated the genetic circuit, it revealed a critical limitation in efficacy. Although *WUS* expression was upregulated approximately 500-fold in hybrid lines, this level of overexpression proved insufficient to guarantee complete lethality, quantified as the inability to germinate or grow past the seedling stage. Phenotypic penetrance was variable, and while many hybrids exhibited severe

developmental arrest or necrosis at the seedling stage, a subset of plants survived when transferred to soil. These survivors displayed only delayed growth and morphological defects rather than total inviability.

For EGI to serve as a viable biocontainment strategy for commercial agriculture, the system must achieve absolute lethality to prevent the introgression of transgenes into wild populations. The survival of hybrid progeny in the initial *WUS* system highlights a threshold problem in the current design. The transition from deleterious to lethal requires a more potent disruption of plant development than was achieved by the single-sgRNA targeting of *WUS*. Several factors may contribute to this incomplete penetrance, including potential insufficient transcriptional drive where the 500-fold increase does not cross the biological threshold required to trigger immediate cell death. Additionally, plants exhibit remarkable plasticity (Sultan, 2000) which potentially allows some hybrids to recover from early *WUS* overexpression once the initial transcriptional burst subsides or is compensated for by homeostatic mechanisms (Somssich et al., 2016).

Building upon the foundational work of Zinselmeier et al., (2025), this chapter focuses on the optimization of the EGI system to eliminate hybrid survivors and ensure robust biocontainment through four primary strategies. While previous efforts focused on the optimization of the PTA machinery, be it the creation of Moontag (Casas-Mollano et al., 2023) or the systematic testing of different activation domains (Zinselmeier et al., 2024), this work seeks to fine tune the design of the constructs and evaluate new targets.

First, we implement a double guide targeting approach to evaluate whether multiplexing sgRNAs at the *WUS* promoter can synergistically increase transcriptional output (Casas-Mollano et al., 2020). By recruiting multiple MoonTag activation complexes to the same promoter region

simultaneously, we hypothesize that we can force a higher density of transcriptional activators, thereby pushing *WUS* expression beyond the recoverable threshold observed in the single-guide pilot study.

Second, we broaden the scope of lethal targets by introducing *ELO1* (Fatty Acid Elongase 1) as a candidate for overexpression. Unlike *WUS*, which functions as a developmental signaling regulator, *ELO1* is involved in fatty acid elongation, a fundamental metabolic process required for proper cell growth and, largely only within root tips (Klepikova et al., 2016; Qi et al., 2019). We posit that disrupting a metabolic pathway outside of its intended tissue may yield more immediate, cell-autonomous toxicity that is less susceptible to the organism-level recovery mechanisms seen with developmental regulators. Additionally, we have communication with collaborators that have tried to overexpress *ELO1* and saw lethality (Cahoon, personal communication).

Third, we aim to boost the baseline efficacy of the dCas9 chassis itself by introducing introns into the coding sequence of the construct. Intron-mediated enhancement (IME) is a well-documented phenomenon in plant biotechnology where the presence of introns can significantly increase mRNA accumulation and translation efficiency (Shaul, 2017). By engineering introns directly into the dCas9 gene following work previously done in cas9 (Grützner et al., 2021), we aim to overcome potential bottlenecks in protein expression, ensuring that high levels of the programmable activator are available to drive the lethal phenotype in hybrid cells.

Finally, we examine the impact of PTA expression levels and timing by exchanging the promoter driving the activation construct. We will compare the original system against alternative promoters: the stronger constitutive *RPS5a* promoter to drive ubiquitous high-level expression,

the *Rpl23* promoter for strong expression, albeit variable across tissues and development, and the *GmGlycinin* promoter to target activation specifically within the seed. This allows us to determine whether global overexpression is superior, or if restricting lethality to specific, vulnerable developmental windows, such as seed maturation, provides a more effective containment mechanism. By addressing the leakiness of the first-generation system through these multi-layered improvements, this chapter seeks to further refine the EGI mechanism in plants.

2.2 Materials and methods

2.2.1 Plasmid Construction and Genetic Assembly

All genetic constructs utilized in this study were assembled via Golden Gate cloning protocols as reported in Chamness et al., (2023). The foundational Programmable Transcriptional Activator (PTA) system employed the MoonTag-dCas9 architecture as previously described (Zinselmeier et al., 2025). The constitutive *Ubiquitin 10* (*AtUbi10*) promoter driving the dCas9 was replaced with three alternative promoters: *Ribosomal Protein S5A* (*pRPS5a*); *Ribosomal Protein L23* (*pRpl23*); *GmGlycinin* (*pGly*) promoter. Furthermore, to augment translational efficiency, 11 introns were inserted into the dCas9 coding sequence based off of Grützner et al., (2021). Single guide RNAs (sgRNAs) targeting the *AtWUS* and *AtELO1* promoters were designed using CRISPOR (Concordet and Haeussler, 2018). For constructs utilizing double-guide targeting, a polyU6 gRNA architecture was engineered to express two distinct guides. All construct maps are listed in Supplemental Table 1.

2.2.2 Plant Material and Growth Conditions

The *Arabidopsis thaliana* Col-0 accession served as the wild-type background for all genetic transformations and hybridization experiments. Plant stocks were maintained in growth

chambers under a long-day photoperiod regime (16 h light/8 h dark) at a constant temperature of 22°C and 50% relative humidity. For purposes of seedling selection and phenotypic characterization, seeds were surface sterilized with 0.6% NaOCl and 10% Silwett-77 for 10 minutes before being plated on 1/2 Murashige and Skoog (MS) medium supplemented with 1% sucrose and 0.8% agar.

2.2.3 Agrobacterium-mediated Transformation

Binary vectors were introduced into *Agrobacterium tumefaciens* strain GV3101 via heat shock. Transformation of *Arabidopsis* plants was achieved utilizing the floral dip method (Clough and Bent, 1998). Positive transformants in the T1 generation were identified through fluorescence screening for the expression of the red fluorescent protein (RFP) in the seed coat.

2.2.4 Promoter Mutant Screening

T2 non-RFP seeds were planted directly to soil and allowed to grow to seedling stage. DNA was extracted utilizing DNAzol reagent by Thermo Fisher Scientific (Waltham, MA) and its corresponding protocol. PCR was conducted utilizing primers purchased from Integrated DNA Technologies (Newark, NJ) and New England Biolabs (Ipswich, MA) Q5 DNA polymerase master mix. Primers are listed in Supplementary Table 2. PCR product was purified with Qiagen (Germantown, Maryland) PCR clean up kit and NEB Exo-Cip before being sent to ACGT (Wheeling, IL) for Sagner sequencing.

2.2.5 EGI Hybridization Assays

To simulate transgene introgression events and evaluate the efficacy of the biocontainment system, hemizygous T1 engineered plants serving as pollen donors were crossed with wild-type

Col-0 females. This experimental design ensured that resultant RFP+ hybrid progeny inherited the PTA construct paternally while retaining a wild-type, susceptible target promoter maternally. Baseline germination and survival metrics were established through null-segregant (RFP-) × wild-type pairings and self-crossed EGI parent lines.

2.2.6 Phenotypic Analysis and Lethality Scoring

Hybrid seeds were harvested and plated on non-selective 1/2 MS media for observation. Germination rates were quantified as the percentage of seeds exhibiting radicle emergence at 8 days after plating. Individuals categorized as "lethal" if they displayed complete necrosis, developmental arrest prior to the first true leaf stage, or complete lack of germination. Surviving seedlings, designated as "escape," were transplanted to soil and monitored for a duration of four weeks to assess long-term viability and morphological aberrations. Effective containment was rigorously defined as the inability of a hybrid individual to reach reproductive maturity.

2.2.7 RNA Extraction and RT-qPCR

Tissue samples were harvested from 20-day-old hybrid escape seedlings and negative controls. Total RNA was isolated from three separate leaves per plant utilizing NEB RNA extraction kit as instructed. NEB Luna Rt-qPCR one step kit was used on a CFX96 Touch Real-Time PCR Detection System. Transcript abundance was normalized to the internal reference gene *PP2A* and relative expression levels were calculated utilizing the ΔΔCt method against wild-type controls. Primers are listed in Supplementary Table 2.

2.3 Results

2.3.1 Generation of Stable *WUS* and *ELO1* Promoter Mutant Lines

To create the new promoter mutants and EGI lines, a two-step transformation process was utilized (Figure 2.1A). First, we utilized CRISPR-Cas9 mutagenesis to generate specific promoter mutations in *Arabidopsis thaliana* that would confer immunity to the PTA. We transformed wild-type plants for *ELO1* mutants and the original EGI line with the g153 promoter mutant for the *WUS* lines with a construct harboring the Cas9 nuclease and sgRNAs targeting the *WUS* or *ELO1* promoters, coupled with an RFP fluorescent marker. In the T2 generation, we screened for RFP-negative seeds and sequenced the promoters to identify segregants that had lost the Cas9 transgene but retained the desired homozygous promoter mutations.

We validated the specific mutations in our candidate lines via Sanger sequencing (Figure 2.1B). For *WUS*, we recovered alleles retaining the original single nucleotide insertions adjacent to the PAM site, while including new mutations of 2 nucleotides within the sgRNA site. For *ELO1*, we identified alleles with complex indels. These mutations effectively disrupt the sgRNA binding site, ensuring that the engineered parent lines remain unaffected by the constitutive PTA. Following this validation, we performed a second transformation using the MoonTag activation system (dCas9-MoonTag) with two different multi guide arrays. This introduction established the complete EGI circuit, where the PTA is present, but the endogenous target is immune due to the promoter mutation.

While the experimental design for the *ELO1* system initially specified the use of sgRNAs targeting sites 1 and 6 of the promoter, retrospective sequence analysis revealed a mismatch in the transformation vectors. The constructs utilized for plant transformation contained sgRNAs targeting guide site 1 and guide site 2. This misalignment had significant implications for the immunity of the engineered lines. Although the *ELO1* promoter mutants contained protective mutations at site 1 and site 6, the sequence at guide site 2 remained wild type. Consequently, the

engineered plants possessed only partial protection against the PTA: they were immune to transcriptional activation driven by guide 1 but remained susceptible to activation by guide 2.

2.3.2 pGly Crosses Without Introns

Crosses were carried out with the hemizygous EGI lines acting as the father to a Col-0 WT background. As shown in Figure 2.2, germination rates were generally high across parental controls and RFP-negative segregants. Only the line targeting *WUS* site 2 showed a lack of parental germination, but this was observed across all stages of line development after the promoter mutant was made (Supplementary Figure 2.1). This parental lethality was saved in the offspring, with both RFP- and RFP+ seeds fully germinating. Lines targeting *WUS* site 4 exhibited 100% germination in all groups, regardless of transgene presence (n = 100 and 27 for RFP+ progeny), indicating no deleterious effect of the PTA overexpression or promoter mutation at this locus.

In contrast, lines targeting *ELO1* demonstrated a genotype-dependent lethality. Parental controls and RFP- segregants in lines L1 and L3 maintained 100% germination, RFP+ individuals showed markedly reduced rates. Specifically, L1 RFP+ seeds germinated at a rate of 31% (n = 16), and L3 RFP+ seeds at 57% (n = 7). Line gly-elo-L2 yielded insufficient seed numbers for robust comparison (n= 0 RFP- and n = 2 RFP+), though the few recovered transgenic seeds did germinate. These data suggest that the PTA can overexpress *ELO1* to a point achieving similar rates of lethality as that previously observed, but still not complete lethality.

2.3.3 Variable Promoter and Intron dCas9 Crosses

Germination assays were conducted to evaluate the viability of intron-containing transgenic lines targeting *WUS* and *ELO1*. As observed in Figure 2.3, lines targeting *WUS* site 4 (gly-L1 and

Rps5a-L1) displayed high viability across all genotypes. Parental controls and RFP- segregants achieved 100% germination, while RFP+ segregants maintained rates of 100% (n = 43) and 98% (n = 51), respectively, suggesting no lethality associated with these targets.

In contrast, lines targeting *WUS* site 2 exhibited genotype-specific reductions in germination. For the *WUS* site 2 target, while RFP- segregants in both lines achieved 100% germination, the RFP+ progeny of Rpl23-L1 showed a marked reduction of 12% (50%, n = 16) compared to a parental baseline of 62% (n = 12). However, much of this can likely be attributed to the reduced fitness of the parental promoter mutant, and indeed in L2 we see a rescuing of the phenotype observed by the parental line.

The most severe phenotypic effects were observed in the *ELO1* lines. Although parental lines displayed variable germination (38%–58%), RFP- segregants recovered to 100% viability in both lines. The presence of PTA and WT binding sites correlated with significant lethality. Specifically, RFP+ seeds from Rpl23-L1 germinated at 52% (n = 40), while Rpl23-L2 showed a drastic reduction to 7% (n = 44), confirming a deleterious effect linked to the transgenic state at this locus.

2.3.4 *ELO1* Escapes Mechanism

To investigate the mechanism of survival in the high-lethality *ELO1* Rpl23-L2 line (which exhibited only 7% viability), we performed RT-qPCR analysis on the three surviving transgenic plants (designated 1, 2, and 3). As shown in Figure 2.4, transcript analysis of the target gene, *ELO1*, revealed no significant reduction in expression among the survivors. *EOL1* transcript levels in plants 1, 2, and 3 were statistically indistinguishable from the parental control (all distinct significance group 'a'), clustering near the normalized baseline (1.0). This suggests that

survival in these individuals was contingent on the maintenance of wild-type *ELO1* expression levels.

Analysis of the transgene components quantified the expression levels of the CRISPR machinery in these survivors. Transcript levels of *dCas9* were significantly lower in all three surviving plants compared to the parental line. Expression profiles for *gRNA* were variable: plants 1 and 2 exhibited significantly reduced *gRNA* levels relative to the parent while plant 3 expressed *gRNA* at levels statistically comparable to the parent, despite the concurrent reduction in *dCas9* expression observed in the same individual.

2.4 Discussion

2.4.1 Target Selection: Metabolic Disruption vs. Developmental Reprogramming

A critical finding of this work is the superior efficacy of targeting the metabolic gene *ELO1* over the developmental regulator *WUS*. Despite the multiplexing of sgRNAs (Double Guide strategy) intended to boost transcriptional output at the *WUS* promoter, lines targeting *WUS* consistently yielded high survivor rates. This was a surprising finding considering that guide 153, the guide utilized in previous efforts (Zinselmeier et al., 2025), was also in each construct targeting WUS. The lack of lethality can potentially be attributed to the inability of the *GmGlycinin* promoter to cause enough transcriptional load to cause lethality, as we saw only a delayed germination phenotype and nothing else (Figure 2.2). This argument is challenged by other results because the Rps5a promoter, which is known to be a very strong constitutive promoter, also lacked any phenotype (Figure 2.3). This could potentially be answered by positional effects of the transgene insertion within the line (Matzke and Matzke, 1998), or the remarkable plasticity that allows plants to buffer or recover from the developmental perturbations caused by ectopic *WUS*

expression (Sultan, 2000). Further replicates and phenotyping will have to be done to discover the true reasoning behind the loss of lethality.

In contrast, the overexpression of *ELO1*, which catalyzes the elongation of very-long-chain fatty acids in root tips (Qi et al., 2019), likely imposes a direct metabolic burden or cytotoxicity that is less easily compensated for by the plant. This was observed across all *ELO1* targeting lines and indeed did yield the greatest lethality observed with only 7% of hybrids surviving. The shift from developmental signaling to metabolic disruption appears to be a more robust strategy for ensuring cell-autonomous lethality.

2.4.2 Synergy of Introns and Spatiotemporal Control

Interestingly, the seed-specific *Glycinin* (*pGly*) promoter failed to induce significant lethality, even with *ELO1* as the target. This indicates that confining overexpression to the embryo maturation phase allows the plant to survive once it transitions to germination, or that the transcriptional burst provided by *pGly* is insufficient to trigger irreversible damage. However, other phenotypes could be observed dependent upon the target gene, such as sterility of developing seeds, but this is contradicted by the fact that no plants showcased sterility in our experiment (supplemental Figure 2.2). The incorporation of introns into the dCas9 coding sequence was implemented to overcome potential limitations in effector protein accumulation via Intron-Mediated Enhancement (IME). When coupled with the division-specific *Rpl23* promoter, this chassis delivered the most potent lethal phenotype observed. The success of the *Rpl23* promoter suggests that having variable but high expression across plant development could lead to the best lethality while also escaping recognition for silencing.

2.4.3 Implications of Partial Protection in *ELO1* Lines

The unintended mismatch between the sgRNAs used for transformation (guides 1 and 2) and the protective mutations in the *ELO1* parent lines (sites 1 and 6) created a unique experimental condition of partial protection. The mistake caused by human error made the engineered parents be immune to activation by guide 1 but remained genetically susceptible to guide 2. The fact that these parent lines remained viable implies that the transcriptional drive provided by a single guide (guide 2) was sub-lethal in the parental background, or that the parent plants were under constant, albeit survivable, metabolic stress. This result is also highlighted in the fact that the no intron *GmGlycinin* parental lines were unaffected, but the intron and Rpl23 promoter constructs saw a marked decrease in germination, likely an effect of increased overexpression. However, in the hybrid context, where both guides target the wild-type allele inherited from the pollen recipient, the combined activity of guide 1 and guide 2 was sufficient to cross the lethality threshold in all lines. This serendipitous finding underscores the dose-dependent nature of EGI lethality: a single guide may be tolerated, but multiplexed activation reduces viability.

2.4.4 Mechanism of Survival and Future Directions

Despite the high mortality rate in the best-performing line (*Rpl23-L2*), a small fraction of hybrids (7%) survived. Our RT-qPCR analysis of the 3 escapes shows that they are not overexpressing *ELO1*. This is correlated with significant downregulation of the *dCas9* transgene or the sgRNAs, however it is unknown if this is caused by a silencing mechanism or is a remanent of the parental line potentially being homozygous for the PTA. While PTA and guide silencing is a possible explanation, silencing of *ELO1* itself is also possible. Unlike *WUS*, *ELO1* is not a necessary gene for the plant, and indeed knock-out mutants of *ELO1* in Arabidopsis have already been created and characterized (Falcone et al., 2007). Our plants do possibly show reduced fitness in terms of natural growth, but further replication will have to be done to confirm this result.

2.5 Conclusion

The optimization of the Engineered Genetic Incompatibility (EGI) system is a prerequisite for its deployment as a biocontainment tool in agricultural settings. While our initial proof-of-concept utilizing the *WUS* promoter demonstrated the mechanistic validity of the system, it failed to achieve the absolute lethality required to prevent gene flow. In this study, we systematically addressed the limitations of the first-generation system by manipulating target selection, transcriptional efficacy, and spatiotemporal expression. Our results identify a specific combination of genetic components, the *Rpl23*-driven, intron-enhanced activation of *ELO1*, that significantly improves containment efficacy, achieving up to 93% lethality in hybrid progeny.

While this showcases a marked increase in comparison to previous efforts, much work is still needed to achieve the desired EGI phenotype. While 93% lethality is high, a biocontainment context requires a stringent 100%. Additionally, the parental lines showing a phenotype inhibit the use of EGI. This phenotype likely arose from the susceptibility to guide 2 within the lines and would be fixed with either introducing guide 6 and removal of guide 2 from the design, as originally intended, or creation of a promoter mutant at site 2. Finally, the lack of *ELO1* overexpression in the escapee lines and parental lines harboring a susceptible Site 2 suggest potential silencing of *ELO1.* More extensive phenotyping, potentially looking at methylation of *ELO1,* will need to be done to confirm the reasoning behind this lack of overexpression and the mode of escape.

2.6 Figures

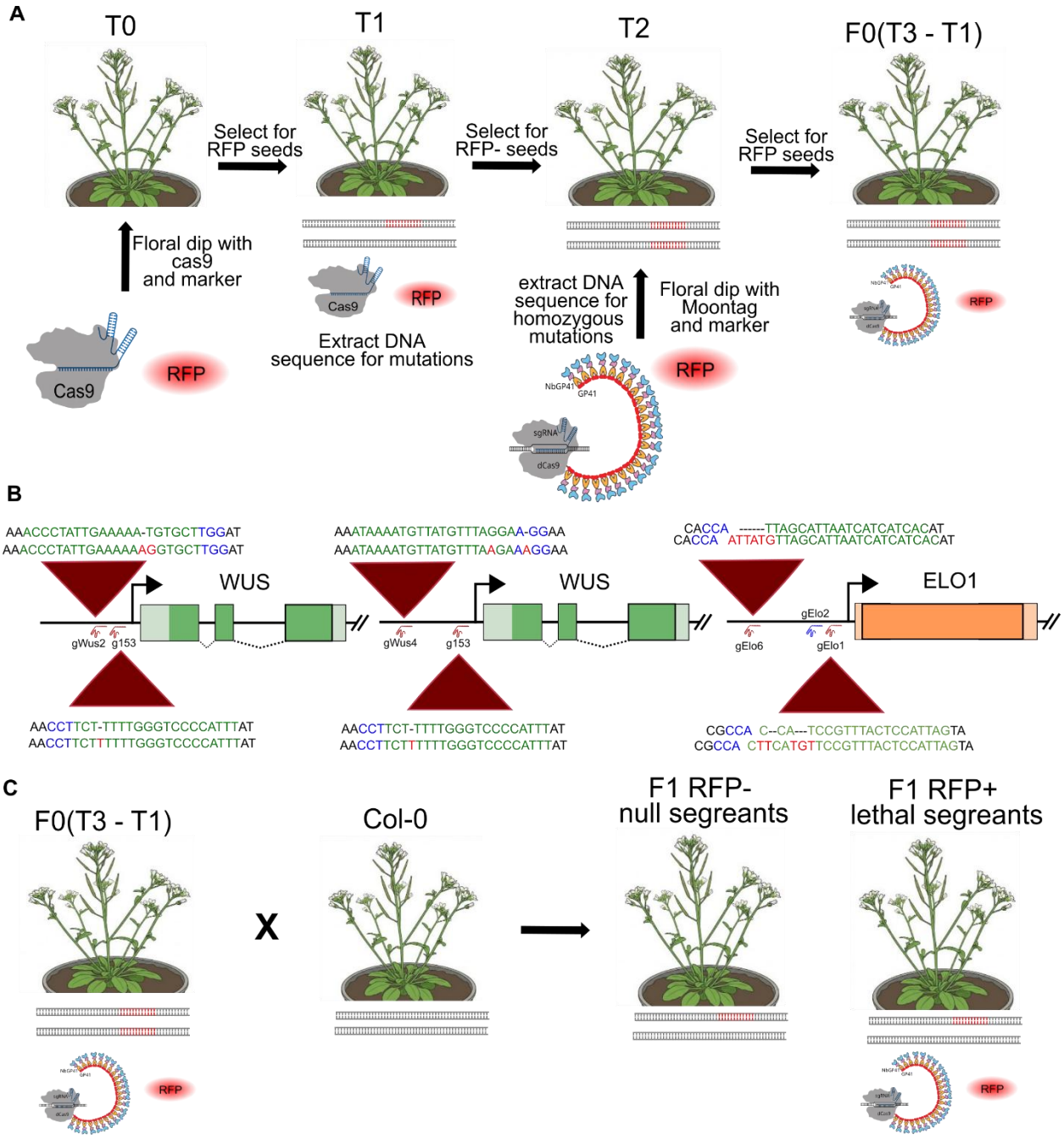

Figure 2.1. Workflow for the generation of EGI lines and characterization of promoter mutants. (A) Schematic overview of the transformation workflow utilized to generate Engineered Genetic Incompatibility (EGI) plants. (B) Validation of the generated promoter mutants. Schematic representation of the *WUSCHEL* (*WUS*) and *ELONGATA 1* (*ELO1*) gene structures showing the sgRNA target sites. Sequence alignments display the specific mutations

(red) generated at the target loci in the engineered lines. WT sequence is always above the mutated sequence. Green is the sgRNA binding site while blue is the PAM site. (C) Experimental design of crossing experiments. The hemizygous EGI parent line crossed to Col-0 WT will create two types of seeds, an RFP- null segreant not containing the PTA, and an RFP+ segreant containing both the PTA and a viable promoter sequence.

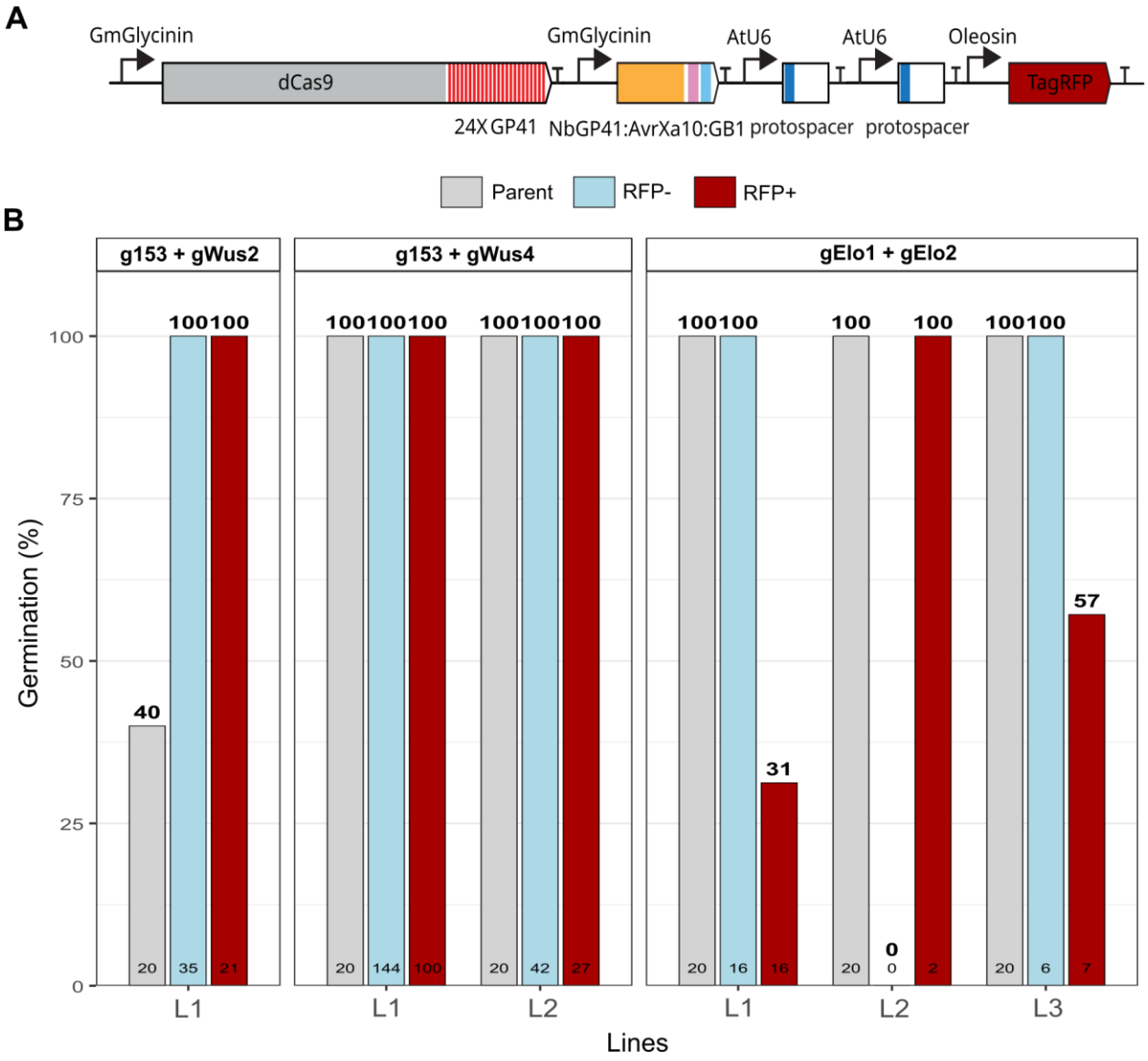

Figure 2.2. Germination viability of *pGly*-driven EGI lines. Germination rates of F1 segregating populations expressing the MoonTag activator under the control of the seed-specific *Glycinin* (*pGly*) promoter. Germination percentage (y-axis) was scored 8 days after plaiting for lines targeting *WUSCHEL* and *ELO1*. Data is shown for Parental controls (EGI self cross RFP+), non-transgenic segregants (RFP-), and transgenic segregants (RFP+). Sample sizes (n) for each

genotype are indicated at the bottom of each corresponding bar. L(number) refers to a unique line resulting from a unique transformation event for the given construct.

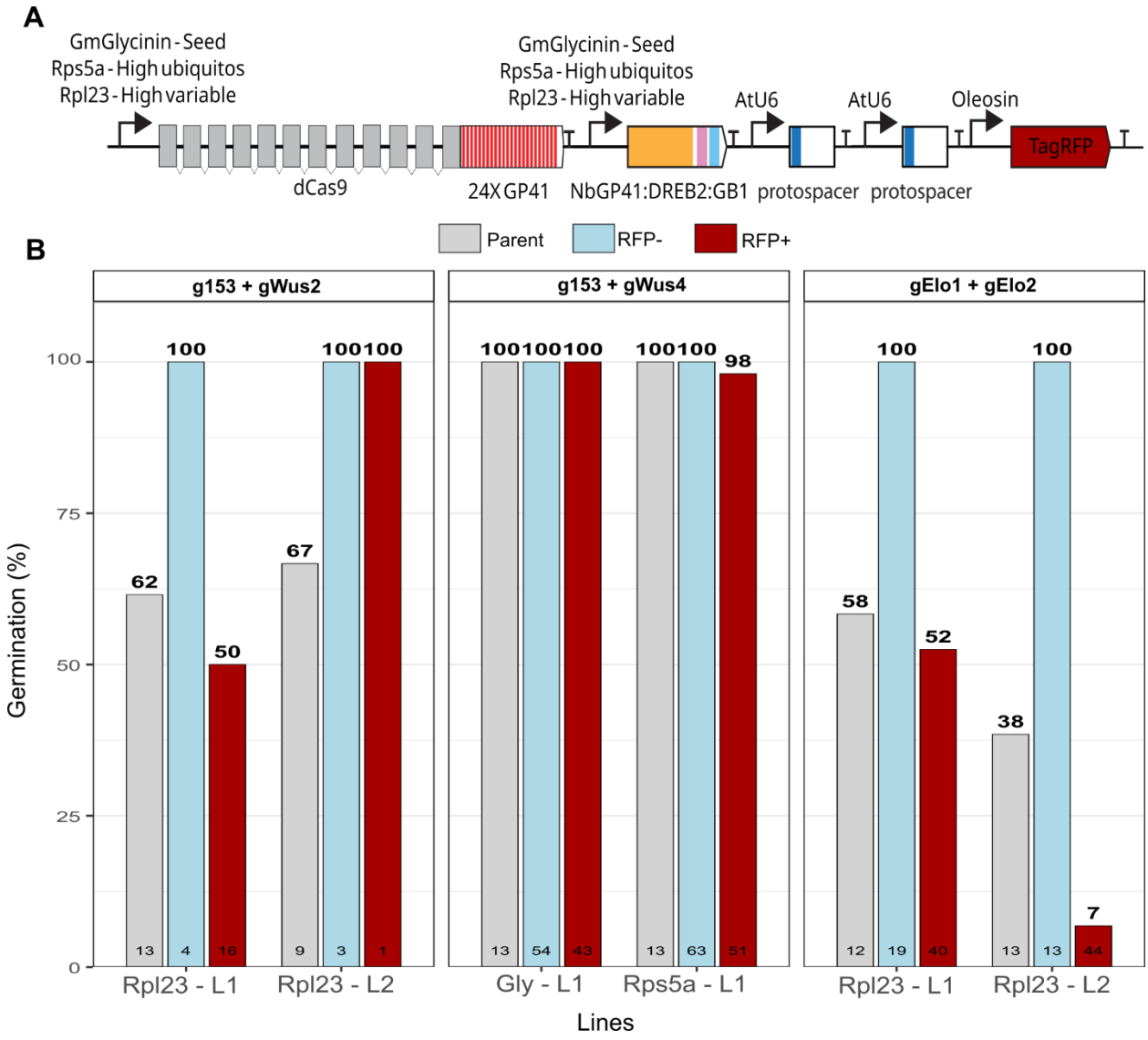

Figure 2.3. Strategies for enhancing transcriptional activation and germination outcomes. (A) Schematic illustration of the optimized PTA constructs. To enhance expression levels, the dCas9 coding sequence was engineered to contain 11 introns. Additionally, the activation complex was placed under the control of three distinct promoters to vary spatiotemporal expression: *pGly* (seed-specific), *pRPS5a* (high ubiquitous), and *pRpl23* (high variable). (B) Germination viability of F1 populations expressing these intron-containing variants. Bar graphs display germination rates for lines targeting *WUS* and *ELO1*. Data is categorized by genotype: Parental (EGI self cross), RFP- (non-transgenic segregants), and RFP+ (transgenic segregants). Sample sizes (n) are indicated at bottom of each bar. L(number) refers to a unique line resulting from a unique transformation event for the given construct.

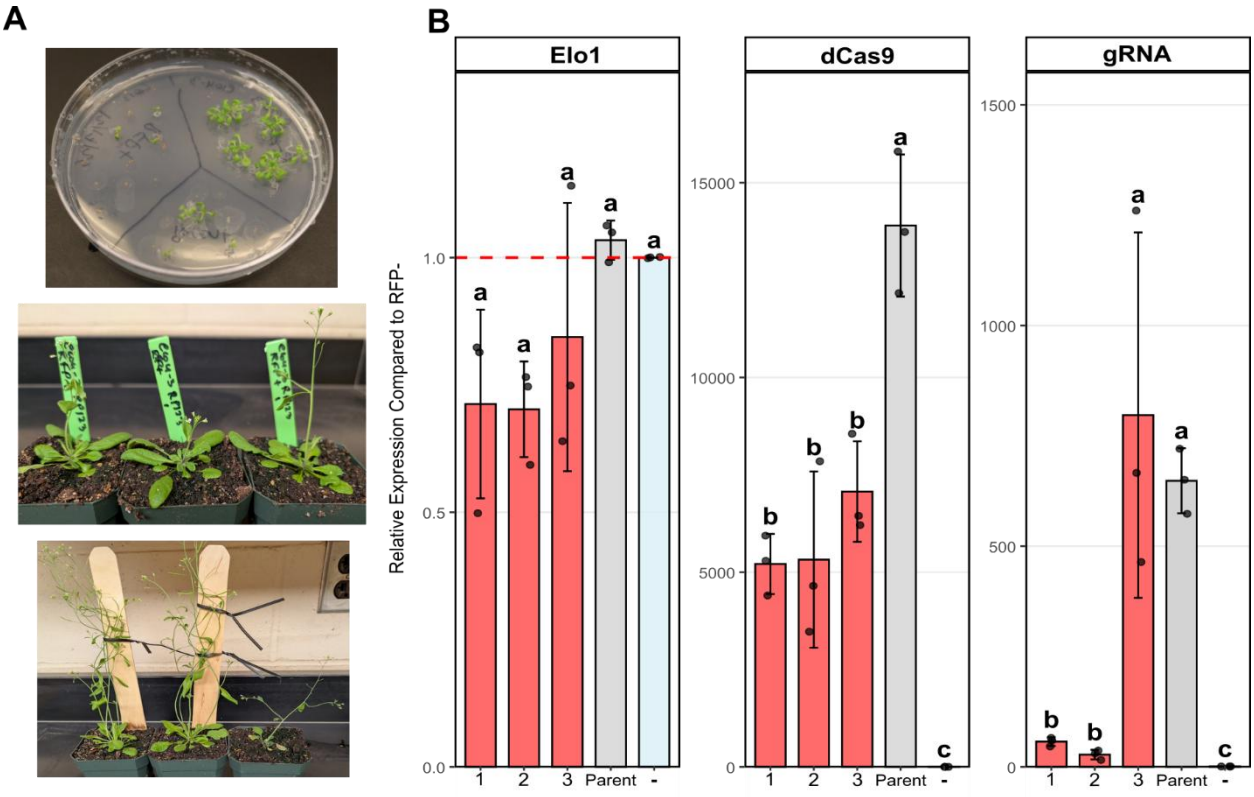

Figure 2.4. Phenotypic and molecular characterization of *Rpl23-elo* survivors. (A) Phenotypic screening of *ELO1 Rpl23-L2* progeny. Images display the crossed population on non-selective media (top), followed by the morphology of the three surviving hybrid seedlings (from left to right, surviving plants 1, 2, and 3) after transfer to soil. Representative non-transgenic segregants (RFP-) and a parental control plant are shown for comparison, illustrating the delayed growth but viable morphology of the escapers. (B) RT-qPCR analysis of gene expression in three individual survivors and controls. Relative transcript abundance of *ELO1* (target), *dCas9* (activator), and *gRNA* was normalized to *PP2A*. Statistical significance was determined using a one-way ANOVA followed by a Tukey's HSD post-hoc test; different letters indicate significant differences between groups ($p < 0.05$

2.7 Supplemental Figures

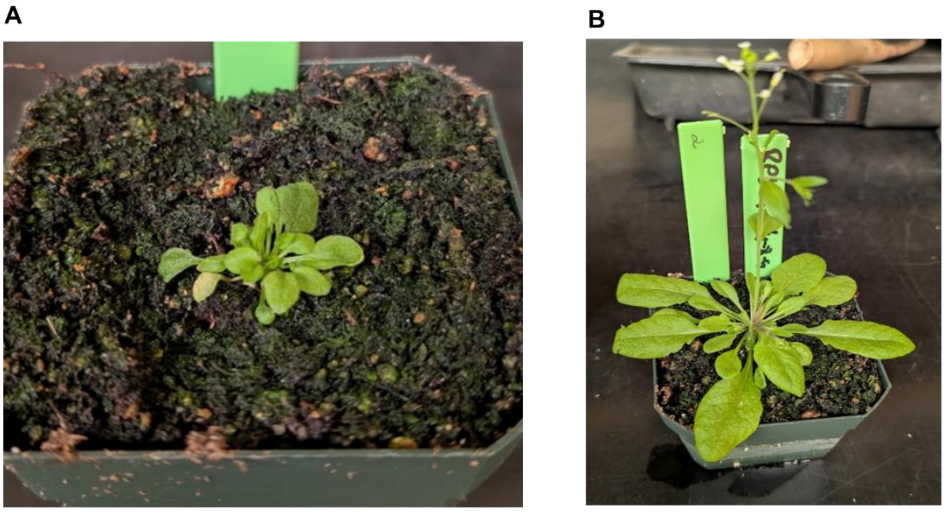

Supplemental Figure 2.1. Comparison of *WUS* site 2 promoter mutant vs same age *WUS* site 4 promoter mutant.

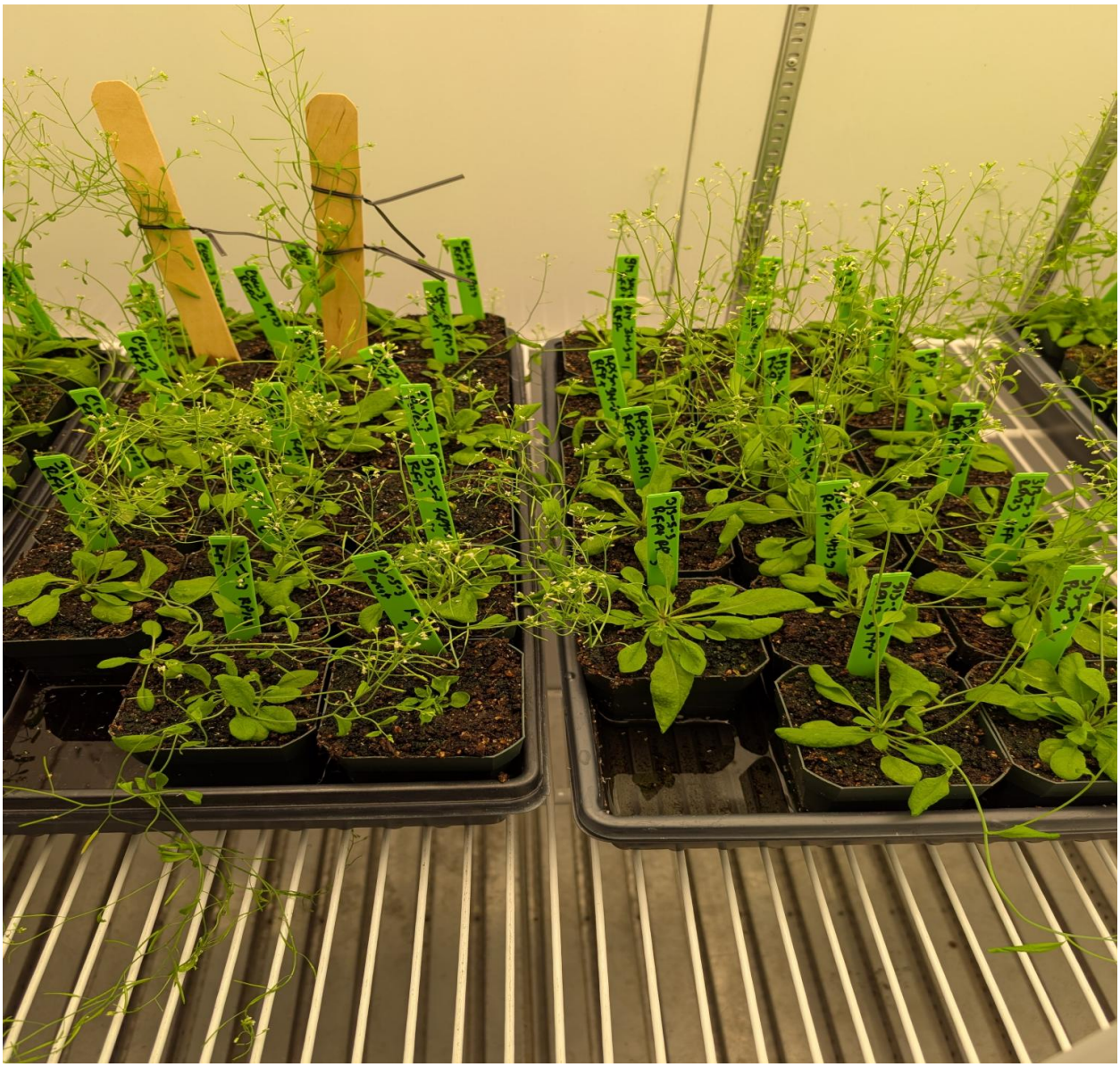

Supplemental Figure 2.2. Photo showcasing normal growth of hybrid plants.

2.8 Supplementary Tables

Plasmid Name	Function	Benchling Link
pACM313	Create promoter mutant in WUS site 2	https://benchling.com/s/seq-PBRJRZ2tfpWq5LjZnB3e?m=slm-TrzIaxMoBp7kMUEq4S1c
pACM314	Create promoter mutant in WUS site 4	https://benchling.com/s/seq-wc4VP2zNzOnZ5gPmsbhL?m=slm-3xxPoBgyQXktIoCFcl0I

pACM315	Create promoter mutant in ELO1 site 1 and site 6	https://benchling.com/s/seq-New9jlHYIqS9Jm9dPfF4?m=slm-VYURnnYjOi41BnA02eJm
gly:Moontag Elo1 lvl2	No intron gly promoter Moontag construct with ELO1 guides 1 and 2	https://benchling.com/s/seq-YArjHIEvAHWRZq1NKtho?m=slm-RyUwlBWiKk7fmGSAt2tp
gly:Moontag wus2 lvl2	No intron gly promoter Moontag construct with WUS guides 153 and 2	https://benchling.com/s/seq-eR62gHPlTLnTbujGXlga?m=slm-fnWecK0QQKzhwTxlua8o
gly:Moontag wus4 lvl2	No intron gly promoter Moontag construct with WUS guides 153 and 4	https://benchling.com/s/seq-9OAJwMUsQLd3OfFlK0ma?m=slm-rkOuEJIGGWczh1a1KoB9
gly:zMoontag wus4 lvl2	Intron gly promoter Moontag construct with WUS guides 153 and 4	https://benchling.com/s/seq-0Q3E8uEZ4ZoIMlVQPRuy?m=slm-VrODrdicFzA477kxytxu
Rps5a:zMoontag wus4 lvl2	Intron Rps5a promoter Moontag construct with WUS guides 153 and 4	https://benchling.com/s/seq-AKhiXJlUj2NKkiGfCzm3?m=slm-hFiuZkN3PyJ3baPC3DSC
Rpl23:zMoontag Elo1 lvl2	Intron Rpl23 promoter Moontag construct with ELO1 guides 1 and 2	https://benchling.com/s/seq-3Eu2lPckL3FJ9v6Yhv4w?m=slm-wA6xBIsik3UE5PGjga2B
Rpl23:zMoontag wus2 lvl2	Intron Rpl23 promoter Moontag construct with WUS guides 153 and 2	https://benchling.com/s/seq-CdoChHzfDRih3bwC5Rwz?m=slm-106RmXqeYBHqzEfgVs6u

Supplementary Table 2.1. List of TDNAs used to transform Arabidopsis.

Primer Name	Sequence
AC-AtWUS-PF1	CTAACTTCTCTGTCCCTTTCAATCC
AC-AtWUS-PR1	CGCTTTCTTGGTCGGCTTGAT
AC-AtWUS-SPR1	GCTCCATGTGTGTTTGATTCGAC
AC-AtELO1-PF1	GTGTGTTAGATGACAAGGCCTAGGAG
AC-AtELO1-PR1	CAAAGAAAACGGTGGAGCCTAGTG
AC-AtELO1-SPR1	GTGGTGGACGAGCCAGTAGGTTAG
AC-AtPP2A-QPF1	TAACGTGGCCAAAATGATGC
AC-AtPP2A-QPR1	GTTCTCCACAACCGCTTGGT
oCORS147_AtElo1_RTqPCRF	CCACGCAACGGTTGTGATTT
oCORS147_AtElo1_RTqPCRR	AACACGAGCCCAACAGGAAA
qSF015_gRNAqF	CTGGAAACAGCATAGCAAGTTGAAA
qSF016_gRNAqR	CTGGAAACAGCATAGCAAGTTGAAA
qSF045_zdCasqF	GTCAGACGCTATCTTGCTCAGT
qSF046_zdCasqR	GATGCTCGTCGTACCTCTTGAT

Supplementary Table 2.2. List of Primers used in the study.

Chapter 3 – Translating EGI From Model to Agronomic Crop

Chapter Summary

Field pennycress (*Thlaspi arvense* L.) is emerging as a sustainable winter annual oilseed capable of providing ecosystem services without displacing food production; however, its mass deployment requires robust biocontainment mechanisms, such as Engineered Genetic Incompatibility (EGI), to prevent gene flow to wild relatives. This study evaluates the translation of the MoonTag-dCas9 Programmable Transcriptional Activator (PTA) system from the model species *Arabidopsis thaliana* to an agronomic context. To validate the system, a multi-tiered strategy was employed via transient protoplast transformation, Tobacco Rattle Virus (TRV) delivery, and sexual hybridization of stable transgenic lines for target genes *WUSCHEL* (*WUS*), *TPXL6*, and *ELO1* promoters. While protoplast assays successfully demonstrated transformation viability, they exhibited extreme variability that prevented reliable quantification of endogenous gene activation. Similarly, TRV vectors achieved systemic infection but failed to consistently drive lethal overexpression of target genes. Definitive validation through stable hybridization revealed a critical translational bottleneck: unexpected toxicity in the T2 parental lines carrying guide RNAs, which violates the EGI requirement for phenotypically normal parents. These findings highlight the physiological constraints of transferring synthetic circuits from model organisms to crops and underscore the necessity for optimized component testing.

3.1 Introduction

3.1.1 Field Pennycress (*Thlaspi arvense* L.): A Novel Winter Annual Oilseed

The global demand for renewable energy sources and sustainable agricultural intensification has necessitated the domestication of novel crops capable of providing ecosystem services without displacing food production (Sedbrook et al., 2014). Field pennycress (*Thlaspi arvense* L.) has emerged as a primary candidate for this role. A winter annual member of the Brassicaceae family, pennycress is uniquely adapted to the temperate climates of the American Midwest, where it can be integrated into the corn (*Zea mays*) and soybean (*Glycine max*) rotation as a cash cover crop (Phippen and Phippen, 2012).

Unlike traditional cover crops that are terminated solely for soil health benefits, pennycress matures in late spring which allows for the harvest of oil-rich seeds prior to the planting of summer commodities (Johnson et al., 2015; Patel et al., 2021). Pennycress seeds typically contain 30–35% oil by weight, with a fatty acid profile highly suitable for hydrotreated renewable jet fuel and biodiesel production (Moser et al., 2009). Furthermore, the crop provides critical ecosystem services including the reduction of nitrogen leaching, mitigation of soil erosion, and suppression of spring ephemeral weeds (Weyers et al., 2019). While wild populations exhibit traits characteristic of undomesticated species such as high seed dormancy, pod shatter, and variable glucosinolate levels, concerted efforts by the scientific community are currently addressing these domestication bottlenecks through traditional breeding, mutagenesis, and gene editing (Basnet and Ellison, 2024; Keadle et al., 2023; McGinn et al., 2019). This ongoing domestication work provides the agronomic foundation upon which advanced biotechnological traits, such as biocontainment, can be layered.

3.1.2 *Arabidopsis thaliana* vs. Pennycress: Translational Imperative

Historically, the elucidation of gene function and metabolic pathways in plant biology has relied heavily on the model organism *Arabidopsis thaliana* (Chang et al., 2016). As a close relative of pennycress within the Brassicaceae lineage, *Arabidopsis* offers extensive genomic resources, a rapid life cycle, and a high degree of transformability. Comparative genomic analyses have revealed substantial synteny between the two species, with pennycress possessing orthologs for over 90% of characterized *Arabidopsis* genes (Dorn et al., 2013). This high degree of sequence homology has been instrumental for the preliminary engineering efforts described in this dissertation, enabling the rapid identification of candidate loci for Engineered Genetic Incompatibility (EGI) based on characterized *Arabidopsis* networks. By leveraging these conserved genetic architectures, our research can effectively translate complex synthetic circuits from a model system to a crop environment with minimal re-engineering of the core genetic logic.

Unfortunately, the translational potential of this workflow is constrained by the inherent physiological and agronomic limitations of the model system. As a diminutive rosette plant with no history of agronomic selection, *Arabidopsis* fails to recapitulate the complex physiological architecture required for field-scale productivity. Traits essential for assessing the robust function of biocontainment tools, such as persistence in soil seed banks, competition in high-density stands, and phenotypic stability under variable abiotic stress, cannot be accurately modeled in the controlled environments typically used for *Arabidopsis* cultivation. Consequently, while *Arabidopsis* serves as an efficient platform for the initial hypothesis testing of circuit topology, it is an insufficient vessel for validating the agronomic utility and evolutionary stability of complex synthetic biology architectures like EGI. Our work, therefore, posits that successful deployment

of biocontainment requires a transitional model that bridges the gap between the genomic tractability of *Arabidopsis* and the physiological reality of a field crop.

3.1.3 Rationale for Engineered Genetic Incompatibility (EGI) in Pennycress

Building upon the foundational proof-of-concept established in *Arabidopsis thaliana*, this research seeks to translate the Engineered Genetic Incompatibility (EGI) system into an agronomic context. Zinselmeier et al., (2025) and chapter 2 of this thesis demonstrate the feasibility of using the MoonTag PTA system to target the *WUSCHEL* (*WUS*) promoter; however, significant hurdles in achieving robust lethality remain a challenge. While the benign promoter mutation successfully protected parental lines, hybrid offspring expressing *WUS* at 100–500 fold excess exhibited incomplete lethality, characterized by necrosis and developmental delays rather than the requisite total incompatibility. The previous chapter expanded upon this framework, achieving 93% lethality in the highest-performing line.

The work presented here expands this experimental framework into field pennycress to address translational gaps and rigorously evaluates a broader suite of potential gene targets. A central objective of this chapter is to establish robust, high-throughput methodologies for validating gene overexpression and consequent lethality in a crop species where traditional stable transformation can be time-prohibitive. To this end, a multi-tiered validation strategy was employed.

Protoplast transformation served as the initial line of inquiry, providing a rapid, transient platform to assess construct functionality at the cellular level. Historically, protoplast systems have been pivotal in plant biology for dissecting signaling pathways and validating synthetic circuits without the temporal constraints of tissue culture (Sheen, 2001; Yoo et al., 2007). In the

context of this study, utilizing isolated mesophyll protoplasts allowed for the high-throughput screening of guide RNA efficiency and dCas9 recruitment efficacy, offering a snapshot of transcriptional activation potential before committing to stable integration.

Subsequently, Tobacco Rattle Virus (TRV)-mediated delivery was employed as a high-throughput vector to bridge the gap between single-cell assays and whole-plant physiology. TRV vectors are well-established tools for Virus-Induced Gene Silencing (VIGS) and, more recently, for the delivery of sgRNAs to induce somatic mutagenesis or transcriptional regulation in established tissues (Ellison et al., 2020). By introducing guide RNAs systemically into PTA-expressing plants, this method aimed to evaluate lethality phenotypes in a developed organismal context, theoretically circumventing the bottleneck of generating stable transgenic lines for every individual guide construct.

Finally, the definitive validation of the system was conducted through the sexual hybridization of stable transgenic lines (Feng et al., 2014; Ricroch et al., 2011). While transient and somatic assays provide preliminary data, the introgression of stable transgenes represents the gold standard for validating heritable agronomic traits. This approach necessitates the crossing of homozygous Programmable Transcriptional Activator (PTA) lines with hemizygous guide-RNA expressing lines, thereby strictly mimicking the mechanistic trigger of the proposed biocontainment strategy. This method evaluates the system not merely as a genetic circuit, but as a robust trait subject to Mendelian segregation and physiological environmental interactions.

This comprehensive approach allows for the systematic evaluation of the established target *WUSCHEL* (*WUS*) alongside novel targets *TPXL6* and *ELO1*. Thus, this chapter details the initial introgression and multi-modal validation of these expanded EGI components into the pennycress

genome, attempting to advance the technology from theoretical verification in a model species to practical validation in a crop chassis.

3.2 Materials and Methods

3.2.1 Plasmid Construction and Genetic Assembly

All genetic constructs utilized in this study were assembled via Golden Gate cloning protocols as reported in (Chamness et al., 2023). The Programmable Transcriptional Activator (PTA) system employed the MoonTag-dCas9 architecture as previously described (Zinselmeier et al., 2025). The constitutive *Ubiquitin 10* (*AtUbi10*) promoter driving the dCas9 and the seed specific *GmGlycinin* (*pGly*) promoter were utilized. Single guide RNAs (sgRNAs) targeting the promoters of the target genes were designed using CRISPOR (Concordet and Haeussler, 2018). For constructs utilizing double-guide targeting, a polyU6 gRNA architecture was engineered to express two distinct guides. All construct maps are listed in Supplemental Table 1.

3.2.2 Plant Material and Growth Conditions

The pennycress accession Spring-32 with the *tt8* mutation served as the wild-type background for all genetic transformations and hybridization experiments. Plant stocks were maintained in growth chambers under a long-day photoperiod regime (16 h light/8 h dark) at a constant temperature of 22°C and 50% relative humidity. For purposes of seedling selection and phenotypic characterization, seeds were surface sterilized with 0.6% NaOCl and 10% Silwett-77 for 10 minutes before being plated on 1/2 Murashige and Skoog (MS) medium supplemented with 1% sucrose and 0.8% agar.

3.2.3 Agrobacterium-mediated Transformation

Binary vectors were introduced into *Agrobacterium tumefaciens* strain GV3101 via heat shock. Transformation of pennycress plants was achieved utilizing the floral dip method (Clough and Bent, 1998) with key variables being taken from McGinn et al., (2018). Positive transformants in the T1 generation were identified through fluorescence screening for the expression of the red fluorescent protein (RFP) in the seed coat, or treatment with 100μM paromomycin.

3.2.4 Protoplast Isolation and Transformation and Rt-qPCR

Protoplasts were isolated and transformed as described in Sychla et al., (2022). After 24 hours, RNA was extracted from the transformed protoplasts utilizing Trizol and its accompanied protocol from Thermo Fisher Scientific (Waltham, MA). One biological replicate equated to an individual protoplast transformation. NEB Luna Rt-qPCR one step kit was used on a CFX96 Touch Real-Time PCR Detection System. Transcript abundance was normalized to the internal reference gene *TaUbi10* and relative expression levels were calculated utilizing the ΔΔCt method against wild-type controls.

3.2.5 Viral Infiltration

Viral delivery of AmCyan and guide RNAs into pennycress were conducted as described in Ellison et al., (2020). Viral infection fluorescent AmCyan photos were taken 8 days post injection. RNA was taken from infected tissue utilizing Trizol and its accompanied protocol. NEB Luna Rt-qPCR one step kit was used on a CFX96 Touch Real-Time PCR Detection System. Transcript abundance was normalized to the internal reference gene *TaUbi10* and relative expression levels were calculated utilizing the ΔΔCt method against wild-type controls.

3.2.6 Lethality Test Crosses

To test the ability for guides to overexpress target genes to the point of lethality, hemizygous T1 engineered plants expressing a guide RNA and TagRFP reporter gene served as pollen donors were crossed with either homozygous lines expressing Moontag under the control of *pAtUbi* or *pGmGlycinin*. This experimental design ensured that resultant RFP+ hybrid progeny had both genes creating the PTA and guide, and the resulting phenotype would be characteristic of a EGI x WT cross. Baseline germination and survival metrics were established through Null-segregant (RFP-) and self-crossed guide RNA parent lines.

3.2.7 Phenotypic Analysis and Lethality Scoring

Hybrid seeds were harvested and plated on non-selective 1/2 MS media for observation. Germination rates were quantified as the percentage of seeds exhibiting radicle emergence at 8 days after plating. Individuals categorized as "lethal" if they displayed complete necrosis, developmental arrest prior to the first true leaf stage, or complete lack of germination, and “escape” if they grew as normal.

3.3 Results

3.3.1 Protoplast Validation of Transformation Protocols and Guide Efficacy

Before initiating time-intensive stable transformations, we sought to establish a rapid validation pipeline for *Thlaspi arvense*. We optimized a protoplast isolation and transformation protocol specifically for pennycress leaf tissue to allow for high-throughput screening of genetic constructs. As shown in Figure 3.1A, we observed robust GFP fluorescence in the isolated protoplasts, confirming the viability of the cells and the efficiency of the transformation method.

Following protocol validation, we utilized this system to screen the efficacy of our designed single guide RNAs (sgRNAs) targeting the *WUSCHEL* (*WUS*) promoter. Protoplasts were co-transformed with the MoonTag-dCas9 activator and vectors containing specific sgRNAs. Figure 3.1B displays the transcriptional response of the endogenous *WUS* target; the results revealed extreme variability associated with this method. Unlike the consistent reporter expression, the quantitative assessment of endogenous gene activation proved highly inconsistent across biological replicates. Multiple approaches to try and mitigate this noise were attempted, including performing additional biological replications and normalizing against dCas9 expression, but none were successful. This high degree of noise prevented any definitive conclusions regarding guide efficacy or activator recruitment from the transient assay, highlighting the limitations of protoplasts for fine-tuning complex synthetic circuits in this species.

3.3.2 Viral Vector Validation of Guide Delivery

Following the inconclusive results from the protoplast assays, we assessed Tobacco Rattle Virus (TRV) as an alternative high-throughput method for validating guide RNA efficacy *in planta*. This system theoretically allows for the systemic delivery of guide RNAs into established tissue, bypassing the need for stable transformation of every guide construct.

We first validated the effectivity of the TRV vector in *Thlaspi arvense* by delivering a cargo expressing the fluorescent reporter AmCyan. We observed successful systemic infection across pennycress plants of both older bolting pennycress (Figure 3.2A) and younger rosette stage pennycress (Figure 3.2B). AmCyan fluorescence was detectable confirming that TRV can effectively replicate and spread within the pennycress host to deliver genetic payloads.

To test the functional reconstitution of the EGI system, we infected stable transgenic pennycress lines, homozygous for the *AtUbi10::MoonTag-dCas9* activator, with TRV vectors carrying sgRNA targeting the *WUS* promoter. We hypothesized that the systemic viral delivery of the guide would recruit the latent activator in somatic cells, leading to measurable overexpression. Figure 3.2C showcases the observed overexpression values of *WUS* based on how progressed the infection was observed to be at time of RNA extraction. Control tissue was fully fluorescent tissue infected without any gRNA. Full fluorescence corresponded to tissue harvested within 24 hours of seeing a full AmCyan signal, but this showcased no significant overexpression in comparison to the control. This same result was observed with pre fluorescent tissue, which was taken ahead of an observed AmCyan signal, and vascular fluorescence, which was vascular tissue with an observed AmCyan signal. The only samples that saw statistically significant overexpression of *WUS* were fully fluorescent tissue that had been infected for 14 days. However, while statistically significant, extreme variability was observed across biological replicates with one not showing any overexpression.

To further test TRV guide infection ability to overexpress native pennycress genes, we targeted the fatty acid gene WRI1. The specific guide utilized, guide 3, was previously confirmed to cause the most overexpression in protoplast systems (unpublished data). Despite this, no observable overexpression was seen from RNA extracted from any full fluorescent leaves, leaves that had an intermediate level of fluorescence, and 14 day full fluorescent tissue, which is contrary to the results observed in *WUS*.

3.3.3 Lethality Validation via Sexual Hybridization

Given the limitations of transient (protoplast) and somatic (viral) validation methods, we proceeded to the definitive test of the system: sexual hybridization of stable transgenic lines. This approach mimics the exact mechanism of biocontainment, where lethality is triggered only upon the union of separated genetic components in the hybrid offspring.

To execute this, we designed a crossing schematic utilizing two distinct parental lineages, as illustrated in Figure 3.3. The maternal recipients consisted of homozygous lines expressing the MoonTag-dCas9 activator driven by either the constitutive *AtUbi10* promoter or the seed-specific *GmGlycinin* promoter. These lines provide the PTA of the system but remain phenotypically normal in the absence of a guide RNA. The paternal pollen donors were selected from T1 populations hemizygous for the target-specific sgRNA arrays and marked with a TagRFP reporter. Table 1 lists the various guide lines that were created, including their target genes and expected phenotype.

By crossing the hemizygous guide-carrying males to the homozygous activator females, we generated F1 progeny that inherit both the latent activator and the targeting guides. This reconstitution of the full synthetic circuit is intended to drive lethal overexpression of the native target gene specifically in the hybrid generation.

3.3.4 Germination Analysis of Hybrid and Parental Populations

To rigorously assess the lethality of the EGI system, we analyzed germination rates across three distinct populations derived from the sexual hybridization experiments: (i) RFP+ T2 hybrid progeny containing both the MoonTag activator and the targeting array; (ii) T2 RFP- hybrid progeny, null segregants lacking the targeting array; and (iii) T2 parent guide lines, self-

pollinated progeny of the pollen donors. Seeds were harvested and plated on media (Figure 3.4A), and germination counts were recorded 8 days post-plating.

As shown in Figure 3.4B, *WUS* targeting guide 39 in the seed promoter parent plants had a germination of 38% (n=8), while RFP- was 100% (n=10) and the parental line was 56% (n=18). *TPXL6* guide 1 in both seed promoter and constitutive promoter parents had a unique phenotype, where RFP+ hybrid seedlings, expected to be lethal, recovered and observed parental line lethality (65% to 100% pGly-L2, 18% to 100% pGly-L3, 15% to 62% pAtUbi-L1, 20% to 100%, pAtUbi-L2). Two multi guide arrays targeting *ELO1* were also tested. Guides 108 and 106 in both the seed and constitutive expression parents saw a decrease in survivability compared to the parent guide line (20% to 7%, 25% to 14%) while guide 108 and 110 only saw a slight decrease when compared to the parent in line 1 (5% to 0%) but in the other lines either no phenotype was observed or a recovery of lethality from the parental line was observed. Across all crosses, RFP- segregants fully germinated, and there was no significant difference in phenotypes between the seed and constitutive promoters driving the Moontag activator complex.

3.3.5 Segregation Analysis of Guide Line Toxicity

The lethality observed in the T2 parent guide lines in Figure 3.4 was an unexpected result and raised a critical question: was this effect driven by the guide RNA constructs themselves, or was it a result of unknown physiological stressors unrelated to the transgene? To definitively answer this, we performed a segregation analysis within the self-pollinated seed lots of the guide-only parents.

Because the T1 parent plants were hemizygous for the guide insertion, selfed T2 progeny segregated for the presence of the transgene. By utilizing the co-segregating TagRFP marker, we

were able to separate the seed population into siblings that inherited the guide array (RFP+) and null segregants that did not (RFP-).

Guides 108 and 110 targeting ELO1 line 2 were the only parents that did not have any observable phenotypic difference from the transgenic RFP+ and the non-transgenic RFP- segregants. All other targets, guide combinations, and lines saw an extreme negative lethal phenotype (*ELO1* g108 and g106 100% to 22%, ELO1 g108 and g110 line 2 100% to 12%, *WUS* g39 100% to 15%, *TPXL6* g1 100% to 0% line 1, 100% to 10% line 2, and 100% to 0% line 3). These results suggest that the previous lethality observed was a factor of the transgenes themselves and not the physiology of the plant.

3.4 Discussion

The translation of synthetic biology from model systems to non-model crops is a pivotal step in the creation of a robust biocontainment strategy, often revealing physiological and technical constraints invisible in the initial design phase (George et al., 2024). The primary objective of this chapter was to validate the EGI system in field pennycress, utilizing the MoonTag-dCas9 PTA to drive lethal overexpression of endogenous targets. While the theoretical framework of EGI relies on a safe parent/lethal hybrid paradigm, our results highlight significant translational bottlenecks where every validation method attempted faced distinct challenges. Transient protoplast assays proved too variable to provide reliable quantitative data, while somatic viral delivery resulted in unreliable overexpression. Even the definitive validation using stable transgenic lines was complicated by unexpected toxicity in the parental guide lines. Consequently, this study highlights the difficulties in translating the EGI construct to applied species and showcases a need for more robust component testing strategies.

3.4.1 Limits of Protoplast Assays for Quantitative Validation

Protoplast assays were deployed as an initial high-throughput filter to screen guide RNA efficacy, aiming to bypass the lengthy generation time of pennycress. While we successfully established a robust transformation protocol (Figure 3.1A), the system failed to provide predictive quantitative data for endogenous gene activation. The extreme variability observed in *WUSCHEL* activation (Figure 3.1B) underscores a fundamental discordance between transient plasmid expression and genomic regulation.

In protoplasts, the chromatin landscape is significantly altered due to the enzymatic stress of cell wall removal and the loss of tissue-specific signaling (Yoo et al., 2007). Consequently, the accessibility of target promoters like *WUS* in a protoplast may not reflect their state in organized tissue. Furthermore, transient assays flood the nucleus with plasmid DNA, creating a high copy-number environment that does not recapitulate the stoichiometry of a stable, single-copy genomic insertion (Sheen, 2001). The stochastic nature of co-transformation, where a cell might receive the activator but not the guide, further dilutes the population-level signal. These results suggest that while protoplasts are excellent for validating the expression of heterologous parts (e.g., GFP), they are insufficient for fine-tuning complex transcriptional regulation of endogenous loci in pennycress. Future validation workflows must prioritize methods that maintain genomic context, such as utilizing protoplasts isolated from stable PTA-expressing lines to reduce experimental variables.

3.4.2 Inconsistency of Viral Delivery for Lethality Screening

The use of Tobacco Rattle Virus (TRV) aimed to bridge the gap between single-cell assays and whole-plant physiology. Although TRV successfully infected pennycress systemically (Figure

3.2), the downstream activation of target genes was inconsistent and failed to trigger robust phenotypic changes. This result stands in contrast to previous reports utilizing TRV for somatic gene editing. Ellison et al. (2020) demonstrated that TRV could efficiently deliver sgRNAs to transgenic *Nicotiana benthamiana* expressing Cas9, resulting in high frequencies of somatic indel mutations. However, a critical distinction exists between the requirements for editing versus activation. Gene editing is a one-and-done event: a single successful cleavage event by the Cas9-sgRNA complex results in a permanent genomic scar that persists regardless of subsequent viral load or complex turnover. In contrast, transcriptional activation via dCas9 is a reversible, equilibrium-dependent process requiring sustained occupancy of the target promoter (Casas-Mollano et al., 2020). Consequently, the transient or fluctuating levels of sgRNA provided by a viral vector may be sufficient to induce a one-time edit but insufficient to maintain the high steady-state binding required to drive hyper-activation of a target gene against homeostatic feedback loops.

Additionally, the architecture of the guide RNA within the viral transcript may necessitate further optimization for activation applications. In the TRV system, the sgRNA is expressed as part of the viral RNA genome and must be recognized and processed by the Cas machinery (Ellison et al., 2020; Weiss et al., 2025). While Cas9 has shown some flexibility in processing guides from longer transcripts (Haeussler and Concordet, 2016), the steric requirements for the dCas9-activator complex may be more stringent. It is possible that the fusion of the bulky MoonTag array to dCas9 hinders the loading of guide RNAs that are not precisely processed at the 5' and 3' ends. Indeed, Ghoshal et al., (2020) saw greater success with guides that had TRNA processing elements. Future iterations should explore the inclusion of self-cleaving ribozymes or tRNA-

gRNA architectures to ensure precise excision of the guide from the viral vector, potentially enhancing loading efficiency and downstream activation.

Despite these challenges, statistically significant overexpression was achieved in select samples (e.g., 14-day fully fluorescent tissue), confirming that the fundamental mechanism of viral-mediated activation is viable in pennycress. Unlike protoplast assays, which suffer from artifactual chromatin states, and stable transformations, which are low-throughput and confounded by insertion effects, TRV delivery offers a unique middle ground by assessing gene regulation in an organismal context with relatively high throughput. If the issues outlined here are resolved in future endeavors, this platform remains the most promising avenue for the rapid, accurate validation of complex synthetic circuits in non-model crops.

3.4.3 Transgene Toxicity in Stable Guide Lines

The most significant and unexpected finding of this study is the intrinsic toxicity associated with the guide RNA parental lines. The segregation analysis (Figure 3.5) definitively linked reduced germination to the inheritance of the guide RNA array, independent of the dCas9 activator. This violates the core tenet of EGI, that the components must be individually inert. There are several possible reasons as to why this phenotype is arising.

First, the fluorescent reporter utilized to track the transgene could itself be a source of cytotoxicity. While TagRFP was selected specifically to avoid the obligate tetramerization and aggregation issues associated with its predecessor dsRed (Merzlyak et al., 2007), the accumulation of fluorescent proteins to high intracellular levels may still generate reactive oxygen species or trigger unfolded protein responses in sensitive tissues (Kalyanaraman and Zielonka, 2017). It is also possible that the reflectance of red light, as noted by the seeds deep red

color, may be disrupting the natural germination machinery, as red light is known to enhance germination (Wei et al., 2023).

Second, in the absence of the dCas9 protein, guide RNAs may be susceptible to processing by the host's endogenous RNA interference (RNAi) machinery, something observed recently in *Arabidopsis thaliana* with the absence of cas9 by Sharma et al. (2022). This mechanism provides a compelling explanation for the rescuing effect observed in certain hybrid crosses (Figure 3.4), where the RFP+ hybrid progeny (containing dCas9) exhibited higher germination rates than their guide-only parents. In the hybrid state, the binding of the dCas9 protein to the sgRNA likely protects it from nuclease degradation and entry into the silencing pathway, thereby mitigating the off-target toxicity observed in the parents.

Finally, the temporal onset of this toxicity, manifesting only in the T2 generation, warrants critical examination. The T1 parental plants, which were hemizygous for the insertion, germinated and grew indistinguishably from wild-type controls alongside the PTA lines. The emergence of toxicity specifically in the T2 generation suggests there may be a dosage-dependent mechanism, potentially linked to the segregation of homozygous individuals (Birchler et al., 2001). It is plausible that a threshold of toxicity (whether from TagRFP accumulation, or siRNA production) is exceeded only when the transgene dosage is doubled in the homozygous state, whereas the hemizygous T1 state remained below this lethal limit. However, this idea is combated by the fact that several lines had overall no germination, and some had full germination. Further research is needed to fully understand the cause of this phenotype.

3.5 Conclusion

This study represents the potential for the translation of EGI from the model species *Arabidopsis* to the agronomic crop pennycress. We systematically evaluated three distinct validation methodologies, protoplasts, viral vectors, and stable transgenics, and found that tools optimized for model organisms can falter when applied to new genetic backgrounds. While protoplast assays and viral delivery offered high-throughput potential, they were limited by variability. Most critically, the definitive stable transformation experiments revealed an unexpected bottleneck: potential guide RNA toxicity. Further research needs to be done to understand the cause of this lethality such that it doesn't interfere with downstream EGI engineering efforts. By resolving these component-level incompatibilities, we move one step closer to establishing a robust biocontainment system capable of securing the future of genetically engineered crops.

3.6 Figures

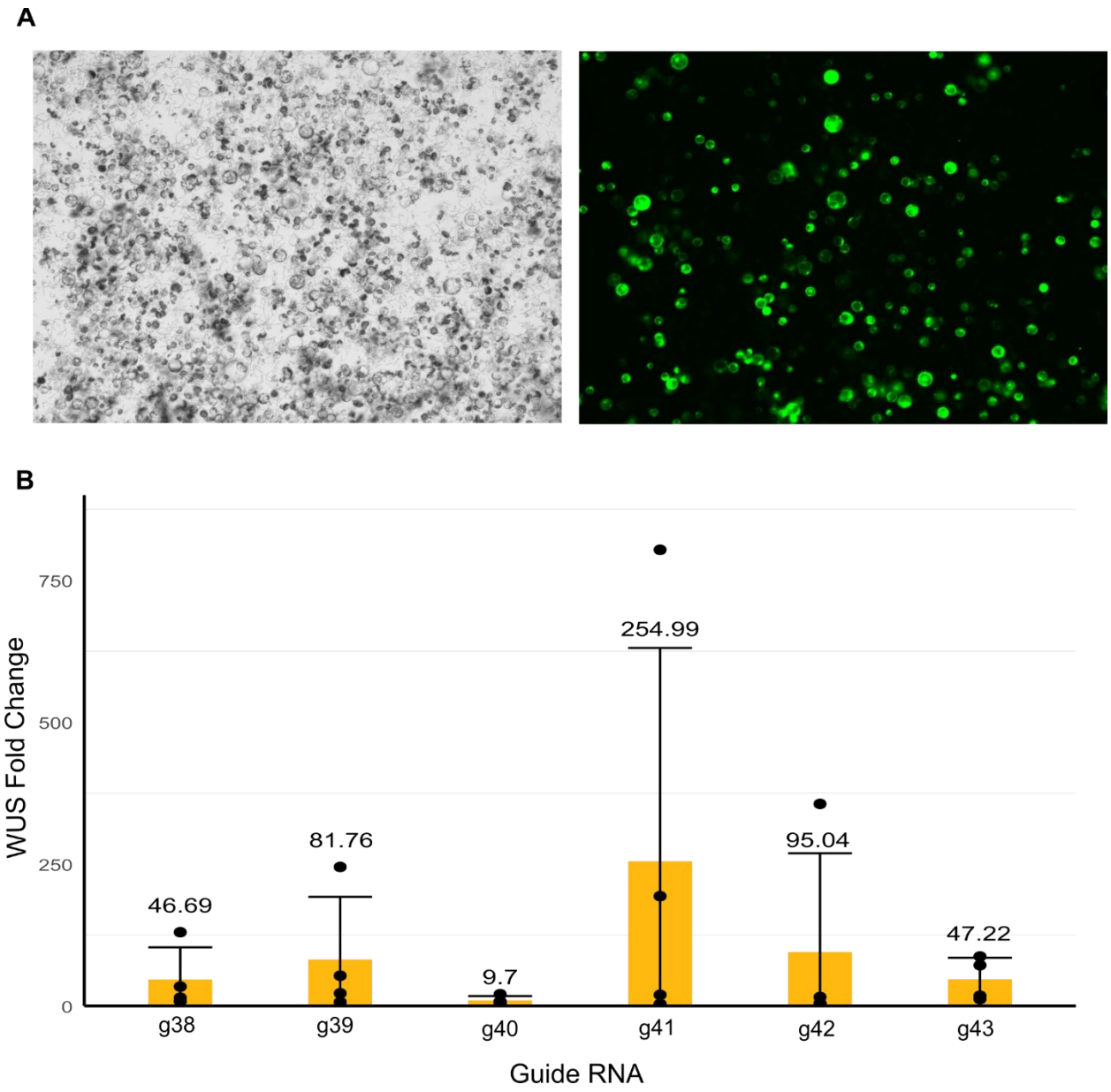

Figure 3.1. Validation of Pennycress Protoplast Transformation and EGI Component Functionality. (A) Representative microscopy image showing successful transient expression of Green Fluorescent Protein (GFP) in *Thlaspi arvense* mesophyll protoplasts, confirming efficient delivery and translation of exogenous DNA. **(B)** Assessment of sgRNAs targeting *WUSCHEL*. Relative expression levels of the native *WUS* gene in protoplasts co-transformed with the MoonTag-dCas9 activator and specific guide RNAs.

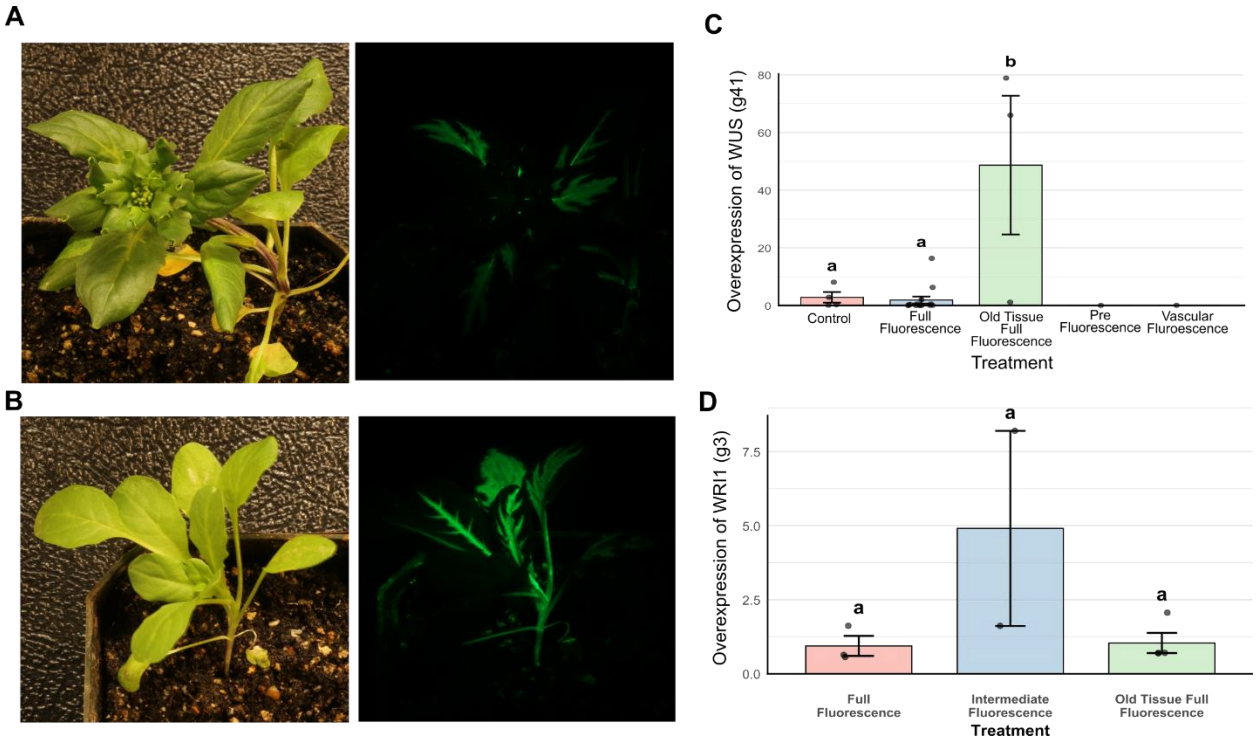

Figure 3.2. Evaluation of Tobacco Rattle Virus (TRV) as a Delivery Vector for EGI Components. Fluorescent imaging of pennycress plants at various developmental stages. (A) Bolting and (B) rosette seedling infected with TRV carrying an AmCyan reporter. The widespread fluorescence indicates successful systemic infection and protein expression across different tissue ages. (C) Rt-qPCR analysis of target gene *WUS* from RNA extracted from homozygous *AtUbi10::MoonTag-dCas9* plants infected with TRV carrying *WUS*-targeting sgRNA. Despite successful infection, the activation of the target gene proved highly variable or not measurably overexpressed. (D) Rt-qPCR analysis of target gene *WRI1* from RNA extracted from homozygous *AtUbi10::MoonTag-dCas9* plants infected with TRV carrying *WRI1*-targeting sgRNA. Statistical significance was determined using a one-way ANOVA followed by a Tukey's HSD post-hoc test; different letters indicate significant differences between groups ($p < 0.05$)

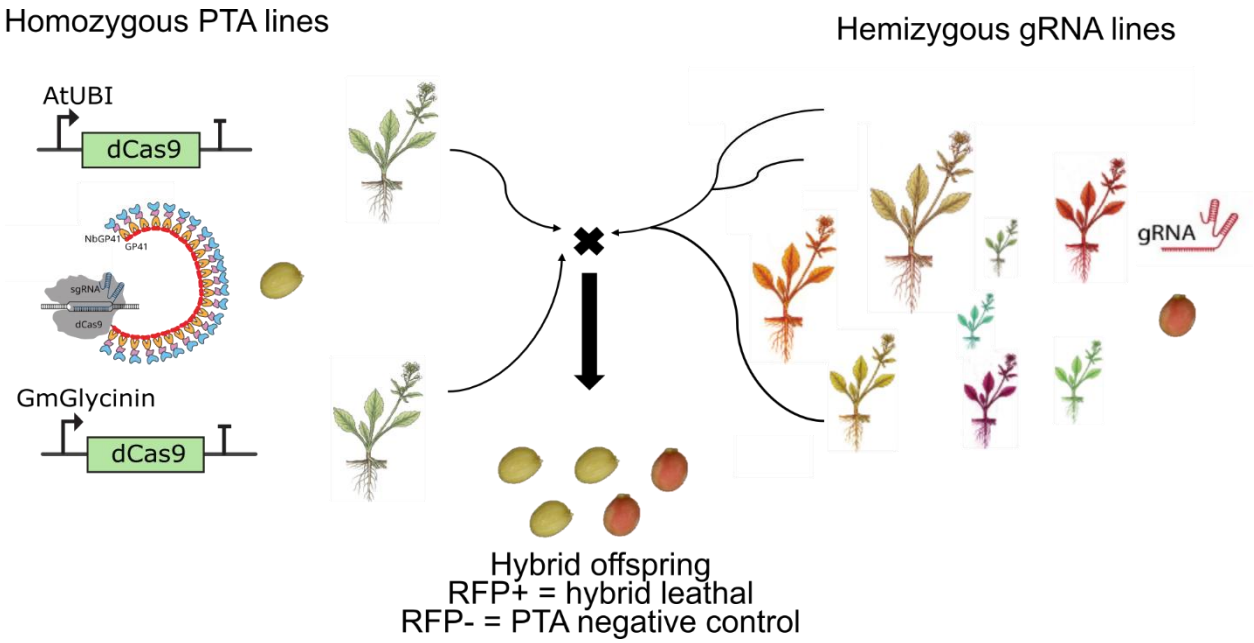

Figure 3.3. Schematic of the Split-Component Crossing Strategy for EGI Validation. The experimental design relies on the segregation of the lethal components into two parental lines to ensure their viability. (Left) The activator female parent is homozygous for the MoonTag-dCas9 construct (driven by *pAtUbi10* or *pGmGlycinin*) without any fluorescent marker. (Right) The guide male parent is hemizygous for the sgRNA array and a TagRFP reporter. (Bottom) The resulting F1 Hybrid reconstitutes the functional complex. The co-inheritance of the activator and the guide RNA triggers the overexpression of the endogenous target gene, leading to programmed lethality in RFP+ seeds. RFP- seeds are null segregants used as controls.

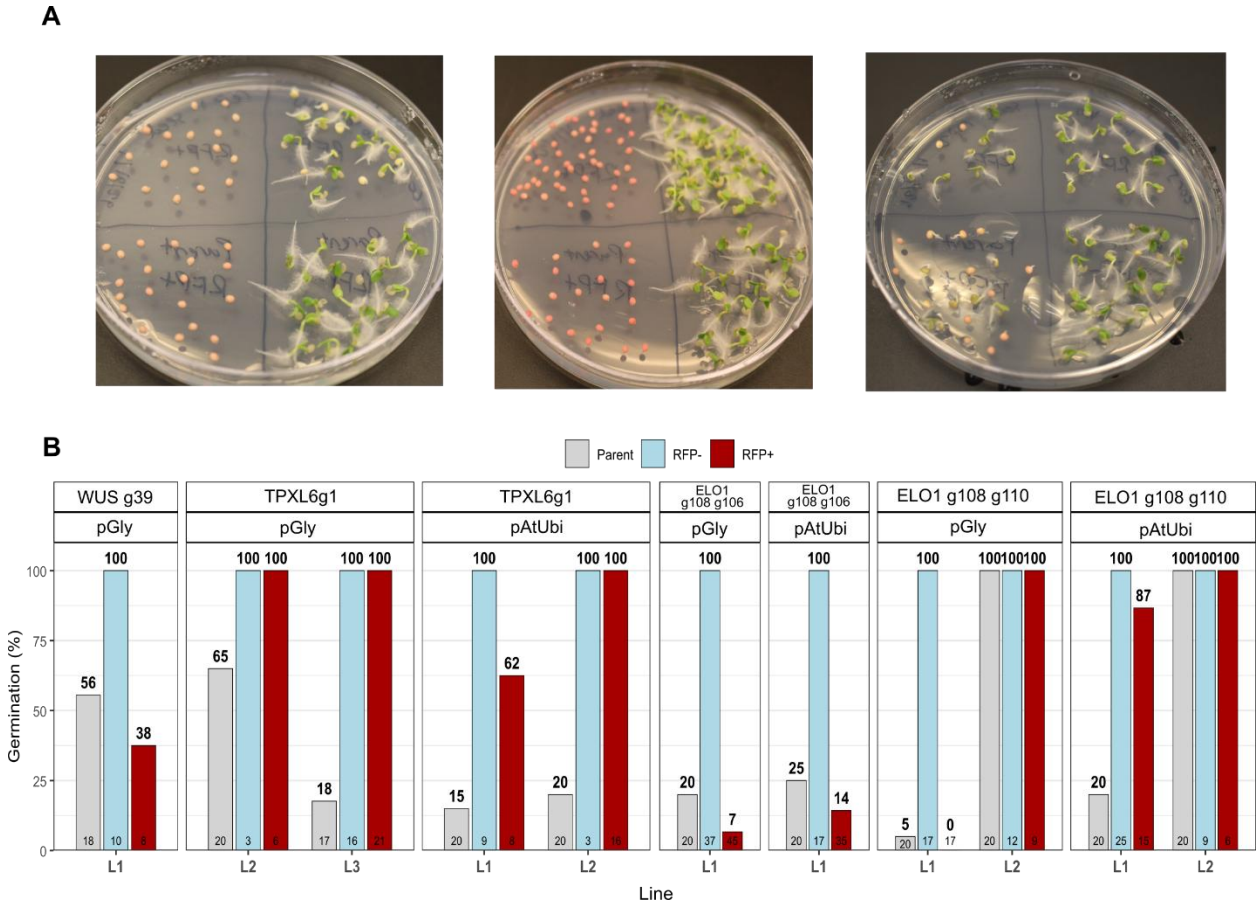

Figure 3.4. Germination Counts of Hybrid and Parental Populations. (A) Representative images of germination for 3 different genotypes at 3 days post plating. (B) Quantitative assessment of seed germination rates across three distinct genotypes. RFP+ F1 hybrid progeny: offspring inheriting both the PTA and the sgRNA, expected to be lethal. T2 RFP- hybrid progeny: null-segregant siblings inheriting only the PTA, expected to be viable. T2 parent guide lines: selfed progeny of the pollen donors expressing only the sgRNA. The graph highlights the germination counts 8 days post-plating. Total seeds tested (n) are at the bottom of each bar. L(number) refers to a unique line resulting from a unique transformation event for the given construct.

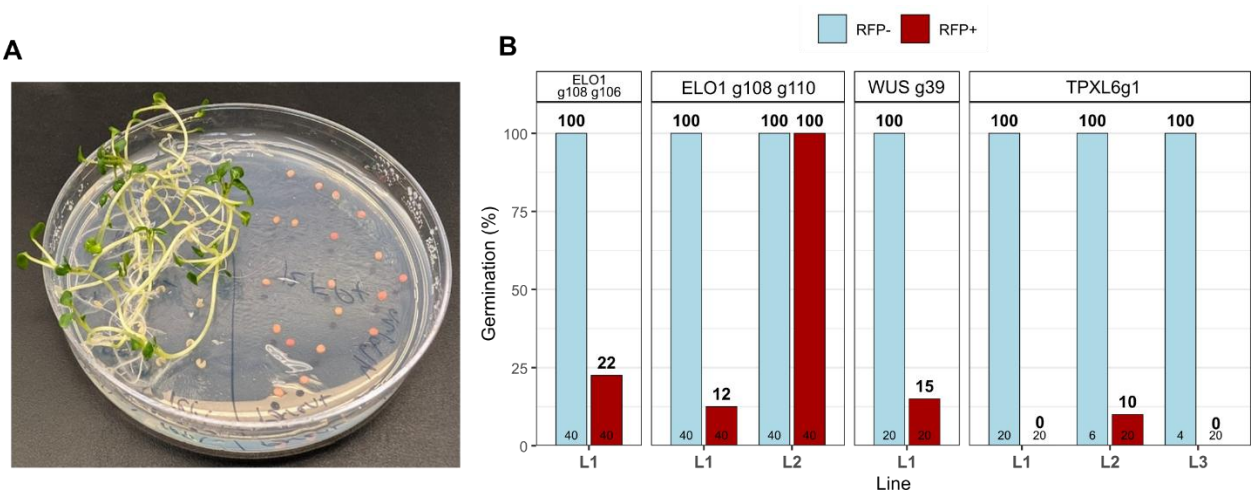

Figure 3.5. Segregation Analysis of Toxicity within Guide RNA Lines. A closer examination of the T2 parent guide lines from Figure 3.4. (A) Seeds from self-crossed guide parents were sorted by fluorescence to distinguish transgenic (RFP+) from null (RFP-) siblings. (B) graph showcasing germination rates 8 days after plating. Total number of seeds t4ested (n) are at the bottom of each bar. L(number) refers to a unique line resulting from a unique transformation event for the given construct.

3.7 Tables

Strategy	Mechanism of Action	Primary Containment Failure Mode
g39, g38, g41	*WUS*	Lethality
g1, g2	*TPXL6*	Lethality
g108 & 106, g108 & 110, g 107 & 111, g111 & 112	*ELO1*	Lethality
g121	*PINOID*	Lethality
g71, g72, g74	*RHD6*	Sterility
g66, g68, g77	*MYC1*	Sterlility

Table 3.1. List of guide lines and their target genes and intended phenotype that were created.

Plasmid Name	Function	Benchling Link
G38 TDNA	Plasmid used to create guide line	https://benchling.com/s/seq-ByiVWh4UlBkz0LWgkaS0?m=slm-mIUzqtXORnZHGpl1armn
G39 TDNA	Plasmid used to create guide line	https://benchling.com/s/seq-D3RynWNx5pHuTCM9sb8P?m=slm-O6ZgSBLn1Q3dSWeYcAwd
G41 TDNA	Plasmid used to create guide line	https://benchling.com/s/seq-HCigkmTV8w6n6ZPWGWez?m=slm-Fo7hILGlxVHTvxZsOyg7
TPXL6g1 TDNA	Plasmid used to create guide line	https://benchling.com/s/seq-4Yz0TGwFUxd9g7UfNVJX?m=slm-PUtyAvucBOHjOF0vXhMj
TPXL6g2 TDNA	Plasmid used to create guide line	https://benchling.com/s/seq-L5CUabi4qG20caApIqyb?m=slm-WYtMkDd4B40A85sP60Fp
G108 & 106 TDNA	Plasmid used to create guide line	https://benchling.com/s/seq-u5AAfdKwfK1t4DcMm15r?m=slm-80CHysXbfi4RK7lo4FU2
G108 & 110 TDNA	Plasmid used to create guide line	https://benchling.com/s/seq-xwthTs1Poa9zvJCsmd93?m=slm-VCC4f2v6mVgPAHDwAMVm
G107 & 111 TDNA	Plasmid used to create guide line	https://benchling.com/s/seq-lKBnSHIRtshBSxM7qpcy?m=slm-SN915ozf7F8kswy7jaee
G110 & 112 TDNA	Plasmid used to create guide line	https://benchling.com/s/seq-U95FnboMnQBzWD24KrQg?m=slm-VBNxgzYxerbRRJ0tHJjr
G121 TDNA	Plasmid used to create guide line	https://benchling.com/s/seq-RPce2teyfIQ8XKWo0zAd?m=slm-RM9r8IRzpXLd9N57NqZB

G71 TDNA	Plasmid used to create guide line	https://benchling.com/s/seq-cAvHewYaXJ5rCqKt82b3?m=slm-MzYFSuhgKzzCZOfS2BFF
G72 TDNA	Plasmid used to create guide line	https://benchling.com/s/seq-bqzhtdK0wXMUnRI9VU2o?m=slm-u2h15zKu18BRPI6Gj2jy
G74 TDNA	Plasmid used to create guide line	https://benchling.com/s/seq-zuJ30k4WSyXZbkyyVS8x?m=slm-I8LvXit6lB8IOq9fGPCq
G66 TDNA	Plasmid used to create guide line	https://benchling.com/s/seq-AHDll8hnavBOpLs7SYEu?m=slm-SxKUZyvyWMEqA6nyTV2u
G68 TDNA	Plasmid used to create guide line	https://benchling.com/s/seq-FXwVCOPxctlcRTtzYS88?m=slm-dCTovUcgJaZEc4Y5iy5h
G77 TDNA	Plasmid used to create guide line	https://benchling.com/s/seq-Udqg3CAw9ST8vmdOvg0y?m=slm-VBP1RPySqdnFJO4XVFIo
Seed:Moon lvl2	Plasmid used to create moontag line	https://benchling.com/s/seq-neOHFx5O98tncs4rwPQW?m=slm-LzKZvZmcSvQRGAs1aQP9
AtUbi:Moon Lvl2	Plasmid used to create moontag line	https://benchling.com/s/seq-Ei7EaAqxJ41fbSs8bM9b?m=slm-A8xrVvWrB0IMUBi58xkj
TRV1	Plasmid used in TRV experiments	https://benchling.com/s/seq-4HNLlgr6lCarG1R7jDjc?m=slm-PcluDx3mx6pf40b1KsGJ
pJPC666	TRV plasmid harboring AmCyan	https://benchling.com/s/seq-dZsZIz9I34KPN5DTDD04?m=slm-G3UogUVWbp7KkGWNRBjp
G41 TRV	TRV plasmid with AmCyan and guide	https://benchling.com/s/seq-ui1e2mRb2gc5yEVCwTlP?m=slm-jpETGvkUvuvyA1WT5h9I
WRI1g3 TRV	TRV plasmid with AmCyan and guide	https://benchling.com/s/seq-AKZKtTVTdjiaDLGgRwXI?m=slm-sQYMqEr03rAgs1y4T8dk
35S:GFP	GFP plasmid used in protoplast experiments	https://benchling.com/s/seq-XbyLES18BHCtfmIEyXqv?m=slm-h2SqU8r3aOMm0LZP6mzU
WUS g38 lvl1	Guide plasmid used in protoplast experiments	https://benchling.com/s/seq-SLMfaZiftVeVjNKAszEM?m=slm-Jaek9upxyGR2eqQpA7cR
WUS g39 lvl1	Guide plasmid used in protoplast experiments	https://benchling.com/s/seq-hNBe80SsunRk63oOpFJF?m=slm-RIKOIiwLMKESOg5gakgJ

WUS g40 lvl1	Guide plasmid used in protoplast experiments	https://benchling.com/s/seq-pxDO8MZXhtJ5HhzVLj96?m=slm-FeIZPTsI8mriJHT095BP
WUS g41 lvl1	Guide plasmid used in protoplast experiments	https://benchling.com/s/seq-IzDyBQEP7O9q3puRxWlR?m=slm-hhxAm8GWQgzPCsbDzlrc
WUS g42 lvl1	Guide plasmid used in protoplast experiments	https://benchling.com/s/seq-dBUx9ALHbk0U9utn6nCF?m=slm-6Dkkkx5TplYtuojeS69V
WUS g43 lvl1	Guide plasmid used in protoplast experiments	https://benchling.com/s/seq-sjX3h7nHd4Uy9EaKNOFH?m=slm-JvKzpRCE41nPRj0cWfAJ
AtUbi:Moontag lvl2	Moontag plasmid used in protoplast experiments	https://benchling.com/s/seq-Ei7EaAqxJ41fbSs8bM9b?m=slm-A8xrVvWrB0IMUBi58xkj

Table 3.2. list of all genetic constructs used in this work

Primer name	Sequence
oCORS50_taubiqf	tacacttcacttggtcttgcgt
oCORS51_taubiqr	tggtctttcccgtcaaggtctt
oCORS46_wusqf	accaagccgaccaagaaagcgg
oCORS47_wusqr	cggctgttggtgaccggact
oCORS130_AmCyanqf	accaagccgaccaagaaagcgg
oCORS131_AmCyanqr	ctctcgtaggacatgccgtc
qSF011b	agactgcttgagcttggataat
qSF012b	gacaacggagaagacgaagag

Table 3.3 list of all primers used in this work

Chapter 4 – Improving Perennial Ryegrass Transformation Protocols with Developmental Regulators

Chapter Summary

The development of genetically modified (GM) or gene edited (GE) turfgrass requires transformation systems that are both efficient and broadly applicable across genotypes. However, traditional *Agrobacterium*-mediated callus culture methods remain limited by low transformation efficiency, extended culture durations, and strong genotype dependence. In this study, we compare a modified classical callus culture protocol with an approach that incorporates the developmental regulator genes *WUSCHEL2* (*wus2*) and *BABY BOOM* (*bbm*), along with an inducible Cre recombinase and a dual luciferase assay to test variable promoter strengths in perennial ryegrass (*Lolium perenne* L.). We show that traditional protocols failed to regenerate plants, despite successful callus formation and transgene expression. In contrast, the developmental regulator system enabled efficient callus induction and plant regeneration independent of genotype. This optimized protocol significantly reduces the time and genotype constraints of perennial ryegrass transformation, offering a practical platform for advanced genetic engineering applications of an important turf and forage grass.

4.1 Introduction

Turfgrass plays a vital role in various landscapes, including recreational areas, sports fields, and urban green spaces. Beyond its aesthetic and functional uses, turfgrass also contributes to environmental sustainability by reducing soil erosion and runoff, and can promote mental wellbeing (Braun et al., 2024). However, turfgrass management presents significant challenges due to its susceptibility to environmental stressors, pathogens, and weed competition (Fan et al., 2020). In recent years, genetic modification has emerged as a powerful tool for plant breeders to target specific improvements in turfgrass, such as introducing genes for enhanced herbicide resistance (Hartman et al., 1994) and stress tolerance (Dai et al., 2003).

Despite the potential advantages of genetically modified (GM) or genetically edited (GE) turfgrass, its widespread adoption is limited by ecological and regulatory concerns. A primary issue is the risk of uncontrolled spread, as GM turfgrass may facilitate gene flow to wild relatives or unintended environments. This concern was exemplified by the escape of a glyphosate-resistant GM creeping bentgrass (*Agrostis stolonifera* L.) from a field trial in Oregon in 2006 (Reichman et al., 2006). To safely release a GM turfgrass, robust biocontainment strategies are essential. Several strategies are currently under development, including apomixis (Wieners et al., 2006), male sterility (Luo et al., 2005), and Engineered Genetic Incompatibility (EGI) (Clark and Maselko, 2020; Maselko et al., 2020; Zinselmeier et al., 2025). However, these approaches are often complex to engineer into a species, and in cases such as EGI, require multiple genetic modifications. A high-efficiency, streamlined transformation protocol is a critical prerequisite for enabling these technologies.

Two main methods have been utilized for turfgrass transformation. Particle bombardment has been used to generate glyphosate-resistant creeping bentgrass (Gardner et al., 2003) and Kentucky bluegrass (*Poa pratensis* L.) (Blume et al., 2010), but suffers from very low efficiency. The second approach, *Agrobacterium*-mediated callus culture, is more commonly used (Singh and Prasad, 2016); this method involves inducing embryonic callus formation using growth hormones, followed by gene transfer via *Agrobacterium*, and then changing the hormones to regenerate roots and shoots from the calluses. However, successful regeneration of viable transgenic plants remains a major hurdle, often limited by genotype specificity and frequent production of albino plants. Furthermore, the callus culture process is time-intensive and prone to multiple failure points, notably from contamination, a key concern in fungal-endophyte containing species such as perennial ryegrass (*Lolium perenne* L.) (Bidabadi and Jain, 2020; Han et al., 2011; Young et al., 2013).

These challenges are not unique to turfgrass. Many monocot species pose similar difficulties in genetic transformation. To address this, Wang et al., (2023) demonstrated a novel strategy involving the developmental regulator genes *Wuschel2* (*wus2*) and *Babyboom* (*bbm*), which promote embryogenesis and callus formation with reduced reliance on exogenous hormones. When paired with a heat-shock-inducible Cre recombinase system, these genes can be excised post-induction, allowing for normal regeneration to proceed. This strategy has proven effective in multiple monocot species but has not yet been tested in perennial grasses.

Perennial ryegrass is a cool-season turfgrass commonly cultivated in northern regions of the United States and across Europe. It is also used as a forage crop in agricultural systems (Bonos and Huff, 2015). Between 2010 and 2019, the United States exported 681 million kilograms of perennial ryegrass seed, generating $194 million in revenue (Petty et al., 2024). Several

Agrobacterium-mediated transformation protocols have been developed for this species, targeting a variety of traits (Bajaj et al., 2006; Grogg et al., 2022; Kumar et al., 2022; Zhang et al., 2020); however, these methods continue to suffer from low efficiency, low throughput, and strong genotype dependence. This genotype specificity is especially problematic given that perennial ryegrass is a cross-pollinated species. Relying on only a few amenable genotypes increases the risk of inbreeding depression and limits breeding progress (Bonos and Huff, 2015).

In this study, we compare the efficacy of traditional *Agrobacterium*-mediated callus culture transformation with the developmental regulator gene approach developed by N. Wang et al. (2023), incorporating *wus2* and *bbm*. We evaluate regeneration rates, promoter performance, and transgene expression to determine the feasibility of this method in perennial ryegrass.

The successful application of this optimized protocol would have far-reaching implications for GM turfgrass. It not only would address a key technical limitation in turfgrass biotechnology, but also enable the implementation of advanced biocontainment strategies. Moreover, the method offers potential for further optimization, increasing its utility for stacking complex genetic traits necessary for next-generation turfgrass varieties.

4.2 Materials and Methods

4.2.1 Key Components

Culture components such as Murshag & Skroog medium; 2,4-D; BA; etc. were all purchased from Phytotech (Lenexa, KS). Enzymes were purchased from New England Biolabs (Ipswich,MA). Synthetic DNA such as the primers for PCR were purchased from Integrated DNA Technologies (Newark, NJ). Plasmid DNA was isolated utilizing Qiagen (Germantown, Maryland) QIAiqiuck spin columns. perennial ryegrass was grown in Sungro (Agawam, MA)

professional potting mix. Three perennial ryegrass cultivars were tested for callus formation: ‘SeaBiscuit’, ‘Pharaoh’, and ‘Arctic Green’. ‘Arctic Green’ was used for transformation.

4.2.2 Protoplast Methods

Protoplast isolation and transformations methods were adapted from Sychla et al. (2022) with key variables being taken from Yu et al. (2017) Briefly, 8 day old seedlings that had been growing in a mist house were finely cut-up and placed in enzyme solution. They were then vacuumed in the dark at 20 inHg for 30 minutes. The tissue was digested for 6 hours in a temperature-controlled room at 25°C. The protoplasts were then cleaned with two centrifugations at 100xg and re-suspensions in 5 ml W5 solution and finally purified with a 0.55 M sucrose gradient. A hemacytometer was used to measure the total amount of protoplasts. Protoplasts were then resuspended in MMG buffer to a concentration of 10^6 protoplasts ml^{-1}. Next, 10 ug of plasmid DNA, 500 ul of protoplasts, and 500 ul of 40% PEG4000 were mixed and let sit for 10 minutes in the dark. Protoplasts had 3.5 ml W5 added to them and then pelleted by centrifugation at 100xg for 5 minutes and washed with W5 solution. Protoplasts were allowed to rest overnight in W5 before readings were taken.

4.2.3 Dual Luciferase Methods

Protoplasts were transformed with plasmids from Chamness et al. (2023) (Supplementary Table 1). After the protoplasts were allowed to rest overnight, they were lysed following instructions from the Dual-Luciferase Reporter Assay System by Promega (Madison, Wi). Luciferase fluorescence measurements were taken with a microplate reader (Glomax). Each biological replicate indicates a separate protoplast transformation. After an initial failed run which didn’t

have any Renilla values, a secondary Renilla plasmid driven by the *35S* promoter was co-transformed to act as the transformation normalization factor.

4.2.4 Media Formulations

All media compositions named throughout are listed in Supplementary Table 2. For the preparation of all media, temperature stable components were mixed and adjusted to a pH of 5.7. The mixture was autoclaved, and the media containers were then cooled under a laminar flow hood. Once the media had cooled to touch, roughly 50°C, temperature sensitive components were added. Subsequently, 25 mL of the media was poured into each petri plate, cooled, sealed, and stored at 4°C until needed.

4.2.5 Seed Sterilization

Seeds of 'Arctic Green' were sterilized in a laminar flow hood following an adapted protocol from Ke and Lee, (1996) with fungicide treatment taken from Bajaj et al. (2006). Seeds were first rinsed with 70% ethanol for 1 minute. The ethanol was then decanted using sterile pipettes and the seeds were rinsed 2-3 times with autoclaved water. Subsequently, 3% sodium hypochlorite (NaOCl) and 1% sodium dodecyl sulfate solution were added, and the seeds were placed on a shaker for 1 hour at approximately 100 rpm (light shaking). After decanting the NaOCl solution, the seeds were rinsed 2-3 times with autoclaved water. Next, 20 mL of 1.5% NaOCl and 1% SDS were added, and the seeds were shaken for an additional 30 minutes. Following decantation, the seeds were rinsed 5-6 times with autoclaved water. Approximately 5 mL of autoclaved water was added to the rinsed seeds, which were deposited onto sterile petri plates containing two pieces of autoclaved filter paper. The plates were sealed and placed at 10°C for 3-7 days of stratification.

4.2.6 Sterile Seed Germination

After stratification, the seeds were removed from the 10°C storage and opened in a sterilized flow hood. The lightest color seeds were selected, and approximately 30 seeds were placed onto an agarose media plate containing fungicide (Supplementary Table 2). After all seeds were placed, the plates were sealed with micropore tape and incubated in a growth chamber at 21°C for two to four weeks.

4.2.7 Original Callus Culture Transformation Methods

Agrobacterium cultures strain AGL1 were grown overnight in LB medium (10g/L tryptone, 5g/L yeast extract, 5g/L sodium chloride) that contained the appropriate antibiotics for the vector utilized (kanamycin), at 28°C and were shaken at 200 rpm. *Agrobacterium* suspensions were pelleted at 4,500 g for 8 minutes, and re-suspended in basal MS medium containing 1% (w/v) glucose and 3% (w/v) sucrose, 400 μM acetosyringone, pH 5.2, at an OD600 of 0.80. Approximately 30 calluses were then placed into 50 mL centrifuge tubes, or until they reached the 5 mL line. Calluses was fully immersed with the *Agrobacterium* liquid culture, shaken for 30 minutes at 100 rpm at room temperature, and then placed onto a petri plate with sterile filter paper to dry. Calluses were placed onto co-cultivation medium (Supplementary Table 2) for 4 days in the dark at 25°C and were then transferred to MS selection plates (Supplementary Table 2) with desired antibiotics (hygromycin) for 2 weeks at 25°C. Calluses were subcultured one time in the same medium with half the concentration of antibiotics. After one month, growing calluses were transferred to MS regeneration medium (Supplementary Table 2) with ¼ original concentration of antibiotics and sub-cultured every 2 weeks until plants were regenerated.

4.2.8 Genetic Construct Creation

All constructs were cloned into TDNA backbones via the MoClo system outlined in Chamness et al. (2023) and utilizing the Golden Gate procedure (Engler et al., 2008). Full constructs are included in Supplementary Table 1.

4.2.9 Developmental Regulator Methods

Agrobacterium strain LBA4404 cultures were streaked from glycerol stocks onto LB plates containing the antibiotics kanamycin and gentamicin at a concentration of 50 μg/ml. Four colonies were selected and inoculated into 50 mL of liquid LB containing 1 μL/mL kanamycin and gentamicin. The cultures grew at 28°C for two days. The OD600 of the cultures was measured, and the cultures were pelleted by centrifugation at 4,500xg for 8 minutes. The pellets were resuspended in infection medium and adjusted to an OD600 of 0.6.

Plantlets were transferred to sterile petri plates, and each plant was excised and placed into the infection medium. The explants were incubated on a shaker for 20 minutes at room temperature. They were then dried on autoclaved filter paper and transferred onto 710N co-cultivation medium (Supplementary Table 2). Sterile filter paper was placed on top of the medium to facilitate transfer. The plates were sealed with parafilm and incubated in the dark at 21°C for two days.

After co-cultivation, explants were transferred to resting media (Supplementary Table 2) for two weeks and subsequently transferred to selection media (Supplementary Table 2) containing kanamycin for two weeks at 21°C in the dark. To induce the heat shock response of the *Hsp17* promoter and activate the Cre recombinase, cultures were incubated at 45°C for two hours.

Explants were then transferred to maturation medium (404) (Supplementary Table 2) without filter paper and incubated at 28°C in the dark for two weeks. Afterward, the explants were moved to a 26°C light condition for one week. Transformed explants were transferred to the rooting medium (Supplementary Table 2) until regeneration or callus death occurred. Once regenerated roots and shoots were observed, they were transferred to soil and grown in the greenhouse.

4.2.10 Transformation Confirmation

After plants had been transferred to the greenhouse, DNA was extracted from a single leaf with DNAzol reagent following manufacturer's instructions. PCRs utilizing Q5 DNA polymerase from NEB were conducted with the genomic DNA following manufacturer's instructions and utilizing primers 5'-gctgctctagccaatacgca-3' + 5'-acgagccggaagcataaagt-3', and 5'-agcacagtggagtagggtat-3' + 5'-attgtcaggttcggttctagtcttctt-3' to confirm transgenesis and *cre* excision. PCR conditions were 98°C for 1 minute, 35 repeats of 98°C for 10 seconds, 68°C for 30 seconds, 72°C for 20 seconds, and a final extension at 72°C for 2 minutes. Conditions for *cre* excision were the same, except for the annealing temperature being 66°C and the extension time being 80 seconds.

4.3 Results

4.3.1 Callus Induction and Transformation Without Developmental Regulators

To assess the feasibility of genotype-independent transformation, we modified methods based on Bajaj et al. (2006) (Figure 4.1A). A new mercury-free seed sterilization protocol was developed that successfully reduced endophyte and surface contamination. Importantly, we found that fungicide treatment was necessary to eliminate the endophyte (Supplemental Figure 4.1). While

early-stage contamination occasionally occurred, contamination-free tissue transferred beyond the seedling stage remained contamination-free for the entirety of the protocol.

Three tissue types were evaluated for callus induction: crown, transition zone (between crown and leaf), and leaf tissue (Figure 4.1B). For each of three tested cultivars (‘SeaBiscuit’, ‘Pharaoh’, ‘Arctic Green’), 40 seedlings each were dissected and placed on a callus induction medium. The crown consistently induced the highest callus formation (Arctic Green - 75% ± 5.6, Pharaoh - 70% ± 9.3, SeaBiscuit - 80% ± 5.0), intermediate zones showed moderate induction (Arctic Green - 32.5% ± 6.4, Pharaoh - 30% ± 6.4, SeaBiscuit - 40% ± 4.7), and leaves rarely produced callus, occurring only once in ‘Arctic Green’ (Figure 4.1C).

Calluses typically formed within one month and could proliferate for up to six months (Figure 4.1D). Calluses were transformed with a plasmid containing hygromycin resistance and RFP (Supplemental Table 4.1). Two weeks post-transformation and antibiotic selection, RFP expression confirmed successful transformation in 74% of 104 calluses (Figure 4.1D, Supplementary Figure 4.3). However, no transformed callus regenerated into plants.

4.3.2 Dual Luciferase Assay

A dual luciferase assay was conducted to characterize optimal promoters for transgene expression in perennial ryegrass (Figure 4.2). The *PvUbi2* promoter demonstrated the highest relative activity, having 5.4 ± 0.25 fold higher expression than CmYLCV. This was followed by the maize and rice ubiquitin promoter, each having 3.55 ± 0.97 and 3.133 ± 0.77 higher fold expression. The promoters Os*EF1a, ZmEf1a, 2x35S* and *Nos* were statistically not different from *CmYLCV*.

4.3.3 Callus Induction & Transformation with Developmental Regulators

To overcome regeneration limitations, we adapted the method of N. Wang et al. (2023) incorporating *wus2* and *bbm* driven by various promoters, with or without *cre* recombinase. Eight constructs were tested in total (Figure 4.3A, Supplementary Table 4.1).

Callus induction was re-evaluated during these experiments and confirmed previous findings that crown tissue yielded the highest callus induction. Intermediate tissue showed reduced rates, and leaf tissue remained non-responsive. This held true whether or not developmental regulators were included (Figure 4.3B).

Following transformation, tissues were subjected to selection and regeneration. Control transformations lacking developmental regulators failed to regenerate, even when surviving selection. In contrast, tissues transformed with *wus2/bbm* constructs successfully regenerated into plants. The role of *cre* recombinase was tested to assess its impact on regeneration: inclusion of *cre* significantly enhanced regeneration rates changing from a mean regeneration of 11.05 ± 3.6% to 34.4 ± 7.6%, with a p-value of 0.0098 (unpaired t-test) (Figure 4.3C).

Promoter strength driving the developmental regulators was tested as it is thought to be a key aspect of inducing regeneration. Contrary to this belief, no statistically significant differences were observed between tested promoter combinations. However, this may be caused by having only two replicates and high variability. The promoter combinations *Nos/3x35S, Nos/3xZmubi, OsUbi,3x35S,* and *OsUbi/3xZmubi* were able to regenerate a total of 49.8%, 25.3%, 21.5%, and 26.6%, equating to a total number of plants of 40, 16, 19, and 28, respectively (Figure 4.3D). Tissue transformed with our negative control plasmid that did not contain the cre and developmental regulators were able to form callus, but none of the callus were able to regenerate. Additionally, of the total 103 plants, 49 were albino and 54 were green and normally growing

(figure 4.3E). There was not a statistically significant difference between promoter strength or inclusion of *cre* in albino and green regeneration.

4.3.4 Genomic Confirmation of Transformation

Regenerated plants were transferred to the greenhouse (Figure 4.4AB) and subsequently had DNA extracted from them. From the first and second replicate, 41 and 32 plants were sampled, respectively. In each sample, the expected band was observed matching the positive control while the no template and four different wild type controls each showed no band (Figure 4.4C, Supplemental Figure 4.2A). Additionally, a PCR spanning the LoxP joining segment of DNA was performed and it revealed that for 55 out of 73 regenerated plants the developmental regulators were not successfully excised (Figure 4.4D, Supplemental Figure 4.2B).

4.4 Discussion

Developing efficient and broadly applicable genetic transformation protocols is essential for advancing trait engineering in perennial grasses such as *Lolium perenne* (perennial ryegrass). However, transformation in this species has been limited by endophyte contamination, lack of genetic resources, and long arduous protocols with low regeneration rates. Our study addresses these challenges by incorporating developmental regulators into transformation workflows, demonstrating a robust strategy that improves regeneration efficiency and circumvents the need for extensive genotype pre-screening. In doing so, we provide a more accessible platform for generating transgenic perennial ryegrass, with potential applications in both basic research and biotechnological innovation.

A key technical barrier in tissue culture is contamination by endophytes, which are typically beneficial in field conditions as they are able to confer pest resistance (Ma et al., 2025), but can

overgrow in sterile environments. To address this, we developed a revised seed sterilization protocol incorporating fungicide treatment. Further improvements could be made to reduce initial contamination observed on seed plates, but plates which were contamination free would remain contamination free for the entirety of the protocol. Additionally, while the removal of endophyte is necessary for transformation, it will likely be beneficial to re-inoculate (Santhanam et al., 2015) the plants after transgenesis to reintroduce positive endophyte effects.

Independent of the cultivar or transformation method, crown tissue consistently produced the highest rates of callus formation. This was followed by the intermediate tissue between crown and leaf, and leaf tissue showing negligible callus induction. This is in line with previous experiments conducted in rice (Hu et al., 2017) which showcase the farther away plant tissue is from the crown, the less likely for callus formation. Although crown tissue offers the best callus generation potential, the intermediate zone may be more suitable for certain experiments, as it allows continued propagation of the source plant. Additionally, other tissues not tested within this work may be suitable such as roots, seeds, and anthers (Ikeuchi et al., 2013; Long et al., 2022).

To gain a greater understanding of promoter activity for the expression of the developmental regulators, a dual luciferase assay was employed. Our dual luciferase assay ranked promoter strengths in perennial ryegrass, with *PvUbi2* and other ubiquitin promoters performing best. While our results confirmed trends observed in previous work by Chamness et al. (2023), the overall fold-change was lower in perennial ryegrass than in rice. This may reflect species-specific differences in promoter activity or relatively higher baseline expression of *CmYLCV* in perennial ryegrass, against which the other promoters were normalized.

Despite extensive experimentation with modified versions of established protocols, including variations in tissue type, hormone concentrations, and antibiotic selection, no viable plant regeneration was observed (data not shown). This suggests that the traditional methods are highly genotype-dependent, a limitation also noted by Bajaj et al. (2006) and Grogg et al. (2022), who both screened for responsive genotypes before proceeding with transformation. In contrast, our adoption of the N. Wang et al. (2023) approach proved effective in generating transgenic plants without first screening for conducive genotypes, removing a large bottleneck in the transformation pipeline. In future work we plan to more rigorously assess these methods in more diverse genotypes and cultivars of perennial ryegrass, as well as other species of turfgrass.

While the adoption of the N. Wang et al. (2023) methods proved to be successful in regenerating transgenic plants, several unexpected results were seen. Within our control callus induction tests, both plants that were transformed with *wus2/bbm* and plants transformed without the developmental regulators formed callus at equal rates. This indicates that the media itself is capable of inducing calluses, and that *wus2* and *bbm* do not increase the efficiency of callus induction. However, despite the ability for callus to be induced, only the plants including *wus2/bbm* resulted in plant regeneration. The inclusion of the developmental genes may enhance regeneration, a finding also noted in several other studies (Gordon-Kamm et al., 2019; Lowe et al., 2016; J. Wang et al., 2023).

The presence of *cre* recombinase was statistically correlated with successful regeneration, consistent with findings in N. Wang et al. (2023): however, the mechanism underlying this effect remains unclear. It was initially hypothesized to be attributed to Cre-mediated excision of the developmental regulators, but PCR analysis of the *cre* excision revealed that only 25% of regenerated plants had the genes excised. Other factors, such as heat-shock treatment, may also

play a role (Dündar et al., 2024), as the control samples without *cre* were not put under a heat shock. No noticeable phenotypic differences have been noted in our plants retaining the recombinase and developmental regulator genes, but negative phenotypes in plants retaining the genes has been noted in other findings (Ikeuchi et al., 2013). Further crossing of the plants may be necessary to remove the genes, or an improved marker system to better track the excision of *cre*, as showcased in Wu et al., (2025), may be desirable.

In conclusion, our study advances the genetic toolkit for perennial ryegrass by demonstrating an effective transformation strategy that eliminates the need for pre-screening of genotypes ability to regenerate and dramatically reduces the overall time of the protocol (Figure 4.5). Future improvements utilized in N. Wang et al. (2023) but not tested here, such as automated tissue sectioning and the inclusion of growth-enhancing compounds like ancymidol, could further increase throughput and consistency. Additionally, the swapping of confirmations markers from *mgfp6* to the RUBY marker as utilized in Wu et al. (2025) could allow for simpler tracking of transformation and successful *cre* excision.

4.5 Figures

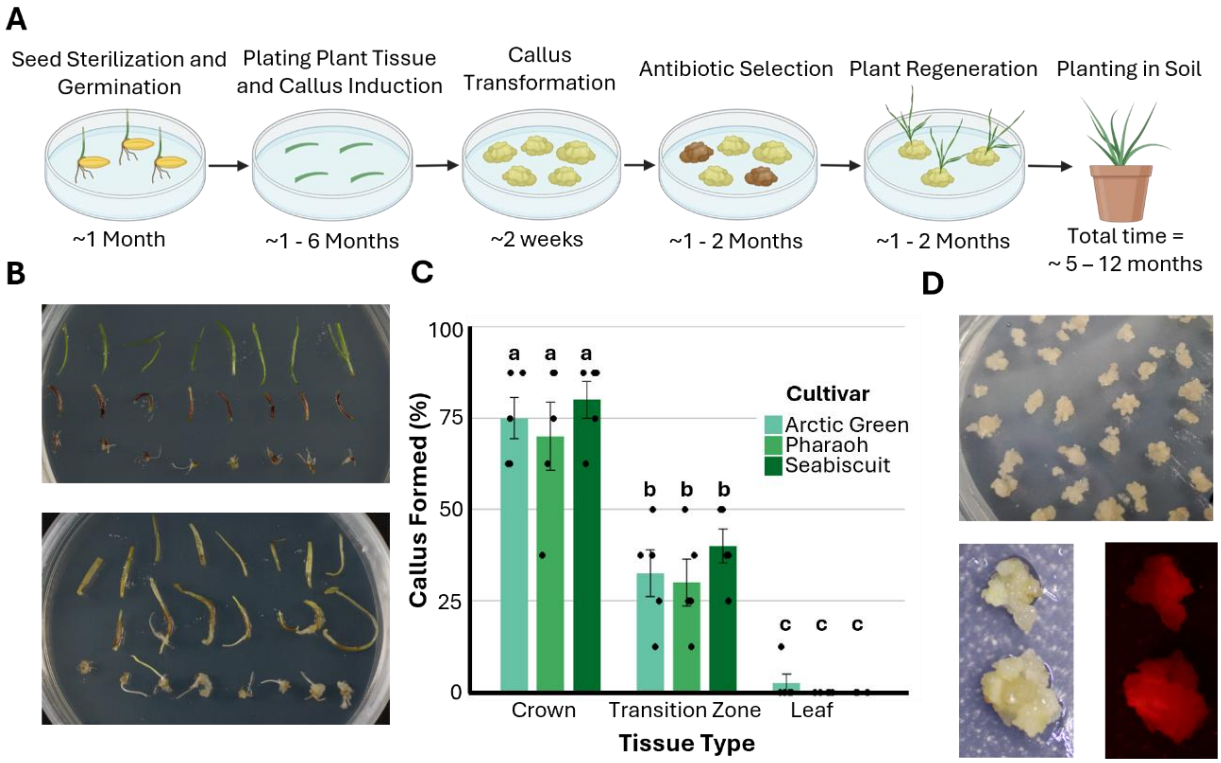

Figure 4.1. Tissue culture and callus formation efficiency in perennial ryegrass.

(A) Schematic overview of the proposed transformation pipeline in perennial ryegrass. (B) Representative images of plated explants before (top) and after (bottom) callus formation. (C) Quantification of callus formation across three tissue types (crown, transition zone, leaf) for three cultivars (‘Arctic Green’, ‘Pharaoh’, ‘Seabiscuit’). Data represent means ± SE (n = 5 biological replicates). Individual data points are shown. Bars sharing the same letter are not significantly different (ANOVA with Tukey's HSD, $p < 0.05$). (D) Representative images of embryogenic calluses prior to transformation (top), post-transformation (bottom left), and showing red fluorescence (bottom right), indicating successful expression of the reporter gene.

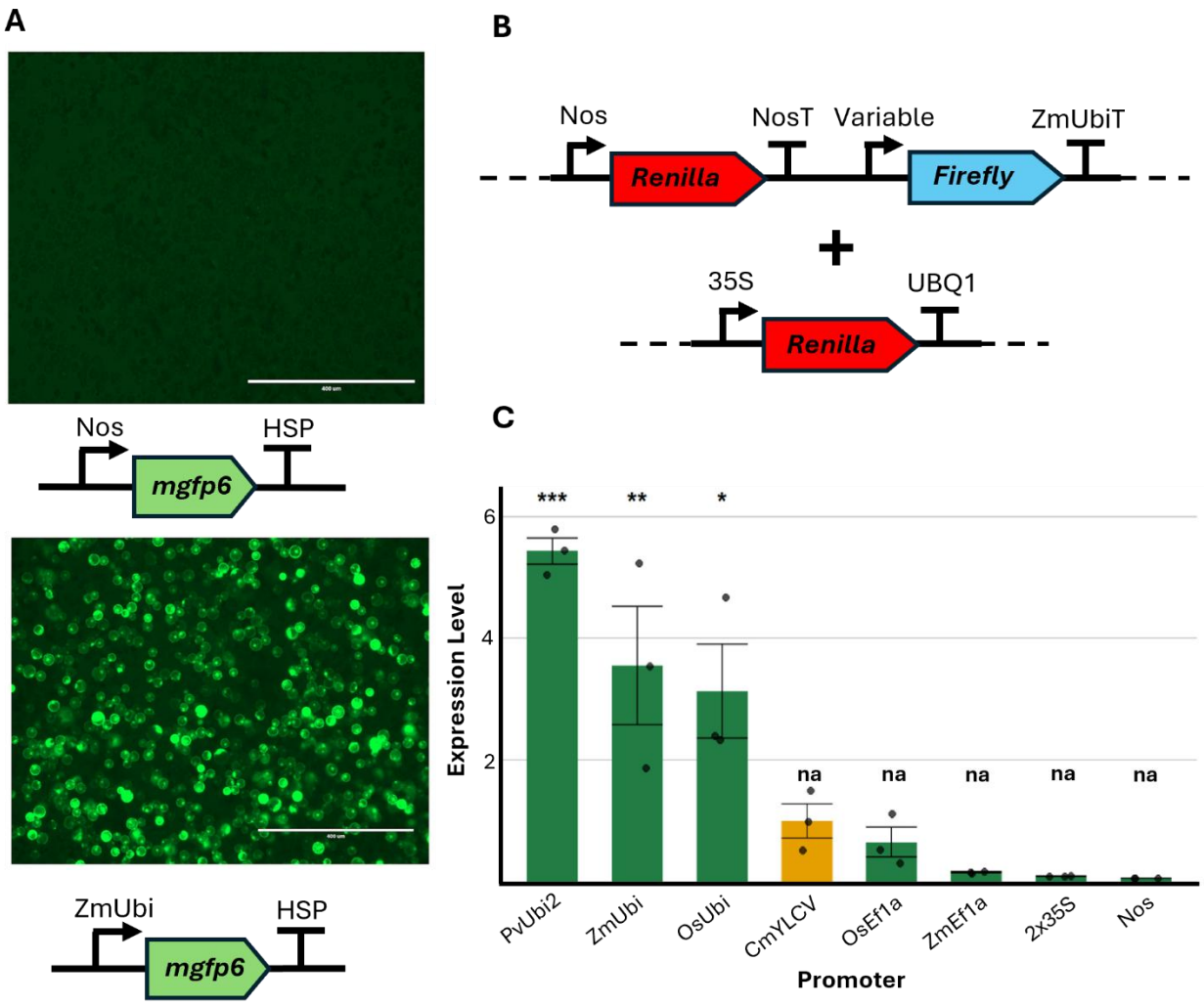

Figure 4.2. Protoplast transformation and promoter activity in perennial ryegrass.

(A) Transient expression of *mgfp6* driven by the Nos (top) or ZmUbi (bottom) promoter in protoplast cells visualized by fluorescence microscopy 24 hours after transformation. Strong fluorescence was observed under the ZmUbi promoter, while little to no signal was detected with the Nos promoter. Scale bars = 400 µm. (B) Schematic of the dual-luciferase reporter constructs used to quantify promoter activity. The experimental construct contains a Firefly luciferase reporter under the control of a variable promoter, and a Renilla luciferase gene driven by a Nos promoter for normalization. A second construct expressing Renilla under the 35S promoter and terminated by UBQ1 was co-transformed due to lack of Renilla signal. (C) Quantification of relative Firefly luciferase activity driven by different promoters in ryegrass protoplasts. Data are normalized to Renilla luciferase and shown as mean ± SD (n = 3). Asterisks indicate statistical

significance compared to the CmYLCV promoter ($p < 0.05$, $\mathbf{p} < 0.01$, $\boldsymbol{p} < 0.001$). “na” indicates expression was not statistically different from CmYLCV.

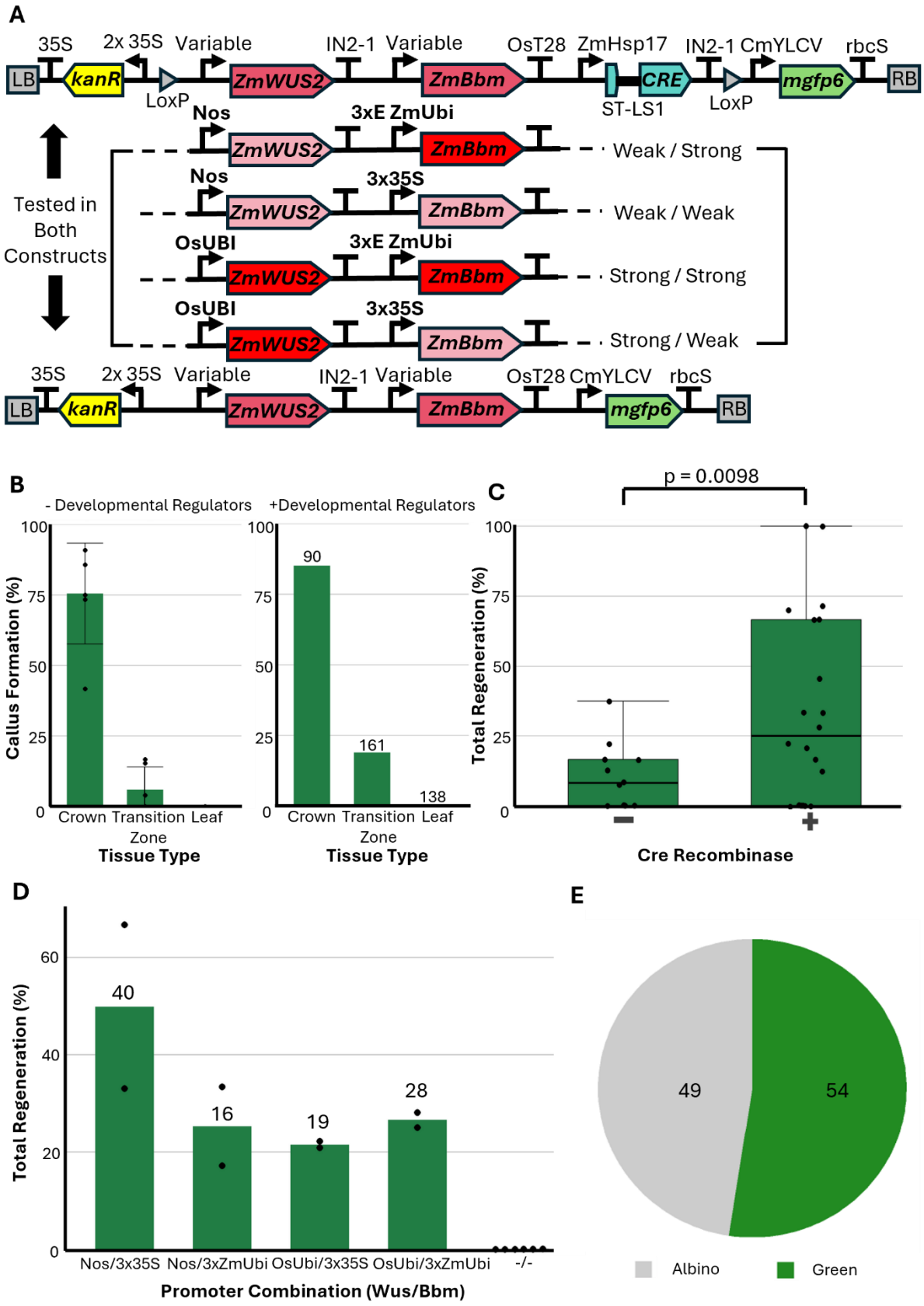
A
35S
2x 35S
Variable
IN2-1
Variable
OsT28
ZmHsp17
IN2-1
CmYLCV
rbcS
LB
kanR
LoxP
ZmWUS2
ZmBbm
CRE
ST-LS1
LoxP
mgfp6
RB
Tested in Both Constructs
Nos
3xE ZmUbi
Weak / Strong
3x35S
Weak / Weak
OsUBI
Strong / Strong
Strong / Weak
B
- Developmental Regulators
+Developmental Regulators
Callus Formation (%)
Crown
Transition
Leaf
Zone
Tissue Type
90
161
138
C
p = 0.0098
Total Regeneration (%)
Cre Recombinase
D
Total Regeneration (%)
40
16
19
28
Nos/3x35S
Nos/3xZmUbi
OsUbi/3x35S
OsUbi/3xZmUbi
-/-
Promoter Combination (Wus/Bbm)
E
49
54
Albino
Green

Figure 4.3. Optimization of regeneration in perennial ryegrass using developmental regulators and Cre-lox recombination.

(A) Schematic of transformation constructs containing maize developmental regulators *ZmWUS2* and *ZmBbm* driven by different promoter combinations (*Nos, 3×35S, ZmUbi, OsUbi*), with or without *cre* recombinase and loxP sites. Constructs were tested in parallel to evaluate the impact of promoter strength and Cre-mediated recombination on regeneration. (B) Callus formation efficiency across three tissue types (crown, transition zone, leaf) in the absence (left) or presence (right) of developmental regulators. Numbers above bars indicate total explants per group. (C) Regeneration frequency with or without *cre* recombinase. Addition of *cre* significantly increased total regeneration percentage ($p = 0.0098$, unpaired t-test). (D) Regeneration efficiencies by *wus2/bbm* promoter combination and a negative control without developmental regulators. The number above each bar represents the total number of regenerated plants. Bullet points represent a full protocol replication, with data from part (C) being averaged into one bullet point per treatment, and the second being a full replication. (E) Distribution of regenerated plants. Of the total regenerated plants, 54 were green and grew normally, while 49 were albino and did not form roots.

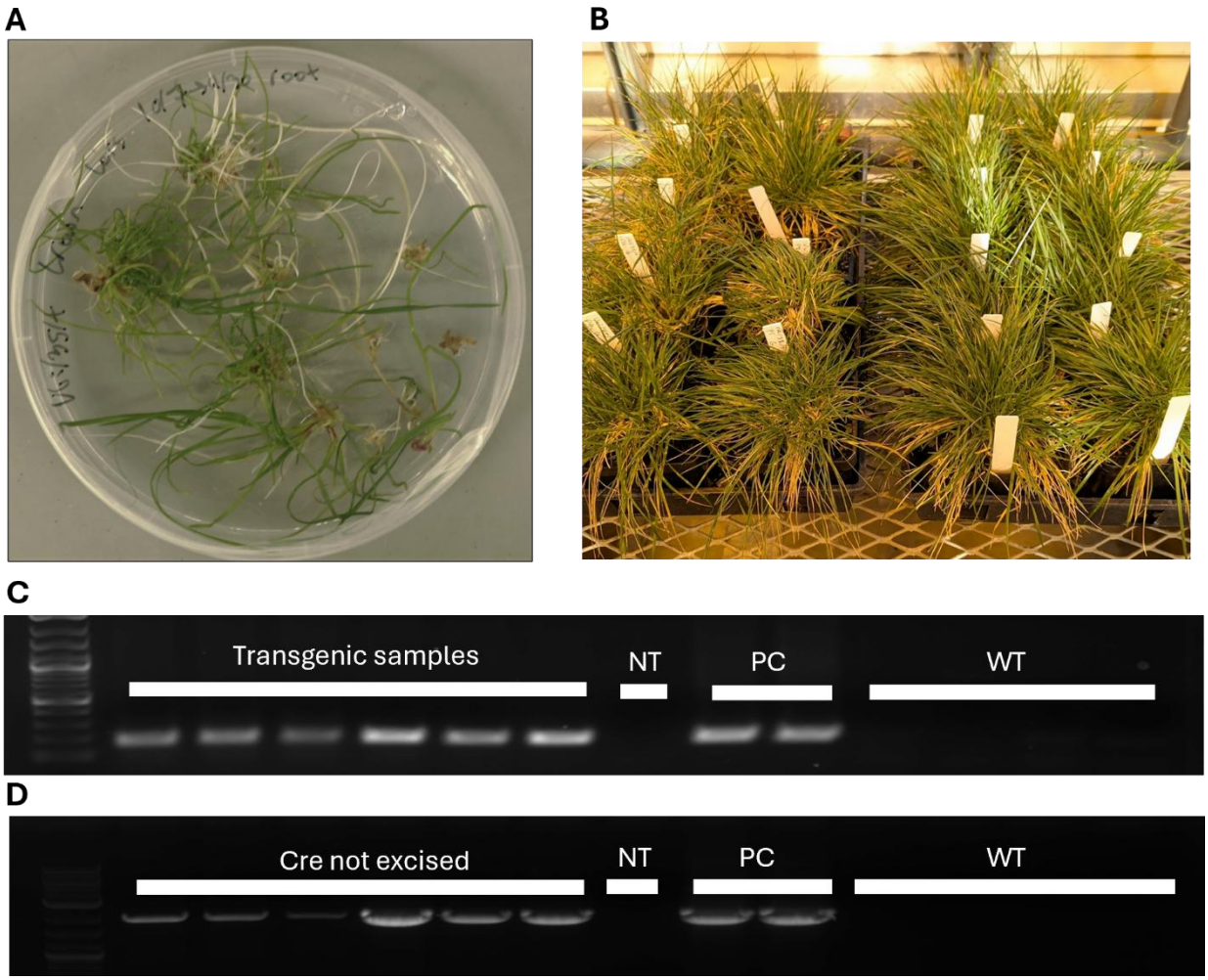

Figure 4.4. Regeneration and molecular validation of transgenic perennial ryegrass.

(A) Regenerated transgenic plantlets prior to soil transfer and (B) established plants growing in the greenhouse. (C) PCR confirmation of transgene presence in regenerated plants. Multiple transgenic samples show amplification of the target band, with no amplification observed in the no template control (NT) or wild-type (WT) samples. Positive control (PC) bands are plasmids Ubi/Zm/+ and nos/35/+. (D) PCR assay detecting Cre-mediated excision of the transgenes.

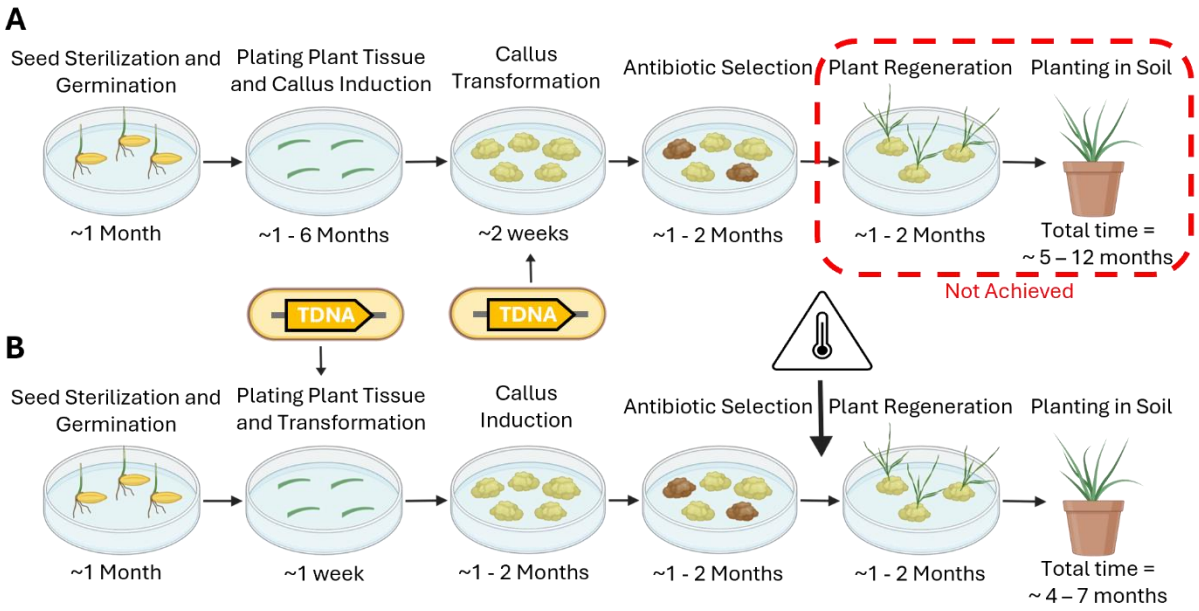

Figure 4.5: Schematic comparison of both protocols

Original callus protocol (A) in comparison to the new developmental regulator protocol (B). The original protocol was longer and unable to regenerate plants, while the new protocol is shorter and succeeded in creating transformed plants.

4.6 Supplementary Tables

Plasmid Name	Description	Benchling Link
Nos::Firefly	Plasmid from Chamness et al. (2023) that tests the strength of the Nos promoter to drive firefly luciferase. Results in fig 2.	**https://benchling.com/s/seq-Wa5Wkt67K2QSKIXC5mky?m=slm-QS9tDo5dc8JCDu83k3dH**
2xCaMV35S::Firefly	Plasmid from Chamness et al. (2023) that tests the strength of the 2xCaMV35S promoter to drive firefly luciferase. Results in fig 2.	**https://benchling.com/s/seq-XVdVYNe0WT45Vq9pREYJ?m=slm-kAyQIezoLtrG7D5OHxe5**
CmYLCV::Firefly	Plasmid from Chamness et al. (2023) that tests the strength of the CmYLCV promoter to drive firefly luciferase. Results in fig 2.	**https://benchling.com/s/seq-LPcZp7rWmbXiBpUR0wd7?m=slm-MnUxDbGyvzqICQWhWz9F**
OsEF1a::Firefly	Plasmid from Chamness et al. (2023) that tests the strength of the OsEF1a promoter to drive firefly luciferase. Results in fig 2.	**https://benchling.com/s/seq-TJvXhVyWEZtrKkOVOzKH?m=slm-wTe2NzXoprw43BZ1CC26**
OsUbi1::Firefly	Plasmid from Chamness et al. (2023) that tests the strength of the OsUbi1 promoter to drive firefly luciferase. Results in fig 2.	**https://benchling.com/s/seq-o4xLJvGIkIy0cb9u7lyB?m=slm-aXa1rU2B2mZ0PlwMFDV4**
PvUbi2::Firefly	Plasmid from Chamness et al. (2023) that tests the strength of the PvUbi2 promoter to	**https://benchling.com/s/seq-fjDAL9WrsitpYo1mpoGe?m=slm-eEU3BVMTXh4rTNAbIilo**

	drive firefly luciferase. Results in fig 2.	
ZmEF1a::Firefly	Plasmid from Chamness et al. (2023) that tests the strength of the ZmEF1a promoter to drive firefly luciferase. Results in fig 2.	**https://benchling.com/s/seq-wa73ejQWpLyIvVsN961g?m=slm-hCz6qd5AwN40RUo1KIjC**
ZmUbi::Firefly	Plasmid from Chamness et al. (2023) that tests the strength of the ZmUbi promoter to drive firefly luciferase. Results in fig 2.	**https://benchling.com/s/seq-ox9Uf4Cv1yyTdM9DKUdc?m=slm-rGLeGtINzFTGfnuXZERH**
35S::Renilla	Plasmid from Chamness et al. (2023) that tests the strength of the 35S promoter to drive firefly luciferase. Results in fig 2.	**https://benchling.com/s/seq-YlKAUxMhXFPKwAeg495k?m=slm-rkiUhXNg4EuPD86AtNnd**
pMOD_A3010	Plasmid from Voytas lab that has the Nos promoter driving mgfp6. Results in fig 2.	**https://benchling.com/s/seq-wPrKh0Gmo5NBxmTEtNSq?m=slm-6HRqa2AFjTnUecBg0Zjl**
pMOD_A3014	Plasmid from Voytas lab that has the ZmUbi promoter driving mgfp6. Results in fig 2.	**https://benchling.com/s/seq-BWg0WjKXHRGmv7HBzalj?m=slm-KMmckhLkvub8kIyXGGfz**
RFP TDNA	Plasmid used to test transformation of original callus culture protocol	**https://benchling.com/s/seq-79Ir1Ecyxsv698e3ZhqK?m=slm-RJPUezz1xjos67dG1BVB**
Negative Control TDNA	Plasmid without developmental regulators used	**https://benchling.com/s/seq-lflKNFTDtn5pdq3NFR3Y?m=slm-562Y83hZsi6r9ddyD72w**

	as a negative control for callus formation and regeneration.	
nos/35s/+ TDNA	Plasmid to test developmental regulator protocol. Nos promoter drives ZmWus, 35s promoter drives Bbm and the plasmid contains the cre recombinase.	**https://benchling.com/s/seq-NdI6yYlUPbtuuHZ5BGsx?m=slm-mMDuEehaeprrqvfIlcEr**
nos/35s/- TDNA	Plasmid to test developmental regulator protocol. Nos promoter drives ZmWus, 35s promoter drives Bbm and the plasmid does not contain the cre recombinase.	**https://benchling.com/s/seq-k4pHKJGayDVZRXrpgGOF?m=slm-QEkAVNxx3f4iP6tPF3eq**
osubi/zmubi/+ TDNA	Plasmid to test developmental regulator protocol. OsUbi promoter drives ZmWus, ZmUbi promoter drives Bbm and the plasmid contains the cre recombinase.	**https://benchling.com/s/seq-nLHbYPheJRICyvGjBmBy?m=slm-pcxE4VEiI20VnmHablkC**
osubi/zmubi/- TDNA	Plasmid to test developmental regulator protocol. OsUbi promoter drives ZmWus, ZmUbi promoter drives Bbm and the plasmid does not contain the cre recombinase.	**https://benchling.com/s/seq-sts5sl8ky6zAyUNHSEVS?m=slm-mgFrbmA7u9ccadrn7Lmm**
osubi/35s/+ TNDA	Plasmid to test developmental regulator protocol. OsUbi promoter drives ZmWus, 35s promoter drives Bbm and the plasmid contains the cre recombinase.	**https://benchling.com/s/seq-7qlxqtK8NH8bSzTLTd6I?m=slm-ZJBIDZNz47Os1SBIeWl4**

osubi/35/- TDNA	Plasmid to test developmental regulator protocol. OsUbi promoter drives ZmWus, 35s promoter drives Bbm and the plasmid does not contain the cre recombinase.	**https://benchling.com/s/seq-cBKXG9jXXulkfBdgMERa?m=slm-nQQdLdP3ntUTXv02dwBP**
nos/zmubi/+ TDNA	Plasmid to test developmental regulator protocol. Nos promoter drives ZmWus, ZmUbi promoter drives Bbm and the plasmid contains the cre recombinase.	**https://benchling.com/s/seq-74TuRaz8cR2tLjBTFx2U?m=slm-vZeVIWvq2sxdcXgvG8e3**
nos/zmubi/- TDNA	Plasmid to test developmental regulator protocol. Nos promoter drives ZmWus, ZmUbi promoter drives Bbm and the plasmid does not contain the cre recombinase.	**https://benchling.com/s/seq-b2m6VSnvBfJCvmC8K42A?m=slm-FQWeIC0bl4QeRX0s25NU**

Supplementary Table 4.1

List of plasmids, their description, and benchling link to full plasmid map for every plasmid used in this paper.

Fungicide Seed Plates	2.2g MS media for ½ strength 0.5g MES buffer 8g phytoblend for 0.8% 15g sucrose for 1.5% 10ml of 4g/L benomyl fungicide stock solution
Culture Plates	4.4g MS media for full strength 0.5g MES buffer 8g phytoblend for 0.8% 30g sucrose for 3% 5ml of 1mg/ml 2,4-D stock solution

Subculture Plates	4.4g MS media for full strength 0.5g MES buffer 8g phytoblend for 0.8% 30g sucrose for 3% 1ml of 0.1mg/ml BA stock solution 2ml of 1mg/ml 2,4-D stock solution
Coculture Plates	4.4g MS media for full strength 0.5g MES buffer 8g phytoblend for 0.8% 30g sucrose for 3% 10g glucose for 1% 1ml of 0.1mg/ml BA stock solution 2ml of 1mg/ml 2,4-D stock solution 1ml of 400mM acetosyringone stock solution
Subculture And Antibiotic Plates	4.4g MS media for full strength 0.5g MES buffer 8g phytoblend for 0.8% 30g sucrose for 3% 1ml of 0.1mg/ml BA stock solution 2ml of 1mg/ml 2,4-D stock solution 1ml of 50mg/ml hygromycin stock solution 250ul of 200mg/ml timentin stock solution
Regeneration Plates	4.4g MS media for full strength 0.5g MES buffer 8g phytoblend for 0.8% 30g maltose for 3% 10ml of 0.1mg/ml BA stock solution 0.5ml of 50mg/ml hygromycin stock solution 250ul of 200mg/ml timentin stock solution

Supplementary Table 4.2

List of every media and its contents used in the original callus culture protocol.

Silver Nitrate Stock	100 mg Silver Nitrate (Preferably Sigma #S7276) 50 mL Di water

N6 Macro Nutrient Stock	1.66 g/L -Calcium Chloride 4.62 g/L -Ammonium Sulfate 4 g/L -Monopotassium phosphate 1.85 g/L -Magnesium Sulfate 28.3 g/L -Potassium nitrate
B5H Minor Salts	3 g/L -Boric acid 10 g/L -Manganese sulfate .25 g/L -Sodium molybdate .75 g/L -Potassium iodide 3.7 g/L -EDTA 2.79 g/L Ferrous sulfate
MS Vitamin Corteva Stock	.4 g/L Glycine .1 g/L Nicotinic acid .1 g/L Pyridoxine HCL .02 g/L -Thiamine HCL
Basal Medium	1.204g/L -Magnesium sulfate, Anhydrous 5 g/L -Maltose
Infection Medium (Make fresh night before)	100mL -Basal Liquid 100 µL/100 mL -Thymidine (50 mg/mL) 200 µL/100 mL -Acetosyringone (100 mM) 100 µL/100 mL -Break-thru (10% v/v)

Co-Cultivation Medium	.33 g/L -Phytotech Gamborg MS .1 g/L -Myo-inositol .7 g/L -L-proline 20 g/L -Maltose 10 g/L -Glucose .5 mL/L -Nicotinic acid (1 mg/mL) .5 mL/L -Pyridoxine (1 mg/mL) 2.5 mL/L -Thiamine (0.4 mg/mL) 0.049 mL/L -Cupric sulfate (100 mM) 4 mL/L -2,4-D (0.5 mg/mL) .5 g/L -MES **PH 5.6** 8 g/L Phytoblend **AUTOCLAVE** 1 mL/L -Acetosyringone (100 mM) 1 mL/L -Ascorbic acid (10 mg/mL) 1.7 mL/L -Silver nitrate (2 mg/mL) 2 mL/L -Thymidine (25 mg/mL)
Resting Medium	4.33 g/L --Phytotech Gamborg MS 60 mL/L -N6 Macronutrient Stock 0.6 mL/L -B5H Minor Salts (1000x) 6 mL/L -NaFe EDTA for B5H (100x) 0.4 mL/L -Eriksson's Vitamins 0.6 g/L -S&H Vitamins powder 1.68 g/L -Potassium Nitrate 0.5 mL/L -Thiamine (0.4 mg/mL) 1.98 g/L -L-proline .3 g/L -Casein Hydrolysate (acid) 1.6 mL/L 2,4-D (0.5 mg/mL) 20 g/L Sucrose .6 g/L Glucose **PH 5.6** 6 g/L Phytoblend **AUTOCLAVE** 1.2 mL/L -Dicamba (1 mg/mL) 1 mL/L -Silver Nitrate (2 mg/mL) 10 mL/L Meropenem (5 mg/mL)
Selection medium	Resting Medium 150mg/L Kanamycin

Maturation Medium	.61 g/L --Phytotech Gamborg MS .1 g/L -Myo-inositol .7 g/L -L-proline 85 g/L Sucrose 5 mL/L -MS Vitamin Stock 1.25 mL/L -Cupric sulfate (1 mg/mL) 1.2 g/L -Ammonium Nitrate 2.52 g/L -Potassium Nitrate .193 g/L -Sodium Phosphate Monobasic .06 mL/L Zeatin (0.5 mg/ml) 2 mL/L IBA (1 mg/ml) **PH 5.6** 6g/L Phytoblend **AUTOCLAVE** 1mL/L -MetaTopolin (0.5 mg/mL) .1 mL/L -Thidiazuron (1 mg/ml) 1 mL/L -ABA (0.1 mM) 2 mL/L -IAA (0.5 mg/mL) 2 mL/L -Meropenem (5 mg/mL)
Rooting Medium	4.33 g/L --Phytotech Gamborg MS .1 g/L Myo-inositol 40 g/L Sucrose 5 mL/L MS Vitamin Cortiva Stock **PH 5.6** 6 g/L Phytoblend **AUTOCLAVE** .5 mL/L -IBA (1 mg/mL) 2 mL/L Meropenem (5 mg/mL)

Supplementary Table 4.3

List of every media and its contents used in the developmental regulator protocol.

4.6 Supplementary Figures

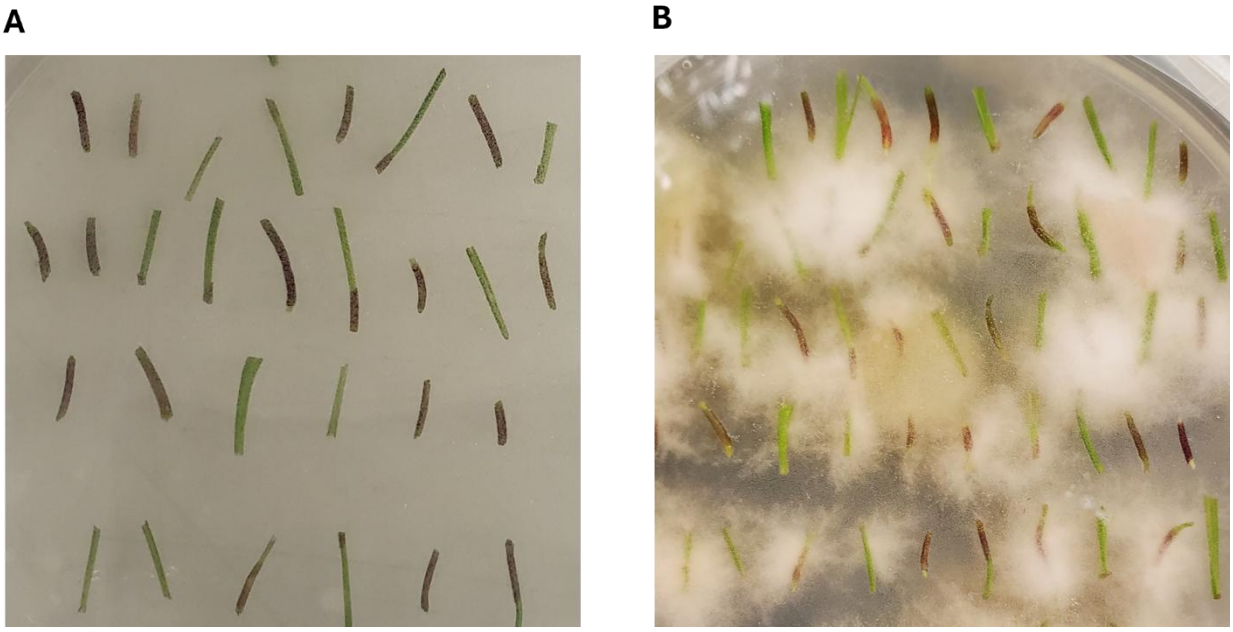

Supplementary Figure 4.1.

Before (A) and after (B) endophyte contamination of tissue on culture induction plates from tissue that was not treated with fungicide.

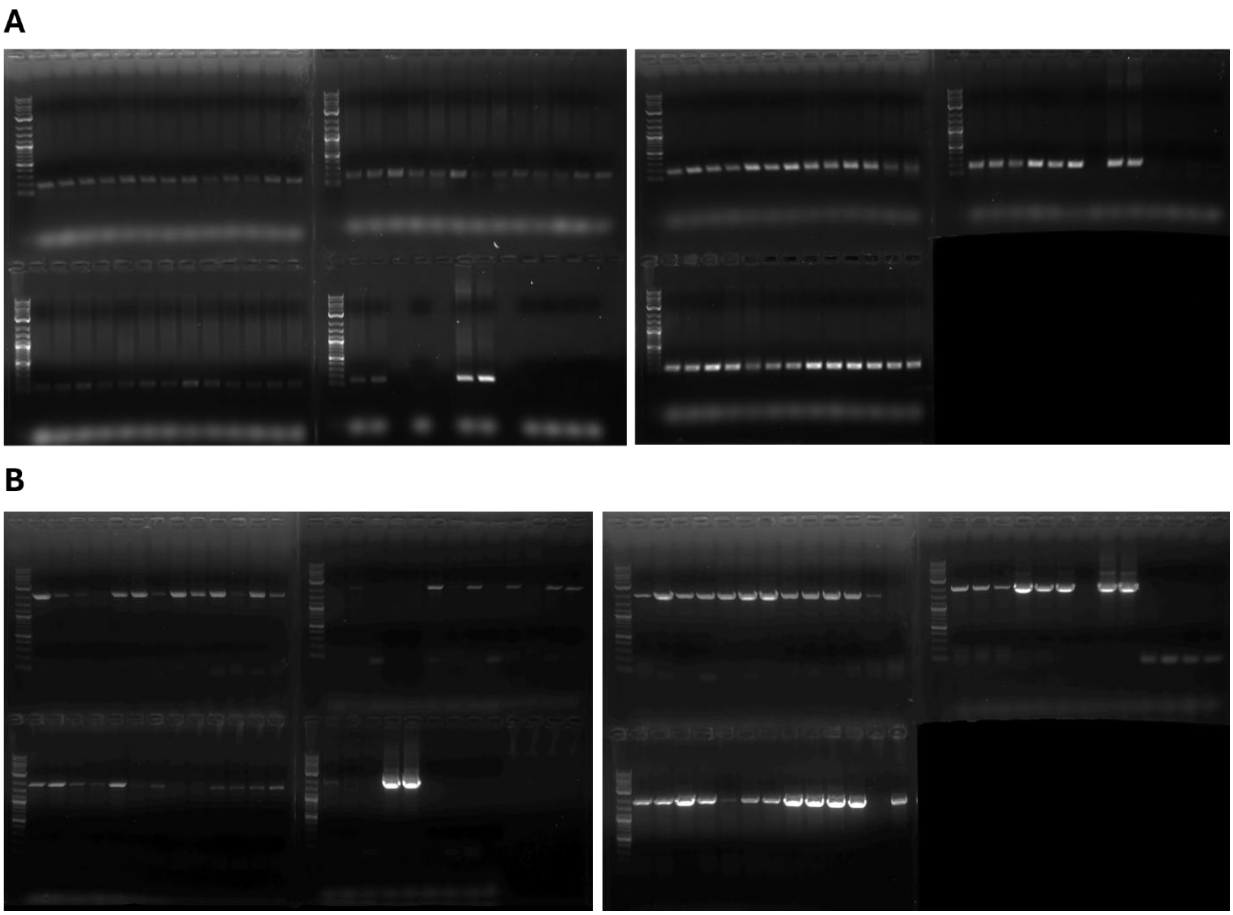

Supplementary Figure 4.2

Full gels for confirmation of transformation (A) and cre excision (B). The first gel image is the first replicate, and the second gel is the second replicate. All wells before the final 6 are tested samples while the final 6 correspond to a no template control, Ubi/Zm/+ and nos/35/+ positive plasmid control, and 4 different wild type controls.

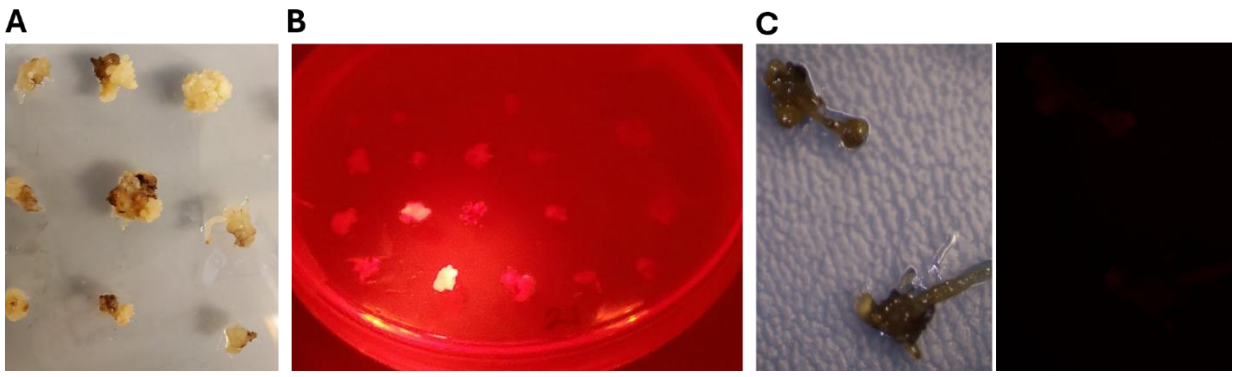

Supplementary Figure 4.3

(A) Callus responding differently to antibiotic selection. (B) Differential expressions of RFP in callus. (C) Dead callus that didn't survive antibiotic selection giving off no RFP signal.

Conclusion and Future Directions For EGI

This research sought to advance the state of Engineered Genetic Incompatibility (EGI) beyond the foundations established by Zinselmeier et al. (2025). In *Arabidopsis*, significant improvements were achieved through optimized genetic construct design, specifically, the use of the *pRpl23* promoter and the insertion of 11 introns into the *dCas9* coding sequence, and the selection of a new target, *ELO1*. These modifications resulted in a peak lethality of 93% in the best-performing line. However, molecular analysis of escape plants via RT-qPCR revealed a critical deviation from previous models. Unlike prior studies where survivors exhibited upwards of 500-fold overexpression of the *WUS* target, the escape plants in this study showed no overexpression of the target gene and reduced expression of the transcriptional activator (PTA). This identifies a novel mechanism of resistance: the silencing of the PTA or the target gene itself, rather than the failure to induce lethal overexpression.

While this silencing mechanism represents a newly identified failure mechanism, it underscores the complexity of maintaining EGI stability. Zinselmeier et al. (2025) previously demonstrated that environmental variables, such as a 3-day cold treatment of the seeds before planting, could compromise lethality. Consequently, these findings highlight the necessity for rigorous stress testing once a 100% lethality proof-of-concept is established. Future validation must subject plants to biotic and abiotic pressures, including light, heat, drought, and salinity, to ensure mechanism robustness. Furthermore, multigenerational studies are essential to determine if EGI components degrade over time. Finally, to ensure broad applicability, analyses of wild population promoter sequences must be conducted to verify that designed guide RNAs remain effective across diverse genetic backgrounds, as suggested by Feltman et al. (2022).

Chapter 3 addressed the translation of the EGI mechanism to the agronomically significant crop pennycress. This effort encountered significant hurdles, as testing methods yielded variable data or were confounded by the lethality of the guide RNA transformation itself. These challenges illuminate a critical bottleneck in the field: the current inability to predict high-efficiency guide RNAs for PTA overexpression without empirical testing. Ideally, future innovations will allow for *de novo* prediction of guide efficacy. In the interim, high-throughput screening methods are required. Hren et al. (2025) successfully utilized whole-genome CRISPRi libraries in cyanobacteria to map fitness impacts; a largely analogous approach using plant protoplasts could revolutionize EGI development. Such a screen would identify genomic targets that induce true lethality, moving the field beyond educated guessing.

Finally, Chapter 4 examined the need for robust transformation protocols to implement EGI in diverse crops. While the use of developmental regulators in recalcitrant crops is a rapidly expanding and promising field (Kelly and Nasti, 2025; Ming et al., 2025; Nasti et al., 2026), technical feasibility is only half the battle. A critical, often overlooked factor is commercial viability. Even if EGI is perfected, the requirement for homozygous double mutations will inevitably delay the release of new cultivars. Future research must therefore assess the breeding industry's willingness to adopt biocontainment technologies, specifically weighing the value of containment against the economic cost of delayed market entry.

In summary, while EGI is not yet ready for deployment in a farmer's field, this dissertation marks a distinct maturation of the technology. The advancements detailed here, and the identification of new challenges, reflect the iterative nature of scientific progress. While new questions have arisen, the path forward is clearer, and we remain within reach of a fully functional proof of concept and the validation of EGI as a viable biocontainment strategy.

Bibliography

Anjanappa, R.B., and Gruissem, W. (2021) Current progress and challenges in crop genetic transformation. *Journal of Plant Physiology*. 261: 153411.

Azhagiri, A.K., and Maliga, P. (2007) Exceptional paternal inheritance of plastids in Arabidopsis suggests that low-frequency leakage of plastids via pollen may be universal in plants. *Plant J*. 52: 817–823.

Bajaj, S., Ran, Y., Phillips, J., Kularajathevan, G., Pal, S., Cohen, D., et al. (2006) A high throughput Agrobacterium tumefaciens-mediated transformation method for functional genomics of perennial ryegrass (Lolium perenne L.). *Plant Cell Rep*. 25: 651–659.

Basnet, P., and Ellison, S. (2024) Pennycress domestication and improvement efforts. *Crop Science*. 64: 535–559.

Bidabadi, S.S., and Jain, S.M. (2020) Cellular, Molecular, and Physiological Aspects of In Vitro Plant Regeneration. *Plants*. 9: 702.

Birchler, J.A., Bhadra, U., Bhadra, M.P., and Auger, D.L. (2001) Dosage-Dependent Gene Regulation in Multicellular Eukaryotes: Implications for Dosage Compensation, Aneuploid Syndromes, and Quantitative Traits. *Developmental Biology*. 234: 275–288.

Blume, C.J., Fei, S.-Z., and Christians, N.E. (2010) Field Evaluation of Reduced-Growth, Glyphosate-Resistant Kentucky Bluegrass in a Noncompetitive Setting. *Crop Science*. 50: 1048–1056.

Bock, R. (2015) Engineering plastid genomes: methods, tools, and applications in basic research and biotechnology. *Annu Rev Plant Biol*. 66: 211–241.

Bohra, A., Jha, U.C., Adhimoolam, P., Bisht, D., and Singh, N.P. (2016) Cytoplasmic male sterility (CMS) in hybrid breeding in field crops. *Plant Cell Rep*. 35: 967–993.

Bollhöner, B., Prestele, J., and Tuominen, H. (2012) Xylem cell death: emerging understanding of regulation and function. *J Exp Bot*. 63: 1081–1094.

Bonos, S.A., and Huff, D.R. (2015) Cool-Season Grasses: Biology and Breeding. In *Turfgrass: Biology, Use, and Management*. Edited by Stier, J.C., Horgan, B.P., and Bonos, S.A. pp. 591–660 American Society of Agronomy, Crop Science Society of America, Soil Science Society of America, Madison, WI, USA.

Botstein, D., Chervitz, S.A., and Cherry, J.M. (1997) Yeast as a Model Organism. *Science*. 277: 1259–1260.

Braun, R.C., Mandal, P., Nwachukwu, E., and Stanton, A. (2024) The role of turfgrasses in environmental protection and their benefits to humans: Thirty years later. *Crop Science*. 64: 2909–2944.

Bucchini, L., and Goldman, L.R. (2002) Starlink corn: a risk analysis. *Environ Health Perspect*. 110: 5–13.

Carter, C.A., and Smith, A. (2006) Estimating the market effect of a food scare: the case of genetically modified starlink corn. *The Review of Economics and Statistics*.

Casas-Mollano, J.A., Zinselmeier, M.H., Erickson, S.E., and Smanski, M.J. (2020) CRISPR-Cas Activators for Engineering Gene Expression in Higher Eukaryotes. *CRISPR J*. 3: 350–364.

Casas-Mollano, J.A., Zinselmeier, M.H., Sychla, A., and Smanski, M.J. (2023) Efficient gene activation in plants by the MoonTag programmable transcriptional activator. *Nucleic Acids Research*. 51: 7083–7093.

Chamness, J.C., Kumar, J., Cruz, A.J., Rhuby, E., Holum, M.J., Cody, J.P., et al. (2023) An extensible vector toolkit and parts library for advanced engineering of plant genomes. *The Plant Genome*. 16: e20312.
Chang, C., Bowman, J.L., and Meyerowitz, E.M. (2016) Field Guide to Plant Model Systems. *Cell*. 167: 325–339.
Charlesworth, D., and Charlesworth, B. (1987) Inbreeding Depression and its Evolutionary Consequences. *Annual Review of Ecology and Systematics*. 18: 237–268.
Chen, L., and Liu, Y.-G. (2014) Male sterility and fertility restoration in crops. *Annu Rev Plant Biol*. 65: 579–606.
Chen, W.-Q., Liu, C., Lu, H., Yang, S., Ma, J., Huang, Y., et al. (2025).
Cheng, Y., Dai, X., and Zhao, Y. (2006) Auxin biosynthesis by the YUCCA flavin monooxygenases controls the formation of floral organs and vascular tissues in Arabidopsis. *Genes Dev*. 20: 1790–1799.
Clark, M., and Maselko, M. (2020a) Transgene Biocontainment Strategies for Molecular Farming. *Front Plant Sci*. 11.
Clark, M., and Maselko, M. (2020b) Transgene Biocontainment Strategies for Molecular Farming. *Front Plant Sci*. 11.
Clough, S.J., and Bent, A.F. (1998) Floral dip: a simplified method for Agrobacterium-mediated transformation of Arabidopsis thaliana. *Plant J*. 16: 735–743.
Concordet, J.-P., and Haeussler, M. (2018) CRISPOR: intuitive guide selection for CRISPR/Cas9 genome editing experiments and screens. *Nucleic Acids Res*. 46: W242–W245.
Culley, T.M., and Klooster, M.R. (2007) The Cleistogamous Breeding System: A Review of Its Frequency, Evolution, and Ecology in Angiosperms. *brev*. 73: 1–30.
Dai, W., Bonos, S., Guo, Z., Meyer, W., Day, P., and Belanger, F. (2003) Expression of pokeweed antiviral proteins in creeping bentgrass. *Plant Cell Rep*. 21: 497–502.
Daniell, H. (2002) Molecular strategies for gene containment in transgenic crops. *Nat Biotechnol*. 20: 581–586.
Dobzhansky, Th. (1936) Studies on Hybrid Sterility. II. Localization of Sterility Factors in Drosophila Pseudoobscura Hybrids. *Genetics*. 21: 113–135.
Dorn, K.M., Fankhauser, J.D., Wyse, D.L., and Marks, M.D. (2013) De novo assembly of the pennycress (Thlaspi arvense) transcriptome provides tools for the development of a winter cover crop and biodiesel feedstock. *The Plant Journal*. 75: 1028–1038.
Drinnenberg, I.A., Weinberg, D.E., Xie, K.T., Mower, J.P., Wolfe, K.H., Fink, G.R., et al. (2009) RNAi in Budding Yeast. *Science*. 326: 544–550.
Dündar, G., Ramirez, V.E., and Poppenberger, B. (2024) The heat shock response in plants: new insights into modes of perception, signaling, and the contribution of hormones. *J Exp Bot*. 76: 1970–1977.
Ellison, E.E., Nagalakshmi, U., Gamo, M.E., Huang, P., Dinesh-Kumar, S., and Voytas, D.F. (2020) Multiplexed heritable gene editing using RNA viruses and mobile single guide RNAs. *Nat Plants*. 6: 620–624.
Ellstrand, Norman C. (2003) Current knowledge of gene flow in plants: implications for transgene flow. *Philos Trans R Soc Lond B Biol Sci*. 358: 1163–1170.
Ellstrand, Norman Carl (2003) Dangerous Liaisons?: When Cultivated Plants Mate with Their Wild Relatives. JHU Press.

Ellstrand, N.C., Meirmans, P., Rong, J., Bartsch, D., Ghosh, A., Jong, T.J. de, et al. (2013) Introgression of Crop Alleles into Wild or Weedy Populations. *Annual Review of Ecology, Evolution, and Systematics*. 44: 325–345.

El-Sappah, A.H., Yan, K., Huang, Q., Islam, Md.M., Li, Q., Wang, Y., et al. (2021) Comprehensive Mechanism of Gene Silencing and Its Role in Plant Growth and Development. *Front Plant Sci*. 12: 705249.

Engler, C., Kandzia, R., and Marillonnet, S. (2008) A One Pot, One Step, Precision Cloning Method with High Throughput Capability. *PLoS One*. 3: e3647.

Falcone, A., Nelissen, H., Fleury, D., Van Lijsebettens, M., and Bitonti, M.B. (2007) Cytological Investigations of the Arabidopsis thaliana elo1 Mutant Give New Insights into Leaf Lateral Growth and Elongator Function. *Ann Bot*. 100: 261–270.

Fan, J., Zhang, W., Amombo, E., Hu, L., Kjorven, J.O., and Chen, L. (2020) Mechanisms of Environmental Stress Tolerance in Turfgrass. *Agronomy*. 10: 522.

Feltman, N.R., Burkness, E.C., Ebbenga, D.N., Hutchison, W.D., and Smanski, M.J. (2022) HUGE pipeline to measure temporal genetic variation in Drosophila suzukii populations for genetic biocontrol applications. *Front Insect Sci*. 2: 981974.

Feng, Z., Mao, Y., Xu, N., Zhang, B., Wei, P., Yang, D.-L., et al. (2014) Multigeneration analysis reveals the inheritance, specificity, and patterns of CRISPR/Cas-induced gene modifications in *Arabidopsis*. *Proc Natl Acad Sci USA*. 111: 4632–4637.

Gardner, D.S., Danneberger, T.K., Nelson, E., Meyer, W., and Plumley, K. (2003) Relative Fitness of Glyphosate-resistant Creeping Bentgrass Lines in Kentucky Bluegrass. *HortSci*. 38: 455–459.

Gelvin, S.B. (2017) Integration of Agrobacterium T-DNA into the Plant Genome. *Annu Rev Genet*. 51: 195–217.

George, D.R., Danciu, M., Davenport, P.W., Lakin, M.R., Chappell, J., and Frow, E.K. (2024) A bumpy road ahead for genetic biocontainment. *Nat Commun*. 15: 650.

Ghildiyal, M., and Zamore, P.D. (2009) Small silencing RNAs: an expanding universe. *Nat Rev Genet*. 10: 94–108.

Ghoshal, B., Vong, B., Picard, C.L., Feng, S., Tam, J.M., and Jacobsen, S.E. (2020) A viral guide RNA delivery system for CRISPR-based transcriptional activation and heritable targeted DNA demethylation in Arabidopsis thaliana. *PLoS Genet*. 16: e1008983.

Gordon-Kamm, B., Sardesai, N., Arling, M., Lowe, K., Hoerster, G., Betts, S., et al. (2019) Using Morphogenic Genes to Improve Recovery and Regeneration of Transgenic Plants. *Plants*. 8: 38.

Greenberg, J.T., and Yao, N. (2004) The role and regulation of programmed cell death in plant–pathogen interactions. *Cellular Microbiology*. 6: 201–211.

Grogg, D., Rohner, M., Yates, S., Manzanares, C., Bull, S.E., Dalton, S., et al. (2022) Callus Induction from Diverse Explants and Genotypes Enables Robust Transformation of Perennial Ryegrass (Lolium perenne L.). *Plants*. 11: 2054.

Grützner, R., Martin, P., Horn, C., Mortensen, S., Cram, E.J., Lee-Parsons, C.W.T., et al. (2021) High-efficiency genome editing in plants mediated by a Cas9 gene containing multiple introns. *Plant Commun*. 2: 100135.

Haeussler, M., and Concordet, J.-P. (2016) Genome Editing with CRISPR-Cas9: Can It Get Any Better? *J Genet Genomics*. 43: 239–250.

Hagemann, R. (2004) The Sexual Inheritance of Plant Organelles. In *Molecular Biology and Biotechnology of Plant Organelles: Chloroplasts and Mitochondria*. Edited by Daniell, H. and Chase, C. pp. 93–113 Springer Netherlands, Dordrecht.

Han, Y., Jin, X., Wu, F., and Zhang, G. (2011) Genotypic differences in callus induction and plant regeneration from mature embryos of barley (Hordeum vulgare L.). *J Zhejiang Univ Sci B*. 12: 399–407.

Hartman, C.L., Lee, L., Day, P.R., and Tumer, N.E. (1994) Herbicide Resistant Turfgrass (Agrostis palustris Huds.) by Biolistic Transformation. *Nat Biotechnol*. 12: 919–923.

Heslop-Harrison, J.S. (Pat), Schwarzacher, T., and Liu, Q. (2022) Polyploidy: its consequences and enabling role in plant diversification and evolution. *Ann Bot*. 131: 1–10.

Hibberd, J.M., Sheehy, J.E., and Langdale, J.A. (2008) Using C4 photosynthesis to increase the yield of rice—rationale and feasibility. *Current Opinion in Plant Biology*., *Genome studies and Molecular Genetics, edited by Juliette de Meaux and Maarten Koornneef / Plant Biotechnology, edited by Andy Greenland and Jan Leach* 11: 228–231.

Hills, M.J., Hall, L., Arnison, P.G., and Good, A.G. (2007) Genetic use restriction technologies (GURTs): strategies to impede transgene movement. *Trends in Plant Science*. 12: 177–183.

Hojsgaard, D., and Hörandl, E. (2019) The Rise of Apomixis in Natural Plant Populations. *Front Plant Sci*. 10: 358.

Hu, B., Zhang, G., Liu, W., Shi, J., Wang, H., Qi, M., et al. (2017) Divergent regeneration-competent cells adopt a common mechanism for callus initiation in angiosperms. *Regeneration (Oxf)*. 4: 132–139.

Huang, C.-Y., and Jin, H. (2022) Coordinated Epigenetic Regulation in Plants: A Potent Managerial Tool to Conquer Biotic Stress. *Front Plant Sci*. 12.

Ikeuchi, M., Sugimoto, K., and Iwase, A. (2013) Plant Callus: Mechanisms of Induction and Repression. *The Plant Cell*. 25: 3159–3173.

Johnson, G.A., Kantar, M.B., Betts, K.J., and Wyse, D.L. (2015) Field Pennycress Production and Weed Control in a Double Crop System with Soybean in Minnesota. *Agronomy Journal*. 107: 532–540.

Kalyanaraman, B., and Zielonka, J. (2017) Green fluorescent proteins induce oxidative stress in cells: A worrisome new wrinkle in the application of the GFP reporter system to biological systems? *Redox Biol*. 12: 755–757.

Kazan, K., and Lyons, R. (2016) The link between flowering time and stress tolerance. *J Exp Bot*. 67: 47–60.

Ke, S., and Lee, C.W. (1996) Plant regeneration in Kentucky bluegrass (Poa pratensis L.) via coleoptile tissue cultures. *Plant Cell Reports*. 15: 882–887.

Keadle, S.B., Sykes, V.R., Sams, C.E., Yin, X., Larson, J.A., and Grant, J.F. (2023) National winter oilseeds review for potential in the US Mid-South: Pennycress, Canola, and Camelina. *Agronomy Journal*. 115: 1415–1430.

Klepikova, A.V., Kasianov, A.S., Gerasimov, E.S., Logacheva, M.D., and Penin, A.A. (2016) A high resolution map of the Arabidopsis thaliana developmental transcriptome based on RNA-seq profiling. *Plant J*. 88: 1058–1070.

Koornneef, M., and Meinke, D. (2010) The development of Arabidopsis as a model plant. *Plant J*. 61: 909–921.

Kumar, R., Kamuda, T., Budhathoki, R., Tang, D., Yer, H., Zhao, Y., et al. (2022) Agrobacterium- and a single Cas9-sgRNA transcript system-mediated high efficiency gene editing in perennial ryegrass. *Front Genome Ed*. 4.
Lee, J.W., Chan, C.T.Y., Slomovic, S., and Collins, J.J. (2018) Next-generation biocontainment systems for engineered organisms. *Nat Chem Biol*. 14: 530–537.
Lombardo, L. (2014) Genetic use restriction technologies: a review. *Plant Biotechnology Journal*. 12: 995–1005.
Long, Y., Yang, Y., Pan, G., and Shen, Y. (2022) New Insights Into Tissue Culture Plant-Regeneration Mechanisms. *Front Plant Sci*. 13.
Lowe, K., Wu, E., Wang, N., Hoerster, G., Hastings, C., Cho, M.-J., et al. (2016) Morphogenic Regulators Baby boom and Wuschel Improve Monocot Transformation. *The Plant Cell*. 28: 1998–2015.
Lu, B.-R., and Snow, A.A. (2005) Gene Flow from Genetically Modified Rice and Its Environmental Consequences. *BioScience*. 55: 669–678.
Luo, H., Kausch, A.P., Hu, Q., Nelson, K., Wipff, J.K., Fricker, C.C.R., et al. (2005) Controlling Transgene Escape in GM Creeping Bentgrass. *Mol Breeding*. 16: 185–188.
Ma, Z., He, J., Shen, Y., Li, Y., Wang, P., and Duan, T. (2025) Impact of Grass Endophyte on Leaf Spot in Perennial Ryegrass Caused by Bipolaris sorokiniana and Subsequent Aphids' Feeding Preference. *Agriculture*. 15: 116.
Maselko, M., Feltman, N., Upadhyay, A., Hayward, A., Das, S., Myslicki, N., et al. (2020) Engineering multiple species-like genetic incompatibilities in insects. *Nat Commun*. 11: 4468.
Maselko, M., Heinsch, S.C., Chacón, J.M., Harcombe, W.R., and Smanski, M.J. (2017) Engineering species-like barriers to sexual reproduction. *Nat Commun*. 8: 883.
Mathieu, O., Reinders, J., Čaikovski, M., Smathajitt, C., and Paszkowski, J. (2007) Transgenerational Stability of the *Arabidopsis* Epigenome Is Coordinated by CG Methylation. *Cell*. 130: 851–862.
Matsumoto, T., Wu, J., Itoh, T., Numa, H., Antonio, B., and Sasaki, T. (2016) The Nipponbare genome and the next-generation of rice genomics research in Japan. *Rice (N Y)*. 9: 33.
Matus-Cádiz, M.A., Hucl, P., Horak, M.J., and Blomquist, L.K. (2004) Gene Flow in Wheat at the Field Scale. *Crop Science*. 44: 718–727.
Matzke, A.J., and Matzke, M.A. (1998) Position effects and epigenetic silencing of plant transgenes. *Curr Opin Plant Biol*. 1: 142–148.
Matzke, M.A., and Mosher, R.A. (2014) RNA-directed DNA methylation: an epigenetic pathway of increasing complexity. *Nat Rev Genet*. 15: 394–408.
McGinn, M., Phippen, W.B., Chopra, R., Bansal, S., Jarvis, B.A., Phippen, M.E., et al. (2018) Molecular tools enabling pennycress (Thlaspi arvense) as a model plant and oilseed cash cover crop. *Plant Biotechnol J*. 17: 776–788.
McGinn, M., Phippen, W.B., Chopra, R., Bansal, S., Jarvis, B.A., Phippen, M.E., et al. (2019) Molecular tools enabling pennycress (Thlaspi arvense) as a model plant and oilseed cash cover crop. *Plant Biotechnol J*. 17: 776–788.
Merzlyak, E.M., Goedhart, J., Shcherbo, D., Bulina, M.E., Shcheglov, A.S., Fradkov, A.F., et al. (2007) Bright monomeric red fluorescent protein with an extended fluorescence lifetime. *Nat Methods*. 4: 555–557.
Moser, B.R., Knothe, G., Vaughn, S.F., and Isbell, T.A. (2009) Production and Evaluation of Biodiesel from Field Pennycress (Thlaspi arvense L.) Oil. *Energy Fuels*. 23: 4149–4155.

Orr, H.A., and Turelli, M. (2001) The Evolution of Postzygotic Isolation: Accumulating Dobzhansky-Muller Incompatibilities. *Evolution*. 55: 1085–1094.
Patel, S., Lenssen, A.W., Moore, K.J., Mohammed, Y.A., Gesch, R.W., Wells, M.S., et al. (2021) Interseeded pennycress and camelina yield and influence on row crops. *Agronomy Journal*. 113: 2629–2647.
Petty, S., Yue, C., and Watkins, E. (2024) Investigating How Nontariff Measures Impact the Turfgrass Seed Trade. *HortTechnology*. 34: 412–423.
Phippen, W.B., and Phippen, M.E. (2012) Soybean Seed Yield and Quality as a Response to Field Pennycress Residue. *Crop Science*. 52: 2767–2773.
Puchta, H. (2005) The repair of double-strand breaks in plants: mechanisms and consequences for genome evolution. *J Exp Bot*. 56: 1–14.
Qi, L., Zhang, X., Zhai, H., Liu, J., Wu, F., Li, C., et al. (2019) Elongator Is Required for Root Stem Cell Maintenance by Regulating SHORTROOT Transcription. *Plant Physiol*. 179: 220–232.
Raman, R. (2017) The impact of Genetically Modified (GM) crops in modern agriculture: A review. *GM Crops Food*. 8: 195–208.
Reichman, J.R., Watrud, L.S., Lee, E.H., Burdick, C.A., Bollman, M.A., Storm, M.J., et al. (2006) Establishment of transgenic herbicide-resistant creeping bentgrass (Agrostis stolonifera L.) in nonagronomic habitats. *Mol Ecol*. 15: 4243–4255.
Ricroch, A.E., Bergé, J.B., and Kuntz, M. (2011) Evaluation of Genetically Engineered Crops Using Transcriptomic, Proteomic, and Metabolomic Profiling Techniques. *Plant Physiol*. 155: 1752–1761.
Salgotra, R.K., and Chauhan, B.S. (2023) Genetic Diversity, Conservation, and Utilization of Plant Genetic Resources. *Genes*. 14: 174.
Santhanam, R., Luu, V.T., Weinhold, A., Goldberg, J., Oh, Y., and Baldwin, I.T. (2015) Native root-associated bacteria rescue a plant from a sudden-wilt disease that emerged during continuous cropping. *Proceedings of the National Academy of Sciences*. 112: E5013–E5020.
Santi, C., Bogusz, D., and Franche, C. (2013) Biological nitrogen fixation in non-legume plants. *Ann Bot*. 111: 743–767.
Schmitz, T.G., Schmitz, A., and Moss, C.B. (2005) The economic impact of StarLink corn. *Agribusiness*. 21: 391–407.
Sedbrook, J.C., Phippen, W.B., and Marks, M.D. (2014) New approaches to facilitate rapid domestication of a wild plant to an oilseed crop: Example pennycress (*Thlaspi arvense* L.). *Plant Science*. 227: 122–132.
Sharma, A.K., and Sharma, M.K. (2009) Plants as bioreactors: Recent developments and emerging opportunities. *Biotechnology Advances*., *Biotechnology for the Sustainability of Human Society* 27: 811–832.
Sharma, V.K., Marla, S., Zheng, W., Mishra, D., Huang, J., Zhang, W., et al. (2022) CRISPR guides induce gene silencing in plants in the absence of Cas. *Genome Biol*. 23: 6.
Shaul, O. (2017) How introns enhance gene expression. *The International Journal of Biochemistry & Cell Biology*., *Splicing* 91: 145–155.
Sheen, J. (2001) Signal Transduction in Maize and Arabidopsis Mesophyll Protoplasts. *Plant Physiol*. 127: 1466–1475.
Simon, M.K., Yuan, L., Che, P., Day, K., Jones, T., Godwin, I.D., et al. (2025).

Singh, R.K., and Prasad, M. (2016) Advances in Agrobacterium tumefaciens-mediated genetic transformation of graminaceous crops. *Protoplasma*. 253: 691–707.
Somssich, M., Je, B.I., Simon, R., and Jackson, D. (2016) CLAVATA-WUSCHEL signaling in the shoot meristem. *Development*. 143: 3238–3248.
Su, Y.H., Tang, L.P., Zhao, X.Y., and Zhang, X.S. (2021) Plant cell totipotency: Insights into cellular reprogramming. *Journal of Integrative Plant Biology*. 63: 228–243.
Sugimoto, K., Gordon, S.P., and Meyerowitz, E.M. (2011) Regeneration in plants and animals: dedifferentiation, transdifferentiation, or just differentiation? *Trends Cell Biol*. 21: 212–218.
Sultan, S.E. (2000) Phenotypic plasticity for plant development, function and life history. *Trends Plant Sci*. 5: 537–542.
Sychla, A., Casas-Mollano, J.A., Zinselmeier, M.H., and Smanski, M. (2022) Characterization of Programmable Transcription Activators in the Model Monocot Setaria viridis Via Protoplast Transfection. In *Protoplast Technology*, Methods in Molecular Biology. Edited by Wang, K. and Zhang, F. pp. 223–244 Springer US, New York, NY.
Upadhyay, A., Feltman, N.R., Sychla, A., Janzen, A., Das, S.R., Maselko, M., et al. (2022) Genetically engineered insects with sex-selection and genetic incompatibility enable population suppression. *eLife*. 11: e71230.
Voytas, D.F. (2013) Plant genome engineering with sequence-specific nucleases. *Annu Rev Plant Biol*. 64: 327–350.
Wang, J., Tan, M., Wang, X., Jia, L., Wang, M., Huang, A., et al. (2023) WUS-RELATED HOMEOBOX 14 boosts de novo plant shoot regeneration. *Plant Physiol*. 192: 748–752.
Wang, N., Ryan, L., Sardesai, N., Wu, E., Lenderts, B., Lowe, K., et al. (2023) Leaf transformation for efficient random integration and targeted genome modification in maize and sorghum. *Nat Plants*. 9: 255–270.
Wei, Y., Wang, S., and Yu, D. (2023) The Role of Light Quality in Regulating Early Seedling Development. *Plants (Basel)*. 12: 2746.
Weiss, T., Kamalu, M., Shi, H., Li, Z., Amerasekera, J., Zhong, Z., et al. (2025) Viral delivery of an RNA-guided genome editor for transgene-free germline editing in Arabidopsis. *Nat Plants*. 11: 967–976.
Weyers, S., Thom, M., Forcella, F., Eberle, C., Matthees, H., Gesch, R., et al. (2019) Reduced Potential for Nitrogen Loss in Cover Crop–Soybean Relay Systems in a Cold Climate. *Journal of Environmental Quality*. 48: 660–669.
Wieners, R.R., Fei, S., and Johnson, R.C. (2006) Characterization of a USDA Kentucky Bluegrass (Poa pratensis L.) Core Collection for Reproductive Mode and DNA Content by Flow Cytometry. *Genet Resour Crop Evol*. 53: 1531–1541.
Wu, R., Chai, Y., Li, Y., Chen, T., Qi, W., Xue, Y., et al. (2025) A visual monitoring DNA-free multi-gene editing system excised via LoxP::FRT/FLP in poplar. *Plant Biotechnol J*. 23: 4017–4029.
Yadav, R.N., Kumar, P.R., Hussain, Z., Yadav, S., Lal, S.K., Kumar, A., et al. (2022) Maintenance Breeding. In *Fundamentals of Field Crop Breeding*. Edited by Yadava, D.K., Dikshit, H.K., Mishra, G.P., and Tripathi, S. pp. 703–744 Springer Nature, Singapore.
Yoo, S.-D., Cho, Y.-H., and Sheen, J. (2007) Arabidopsis mesophyll protoplasts: a versatile cell system for transient gene expression analysis. *Nat Protoc*. 2: 1565–1572.

Young, C.A., Hume, D.E., and McCulley, R.L. (2013) FORAGES AND PASTURES SYMPOSIUM: Fungal endophytes of tall fescue and perennial ryegrass: Pasture friend or foe?12. *J Anim Sci*. 91: 2379–2394.

Zapiola, M.L., Campbell, C.K., Butler, M.D., and Mallory-Smith, C.A. (2008) Escape and establishment of transgenic glyphosate-resistant creeping bentgrass Agrostis stolonifera in Oregon, USA: a 4-year study. *Journal of Applied Ecology*. 45: 486–494.

Zhang, Y., Ran, Y., Nagy, I., Lenk, I., Qiu, J.-L., Asp, T., et al. (2020) Targeted mutagenesis in ryegrass (Lolium spp.) using the CRISPR/Cas9 system. *Plant Biotechnology Journal*. 18: 1854–1856.

Zinselmeier, M.H., Casas-Mollano, J.A., Cors, J., Ferreira, S.S., Voytas, D.F., and Smanski, M.J. (2025) Towards engineering hybrid incompatibility in plants. *Plant Biotechnology Journal*. 23: 2752–2754.

Zinselmeier, M.H., Casas-Mollano, J.A., Cors, J., Sychla, A., Heinsch, S.C., Voytas, D.F., et al. (2024) Optimized dCas9 programmable transcriptional activators for plants. *Plant Biotechnol J*. 22: 3202–3204.